ACUSTICA

Vol. 3 1953 No. 3

THE PRACTICAL REPRESENTATION OF STANDING WAVES IN AN ACOUSTIC IMPEDANCE TUBE

by W. K. R. LIPPERT

Division of Building Research, C.S.I.R.O., Melbourne, Australia

Summary

It is shown that the envelope curves of the standing waves along the whole of an acoustic impedance tube with attenuation can be represented with the aid of diagrams. Suitable diagrams for easy application to impedance measurements are given and their usefulness is discussed in some specific cases.

The position of the pressure minima are measured with different orifices of the probe tube and the resultant shifts of position are discussed.

Special test measurements with a rigid terminal are proposed for specifying the tube performance.

Sommaire

On montre que les enveloppes des ondes stationnaires dans un tube absorbant à impédance acoustique peuvent être représentées à l'aide de diagrammes. On donne des diagrammes utilisables dans les mesures d'impédance acoustique, et on démontre l'utilité de la méthode proposée par quelques exemples expérimentaux.

Les positions des minima des ondes stationnaires ont été mesurées avec différents orifices du petit tube sonde; on discute les variations correspondantes de position.

On propose de faire quelques expériences propres à caractériser la qualité d'un tube acoustique.

Zusammenfassung

Es wird gezeigt, daß die Umhüllungskurven der stehenden Wellen in einem akustischen Impedanzrohr mit Dämpfung längs des ganzen Rohres mit Hilfe von Diagrammen dargestellt werden können. Geeignete Diagramme für den praktischen Gebrauch bei Impedanzmessungen werden angefertigt, und ihre Nützlichkeit wird an Hand einiger Messungen diskutiert.

Die Lage der Schalldruckminima wird mit verschiedenen Öffnungen des Abtastrohres gemessen, und die sich ergebenden Verschiebungen werden diskutiert.

Besondere Prüfmessungen mit starrem Abschluß werden vorgeschlagen, um die Güte eines Impedanzrohres zu kennzeichnen.

1. Introduction

The transmission line method is the most widely used one for measuring the absorption coefficient or the specific acoustic impedance of a material. A smooth rigid-walled tube has a source of sound at one end and the sample under test at the other and the acoustic impedance can, as is well known, be found by measurements of the standing waves along the tube.

The method requires the measurement of the pressure in the tube without disturbing the sound field, and several approaches to the solution of this problem are known [1]···[6]. That of TAYLOR [1], improved by SCOTT [5], uses a long smallbore probe tube to measure the sound pressure in the main tube. The probe tube is moved along the main tube and is terminated by a microphone outside the main tube.

This method is frequently used because of its simplicity and accuracy. SCOTT has shown that it is not permissible to assume that the tube attenuation is negligible when precise measurements are required and he derived the relevant theory. The practical application of this theory is lengthy, particularly when the standing wave has been explored by recording sound pressure by a high speed level recorder. BERANEK [7] discussed SCOTT's theory and showed how to derive the specific acoustic impedance from measured data from part of the standing wave close to the sample. However, in the course of the present work it was found preferable to use the record along the whole of the tube, and suitable diagrams as presented below were found particularly useful. With these diagrams a sensitive method is available for detecting irregularities in the operation of the equipment, extrapolation of minima to zero distance is easier and the whole provides an improvement in the specification of tube performance.

2. The envelope function

Acoustic impedance tube theory for a tube with attenuation is given in text books [7] and it is necessary only to quote the results here. The ratio of the Mth pressure maximum to the Nth pressure minimum is

$$\left(\frac{|P_{max}|}{|P_{min}|}\right)_{M,N} = \tag{1}$$

$$\sqrt{\frac{2\cosh^2(\alpha D_M + \psi_1) - \frac{\alpha^2}{2k^2}\sinh^2 2(\alpha D_M + \psi_1)}{2\sinh^2(\alpha d_N + \psi_1) + \frac{\alpha^2}{2k^2}\sinh^2 2(\alpha d_N + \psi_1)}}$$

and the distance d_N of the Nth pressure minimum (counted from the sample) is

$$\frac{d_N}{\lambda} = \frac{2N-1}{4} - \frac{\psi_2}{2\pi} - \frac{\alpha}{2k^2\lambda}\sinh 2(\alpha x + \psi_1), \tag{2}$$

wherein α is the attenuation constant for the sound wave due to energy losses at the side walls of the tube and in the gas,

$f = \omega/2\pi$ is the frequency,
c is the wave velocity,
λ is the wavelength,
$k = \omega/c = 2\pi/\lambda$ is the wave number,
x is the distance from the sample surface,
d_N is the distance of the Nth minimum from the sample surface,
D_M is the distance of the Mth maximum from the sample surface,
P_i is the pressure of the incident wave,
P_r is the pressure of the reflected wave and $\psi = \psi_1 + j\psi_2$ is given by

$$P_r/P_i = e^{-2\psi} = e^{-2(\psi_1 + j\psi_2)}. \tag{3}$$

The values of ψ_1 and ψ_2 are calculated by substitution of experimental values of $(P_{max}/P_{min})_{M,N}$ and d_N/λ in equations (1) and (2) and the acoustic impedance ratio is then

$$\frac{Z}{\varrho c} = \frac{R}{\varrho c} + j\frac{X}{\varrho c} = \frac{1}{1 - j\frac{\alpha}{k}}\coth(\psi_1 + j\psi_2) \approx \tag{4}$$

$$\approx \coth(\psi_1 + j\psi_2),$$

wherein Z is the acoustic impedance,
R is the acoustic resistance,
X is the acoustic reactance,
and ϱ is the density of the medium.

The ratio of the maximum to the minimum pressure in the tube is commonly measured by moving the probe tube at constant speed and recording the sound pressure with a high speed level recorder. A typical record is given in Fig. 1. The curves

$$P = A\sqrt{2\cosh^2(\alpha x + \psi_1) - \frac{\alpha^2}{2k^2}\sinh^2 2(\alpha x + \psi_1)} \tag{5}$$

and

$$P = A\sqrt{2\sinh^2(\alpha x + \psi_1) + \frac{\alpha^2}{2k^2}\sinh^2 2(\alpha x + \psi_1)}, \tag{6}$$

where A is a constant depending upon the sound pressure level, will enclose the whole of the recorded trace and hence are envelope curves.

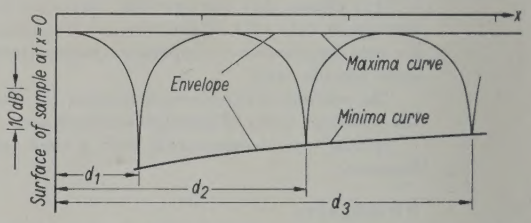

Fig. 1. A typical record of the sound pressure with a high-speed level recorder.

These curves have been superimposed on Fig. 1. The curve which encloses the maxima (cf. eq. (5)) is practically a straight line since αx is usually small. The envelope curves (cf. eq. (5) and (6)) will be separated by an ordinate (in dB) which may be called the envelope value $L(x)$ such that

$$L(x) = \tag{7}$$

$$20\log\sqrt{\frac{2\cosh^2(\alpha x + \psi_1) - \frac{\alpha^2}{2k^2}\sinh^2 2(\alpha x + \psi_1)}{2\sinh^2(\alpha x + \psi_1) + \frac{\alpha^2}{2k^2}\sinh^2 2(\alpha x + \psi_1)}}$$

which can be readily transformed to

$$L(x) = \tag{8}$$

$$20\log\left[\coth(\alpha x + \psi_1)\sqrt{\frac{1 - \frac{\alpha^2}{k^2}\sinh^2(\alpha x + \psi_1)}{1 + \frac{\alpha^2}{k^2}\cosh^2(\alpha x + \psi_1)}}\right].$$

It will be observed that the shape of the envelope curve for a given tube and frequency depends on the tube attenuation and the impedance of the sample. The value of ψ_2 (the phase change caused by the sample) does not affect the envelope; a change in ψ_2 affects both the value and position of the maxima and minima in such a way that the envelope curves are unaltered.

Before discussing the envelope curves further it is desirable to distinguish two cases: case A including highly reflecting to normally absorbent samples, say $\psi_1 \leqq 0.6$, and case B with highly absorbent samples, say $\psi_1 > 0.6$.

3. The envelope function for highly reflecting to normally absorbent samples (Case A)

When $\psi_1 \leqq 0.6$, i.e. when $|P_r|/|P_i| \geqq 0.3$, the envelope function $L(x)$ can conveniently be divided into two parts

$$L(x) = L_1(x) - L_2(x) \tag{9}$$

where $L_1(x) = 20 \log \coth (\alpha x + \psi_1)$, (10)

$$L_2(x) = 10 \log \left[\frac{1 + \frac{\alpha^2}{k^2} \cosh^2 (\alpha x + \psi_1)}{1 - \frac{\alpha^2}{k^2} \sinh^2 (\alpha x + \psi_1)} \right]. \tag{11}$$

$L_1(x)$ may be called the principal envelope function because it largely determines the envelope; $L_2(x)$ is the correction function, small compared with $L_1(x)$. The relation between the various functions and envelope curves is shown diagrammatically in Fig. 2.

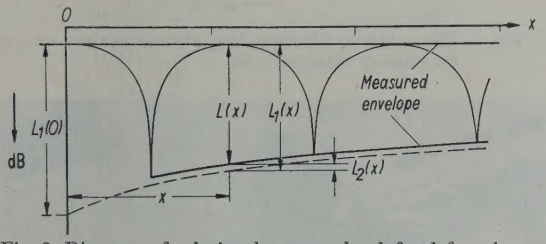

Fig. 2. Diagram of relation between the defined functions and envelope curves.

The principal envelope function $L_1(x)$ has been plotted against αx in Fig. 3 for various values of $L_1(0)$ and for ease of application a set of scales of the distance x for different values of α is given. In Fig. 4 the correction function $L_2(x)$ is plotted against $(\alpha x + \psi_1)$ for various values of the parameter α/k; it will be observed that the value of $L_2(x)$ depends primarily on the value of α/k.

The attenuation constant α may be calculated with sufficient accuracy for a smooth rigid-wall tube when the size and frequency are known [7]···[12]. BERANEK [7] recommends that the values obtained from KIRCHHOFF's equation be increased about 8 per cent in magnitude when predicting the attenuation and this gives an attenuation constant α in nepers per cm

$$\alpha = 1.59 \cdot 10^{-5} \cdot f^{1/2} \cdot \frac{U}{S}, \tag{12}$$

wherein f is the frequency in c/s,
U is the circumference of the tube in cm,
S is the area of the tube in cm².

For normal frequencies and dimensions, the attenuation constant α is a very small quantity and consequently α/k is normally much smaller than unity.

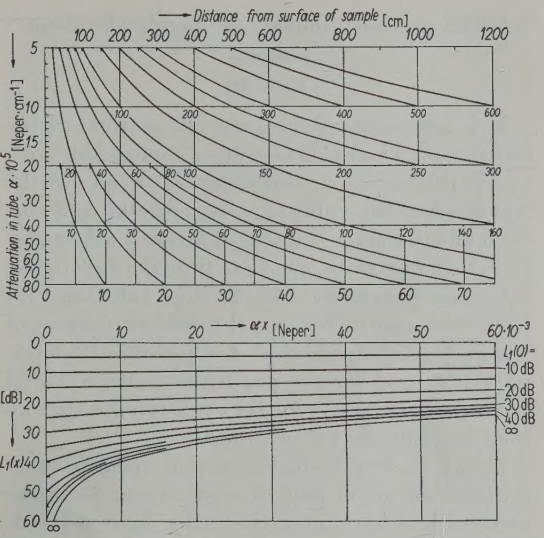

Fig. 3. The principal envelope function $L_1(x)$ plotted against αx for various values of $L_1(0)$ and a set of scales for different values of α.

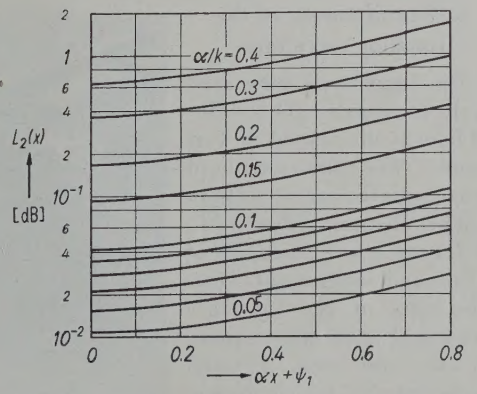

Fig. 4. The correction function $L_2(x)$ plotted against $\alpha x + \psi_1$ for various values of α/k.

If now it be required to determine ψ_1 corresponding to a particular curve recorded in the impedance tube, the values of $L_2(x)$ are found from the value of α/k and from Fig. 4[1] and the curve of $L_1(x)$ drawn from the experimental values according to Fig. 2. This is fitted to the curves of Fig. 3 and the corresponding value of $L_1(0)$ obtained. ψ_1 can then be found from the relation

$$L_1(0) = 20 \log \coth \psi_1. \tag{13}$$

In practice of course the value of $L_2(x)$ is small and for the usual case negligible and the measured curve $L(x)$ is fitted directly to the curves in Fig. 3 and $L_1(0)$ and ψ_1 determined as before.

[1] It is, of course, permissible to determine $L_2(x)$ in Fig. 4 by making a rough estimate for $\alpha x + \psi_1$ or taking it as zero.

4. The envelope function for highly absorbent samples (Case B)

It is not practicable to use the method of the last section when $L_2(x)$ becomes comparable with $L_1(x)$; this occurs or can occur sometimes in the region when the value of ψ_1 exceeds 0.6 and corresponds to values of $L_1(0)$ of about 5 dB or less. It is then better to use $L(x)$ directly and to use α/k as the parameter. The envelope function $L(x)$ is plotted against $\alpha x + \psi_1$ for different values of α/k in Fig. 5.[2] From this, it is possible to determine $(\alpha x + \psi_1)$ for the particular value α/k and the measured value of $L(x)$ at distance x. ψ_1 can then be obtained by subtraction.

It can be seen from Fig. 5 that there is theoretically an upper limit of ψ_1 that can be measured with a particular tube; the limit depends on the parameter α/k but is in general so near to 100 per cent absorption coefficient as to be unimportant.

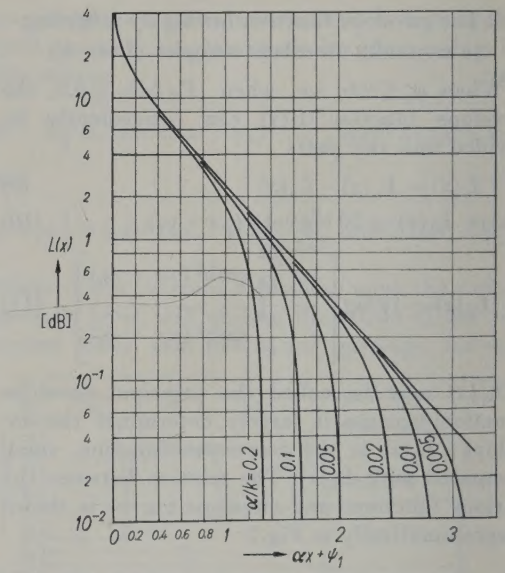

Fig. 5. The envelope function $L(x)$ plotted against $\alpha x + \psi_1$ for various values of α/k.

5. Measurements of the standing wave ratio

The impedance tube used in the measurements described here is illustrated in Fig. 6 and 7. The tube is made of brass, square in cross-section, and has an internal dimension of 7.5 cm, a wall thickness of 0.9 cm and a length of 170 cm. The ends of the tube are machined accurately square to the tube axis. A small probe tube 4.7 mm in diameter rests on the bottom of the main tube and is bent upwards at the end so that the orifice is on the axis of the tube. The probe tube area is about 0.5 per cent of the main tube area and errors due to the probe can be expected to be smaller than this [13]. The impedance tube was terminated as required by a heavy steel plate (4 cm thick), a brass plate (1.0 cm thick) or a sample contained in a holder; these plates and the sample holder can be seen in Fig. 7. Precautions were taken throughout the design to avoid unwanted vibrations in the microphone or the tube, to shield the microphone and to mount it resiliently. The loudspeaker box was

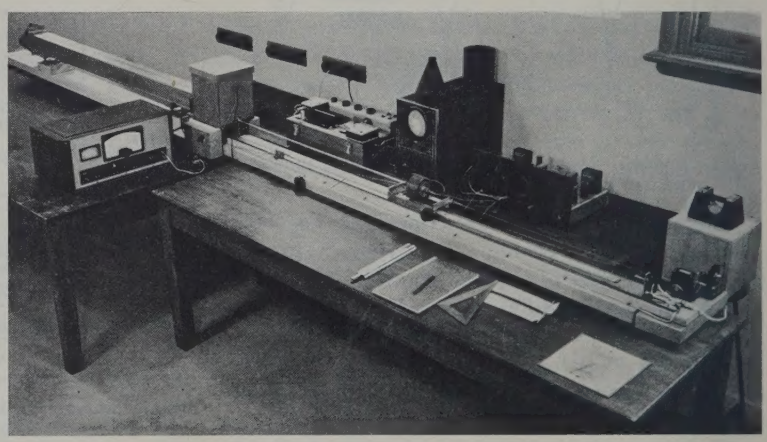

Fig. 6. The acoustic impedance tube.

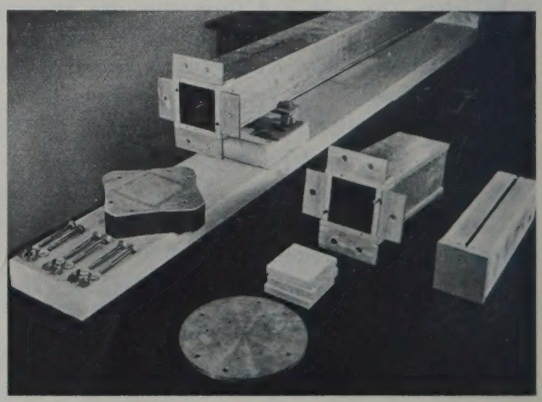

Fig. 7. The end of the main tube with the different terminals and the sample holder.

[2] Although for the measurement of the standing wave ratio of highly absorbent samples a recorder or meter with linear sensitivity is normally and preferably used instead of a high-speed level recorder with logarithmic sensitivity, the scale for $L(x)$ in Fig. 5 has been given in dB for reason of uniformity.

decoupled from the main tube and from the probe tube where it passed through the speaker box. With these precautions and the use of a tuned amplifier (having a Q of about 6) the noise level when the orifice of the probe tube was sealed was almost 65 dB below the level at the maxima (see Fig. 10c).

The attenuation constant α of the impedance tube and the parameter α/k are plotted against frequency in Fig. 8, and since α/k does not exceed 0.005 at any point, the correction $L_2(x)$ is always negligible. The measured envelope curves from the examples of Fig. 9a and 9f can therefore be directly compared with the curves of Fig. 3; such comparison showed good agreement of experimental and theoretical values along the whole length of the tube. This provides an excellent check that the conditions in the tube are satisfactory.

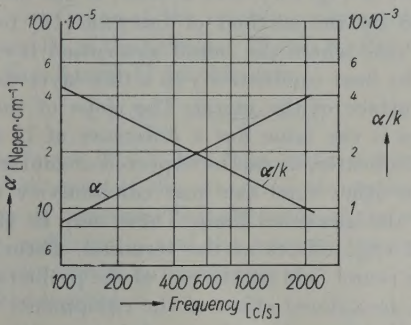

Fig. 8. Attenuation constant α of the main tube and ratio of α to the wave number k plotted against frequency.

The usefulness of this method of checking is shown by results obtained when errors were deliberately introduced; these are illustrated in Fig. 10. The curve of Fig. 10a would normally be considered acceptable but the use of the envelope curves (Fig. 3) shows that a mistake is being made. It was, in fact, caused by a deliberate increase in the speed of movement of the probe tube and a decrease in writing speed of the level recorder. It is interesting to observe that 44 dB would be the value of $L_1(0)$ used for calculating ψ_1 based on previous methods whereas 60 dB is the correct figure. During early work, the curve of Fig. 10b was obtained at low frequency and was recognized as incorrect since the curve passes the $L_1(x)$ line for complete reflection. Examination of the output at the minimum showed a sinusoidal voltage with low noise. The curve was recorded again with a higher valued potentiometer in the level recorder, the probe was sealed and the noise measured. The curves are given in Fig. 10c. The noise level was obviously low enough. Finally it was found that the trouble was

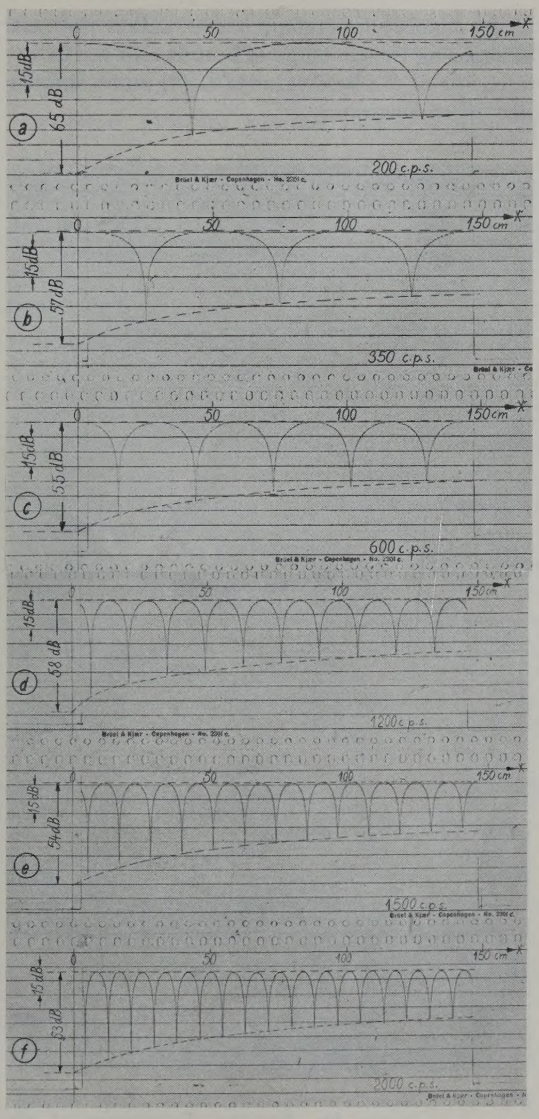

Fig. 9a···f. Records with envelope curves for a rigid terminal and different frequencies.

caused by a very small coupling between the loudspeaker box and the main tube. After this had been removed, the correct result was obtained as shown in Fig. 10d. In most impedance tubes wherein high precision is sought, the checking necessary to ensure correct working takes a great deal of time and care. This can be greatly reduced by adopting the envelope technique described here.

A further advantage of the use of the envelope curve over the whole tube is illustrated in Fig. 10e. Herein the minima of the recorded curve do not lie accurately on a smooth curve (undoubtedly owing to inherent small irregularities) but the use

of the family of envelope curves makes the task of choosing the envelope of best fit and the determination of the best value of $L_1(0)$ much simpler and more accurate.

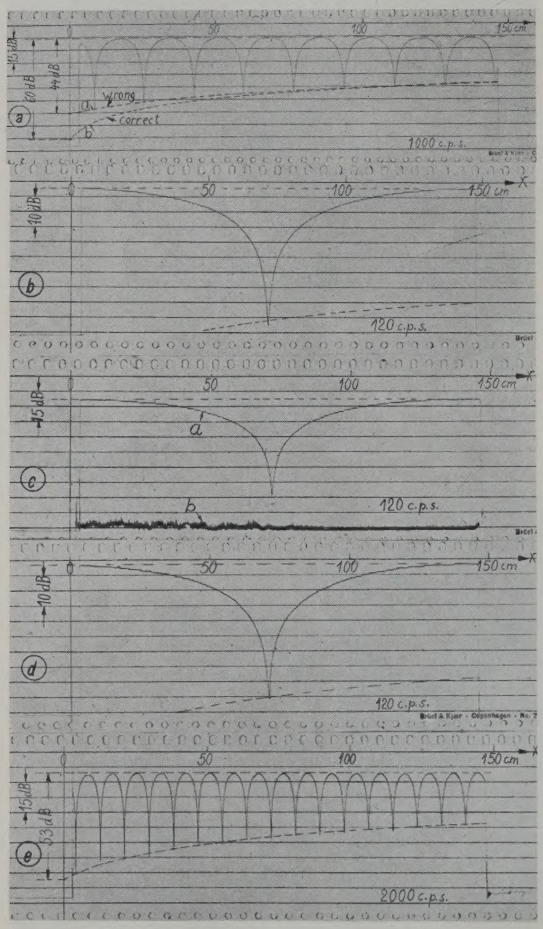

Fig. 10a···e. Records to illustrate the use of the envelope curves for detecting disturbances of the equipment.

6. Measurement with a highly reflecting terminal

In order to check the working conditions of an impedance tube or to determine the limits of accuracy for the difficult measurements of hard materials it is necessary or desirable to study the apparent impedance of a very hard terminal. The measured values of $L_1(0)$ for a ground steel plate 4 cm thick as obtained with the equipment described above, are plotted against the frequency in Fig. 11, the technique of the envelope function being used in the measurement (cf. Fig. 9a···f). Several methods of fixing and sealing the plate were used and all gave essentially the same result. The corresponding absorption coefficients (cf.

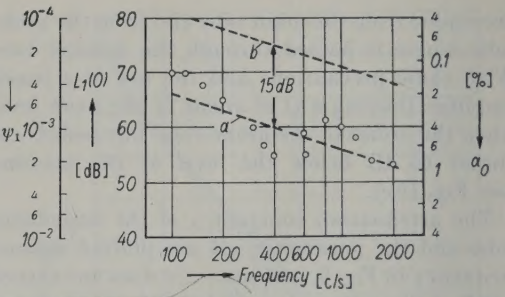

Fig. 11. Values of $L_1(0)$, ψ_1 and absorption coefficient a_0 for a rigid terminal plotted against frequency.
(a) average of measured values,
(b) theoretical limit caused by heat conductivity only.

curve a) are 0.2 per cent at 100 c/s, 0.5 per cent at 500 c/s and 0.9 per cent at 2000 c/s.

The theoretical limit is for this measurement plotted in Fig. 11 (curve b) also; it has been obtained by the method of CREMER [14] for the ideal case where the sound absorption is caused only by heat conductivity in a thin layer close to the surface of the metal. The slope of the two curves is the same but a difference of 15 dB in level indicates, as can be expected of course, that effects other than the heat conductivity determine the measured limit. These may be the so-called edge effects at the terminal, disturbance of the sound field by the end of the probe tube or some unexplored effect of the equipment.

In the first place the resolving power of the tube in connection with the possible error must be discussed. With a highly reflecting terminal, the first minimum occurs at a distance close to a quarter of a wavelength from the sample surface. For a given sound level at maxima, the level at the first pressure minimum is determined partly by the attenuation (α) of the tube and partly by sound absorption (ψ_1) of the terminal. A factor of the resolving power D_1 may be defined as the ratio of the pressure at the first minimum with zero tube attenuation to the pressure at the first minimum for zero energy absorption at the terminal.

Now for highly reflecting samples

$$a_0 = 1 - \left(\frac{|P_r|}{|P_i|}\right)^2 = 1 - e^{-4\psi_1} \approx 4\psi_1 \qquad (14)$$

and from eq. (10)

$$D_1 = \frac{4\psi_1}{\alpha\lambda} = \frac{a_0}{\alpha\lambda} = \frac{a_0}{2\pi}\left(\frac{k}{\alpha}\right) \qquad (15)$$

and consequently for a constant a_0 the factor D_1 is proportional to the square root of the frequency. If, alternatively, $L_1(0)$ is determined from a

minimum other than the first, the corresponding resolving power $D(x)$ becomes

$$D(x) = \frac{\psi_1}{\alpha x} = \frac{a_0}{4\alpha x}. \tag{16}$$

For constant a_0 and x, the factor $D(x)$ is inversely proportional to the square root of the frequency. The use of minima at some distance from the sample is therefore a disadvantage at higher frequencies; however, the proposal made earlier that the record of the standing wave along the whole tube be used in determining $L_1(0)$ has the advantage that hidden disturbances can be recognized and eliminated. To avoid an overestimate of the accuracy, consider the resolving power of the tube at a point about half its length.

The measured absorption coefficient of Fig. 11 increases with frequency in such a way that the factor $D(x)$ is independent of frequency. Therefore, the factor of the resolving power taken at the middle of the tube ($x = 75$ cm) is after eq. (16) and Fig. 8 and 11 in this case

$$D(x = 75\text{ cm}) \approx 0.08. \tag{17}$$

If the factor $D(x)$ is less than unity, it is obvious that the error of the measured absorption coefficient a_0 increases. Call the error of the absorption coefficient ε_a and the error in the pressure ratio maximum to minimum ε_m.

Then it yields

$$\left(\frac{|P_{max}|}{|P_{min}|}\right)_{measured} = \left(\frac{|P_{max}|}{|P_{min}|}\right)(1 \pm \varepsilon_m) \tag{18}$$

and

$$a_{0\,measured} = a_0(1 \pm \varepsilon_a) \tag{19}$$

and ε_a and ε_m are related

$$\varepsilon_a = \left(1 + \frac{1}{D(x)}\right)\varepsilon_m. \tag{20}$$

For measurements of the envelope curve from a single tube record, the error may be estimated at ± 0.5 dB corresponding to $\varepsilon_m = 0.05$. Repetition and good experimental conditions may reduce these to ± 0.1 dB, $\varepsilon_m = 0.01$. The scattering of measurements shown in Fig. 11 can be explained from eq. (17) and (20) and the tube conditions for determining the standing wave ratio with highly reflecting samples are as good as can be expected.

7. The shift of position of the pressure minimum

The complex value of the acoustic impedance is determined from the relative position of the pressure minimum and the sample as well as from the standing wave ratio (cf. eq. (4)). Normally the position d_1 of the first minimum (cf. Fig. 1) is chosen. The value of ψ_2 is then found by the use of eq. (2); the wave length is preferably determined from the average distance between two successive pressure minima $\left(\text{e.g. } \frac{\lambda}{2} = \frac{d_N - d_1}{N-1}\right)$. The distance of a minimum depends to some extent on tube attenuation (eq. (2)) as discussed by SCOTT [5]. Let the change in position of the minimum with and without attenuation be δx, then

$$\delta x = -\frac{\alpha}{2k^2}\sinh 2(\alpha x + \psi_1) \tag{21}$$

and in all practical cases δx is small for ψ_1 small. The effect of the attenuation on the position of minima is therefore small for hard materials but it is necessary to check and investigate the accuracy of the position of the first minimum for a highly reflecting sample.

As the size and plane of the orifice of the probe tube vary frequently with different impedance tubes, four types of probe tube orifice have been used with the equipment described; their sections are given in Fig. 12. The difference Δx between the measured position d_1 and a quarter of a wavelength is plotted against the frequency in Fig. 13

$$\Delta x = d_1 - \frac{\lambda}{4}. \tag{22}$$

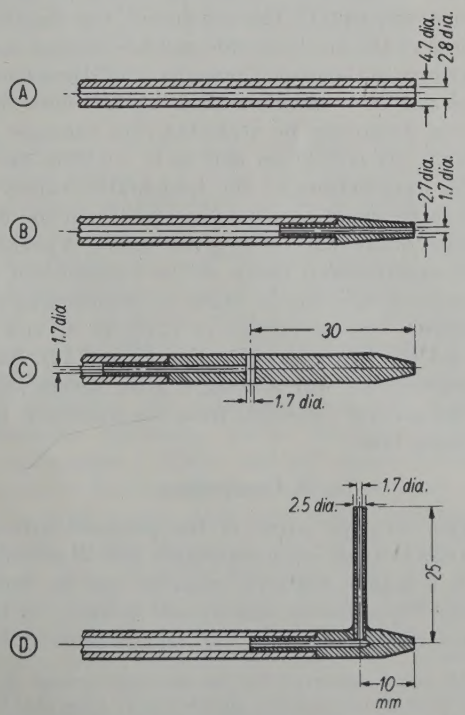

Fig. 12. Cross-sections of probe tube orifices used in the measurements of Fig. 13.

Reproducibility of the order of ± 0.01 cm was achieved, and there was no significant difference by using different methods of fixing and sealing the end plate (steel 4 cm thick).

The curves of Fig. 13 indicate that appreciable errors can be introduced by having the orifice perpendicular to the plane of the main tube (end pieces A and B) and that the effect is greater with larger orifices. End pieces C and D having orifices

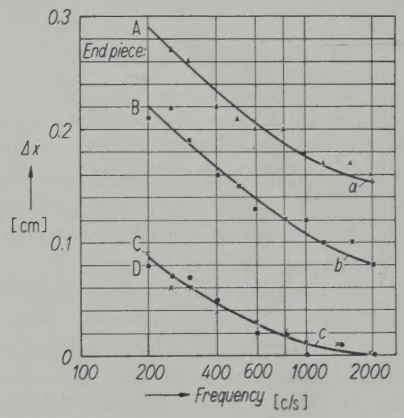

Fig. 13. Measured difference Δx of the position of the first minimum and a quarter of a wave length plotted against frequency for different tube orifices.

parallel to the axis of the tube, gave values of Δx much smaller than A and B which moreover were nearly equal.[3] The end piece C was therefore chosen as the most suitable and was the one used elsewhere in the work. Comparison of Δx as measured and δx as calculated from eq. (21) show that δx can invariably be neglected. For example, at 200 c/s, Δx is 0.09 cm and δx is -0.0005 cm.

An examination of the measurable values of ψ_2 can be made in a manner similar to the discussion of the limits of ψ_1 given earlier. A practicable experimental check of the condition of an impedance tube can be made by determining the frequency characteristics of $L_1(0)$ or a_0 and of Δx (as has been shown in Fig. 11 and 13). Such characteristics will provide a good specification of the accuracy possible from the particular impedance tube.

8. Conclusions

The envelope curve of the pressure-distance relation in an acoustic impedance tube as recorded with a high-speed level recorder can be determined theoretically and its use is likely to improve the accuracy of the measurements. For highly reflecting samples, the family of curves for different envelopes is represented by taking the absorption of the sample ($L_1(0)$ or ψ_1) as parameter and for highly absorbent samples the curves have the ratio of attenuation to wave number (α/k) as parameter. Disturbing effects in the equipment can be rapidly detected by closing the tube with a rigid terminal, recording a pressure-distance curve and comparing this with theoretically derived curves.

A definition of the resolving power of an impedance tube is proposed and discussed. The size and plane of the probe tube orifice is important — in particular the plane should be parallel to the tube axis. Test measurements with a rigid terminal whose results are plotted against frequency as shown in some examples provide a practicable method for specifying the tube performance and the accuracy of measurements possible with an impedance tube.

[3] It may be observed that the measured increase of Δx with lower frequencies does not necessarily mean that it is caused by the orifice of the probe tube and could not be avoided with other equipment.

Acknowledgments

The author desires to acknowledge the assistance of Mr. A. W. Wilson in designing and constructing the equipment.

(Received 25th August, 1952.)

References

[1] Taylor, H. O., A direct method of finding the value of materials as sound absorbers. Phys. Rev. **2** [1913], 270—287.

[2] Wente, E. C. and Bedell, E. H., Measurement of acoustic impedance and the absorption coefficient of porous materials. Bell Syst. Tech. J. **7** [1928], 1—10.

[3] Hall, W. M., An acoustic transmission line for impedance. J. acoust. Soc. Amer. **11** [1939], 140—146.

[4] Sabine, H. J., Notes on acoustic impedance measurements. J. acoust. Soc. Amer. **14** [1942], 143—150.

[5] Scott, R. A., An apparatus for accurate measurement of the acoustic impedance of sound absorbing materials. Proc. phys. Soc. **58** [1946], 253—264.

[6] Beranek, L. L., Some notes on the measurements of acoustic impedance. J. acoust. Soc. Amer. **19** [1947], 420—427.

[7] Beranek, L. L., Acoustic measurements. John Wiley & Sons Inc., New York 1949.

[8] Morse, P. M., Vibration and sound, 2nd Ed. McGraw-Hill Book Co., New York 1948.

[9] Waetzmann, E. and Wenke, W., Schalldämpfung in Rohren und Schläuchen. Akust. Z. **4** [1939], 1—9.

[10] Fay, R. D., Attenuation of sound in tubes. J. acoust. Soc. Amer. **12** [1940], 62—67.

[11] Beranek, L. L., Precision measurements of acoustic impedance. J. acoust. Soc. Amer. **12** [1940], 3—13.

[12] Lord Rayleigh, Theory of sound. Macmillan, London 1897.

[13] Zwikker, C. and Kosten, C. W., Sound absorbing materials. Elsevier Publ. Co., Inc., New York, Amsterdam, etc. 1949.

[14] Cremer, L., Über die akustische Grenzschicht vor starren Wänden (On the acoustic boundary layer at rigid walls). Arch. elekt. Übertragung **2** [1948], 136—139.

DIE MESSUNG DER TRITTSCHALLDÄMMUNG VON DECKEN MIT SINUSFÖRMIGER ERREGUNG

Von THOMAS LANGE

III. Physikalisches Institut der Universität Göttingen

Zusammenfassung

Es wird die Trittschalldämmung von Fußböden bzw. Decken in Gebäuden gemessen. Die Anregung der Decke zu Schwingungen erfolgt sowohl mit dem üblichen Hammerwerk als auch sinusförmig mit einem elektromagnetischen System. Die Differenz beider Trittschallpegel-Kurven stimmt mit dem Schlagspektrum des Hammerwerkes überein. Messungen auf dem Bau beweisen die Brauchbarkeit des Verfahrens zur Messung der Trittschalldämmung von Decken bei sinusförmiger Anregung, welches eine Reihe von Vorteilen bietet. Die Amplituden der Biegeschwingungen einer gemessenen Decke nehmen bei punktweiser Erregung mit der Wurzel aus dem Abstand ab.

Summary

This paper describes investigations of the sound pressure level of impact sound. The vibrations of the ceiling are produced both by the usual hammer machine and by an electromagnetic system for sinusoidal excitation. The difference of both sound pressure levels is in agreement with the spectrum of the impacts with the hammer. Measurements in buildings demonstrate the adequacy of the method of sinusoidal excitation. This method has several advantages. In the case of excitation at one point the amplitudes of flexural waves on a floor decrease with the square root of the distance.

Sommaire

Mesure de la transmission sonore des bruits de choc dans les bâtiments. Les vibrations d'un plancher sont produites non seulement par la machine à frapper (à marteaux) mais aussi par un système électromagnétique excitant seulement une fréquence. La différence des niveaux sonores moyens produits dans le local de réception s'explique par le spectre des chocs des marteaux. Dans les bâtiments, des essais avec le système électromagnétique montrent l'utilité de cette méthode d'excitation, qui possède plusieurs avantages. Les amplitudes mesurées des vibrations de flexion d'un plancher diminuent avec la racine carrée de la distance du point excité.

1. Einleitung

Die Trittschalldämmung von Fußböden bzw. Decken in Gebäuden wird nach einem genormten Verfahren [1], [2] gemessen, indem man ein bestimmtes Hammerwerk auf den Fußboden stellt, das stoßweise die Decke zu Schwingungen anregt. In dem darunter liegenden Raume mißt man den mittleren absoluten Schallpegel in Frequenzbändern von Oktavbreite. Im folgenden wird untersucht, wie die stoßweise Erregung durch eine sinusförmige ersetzt werden kann.

2. Messungen mit dem Hammerwerk nach DIN 52210

Zunächst sei über einige Untersuchungen mit dem Hammerwerk berichtet, das den internationalen Normen [2] entsprach bis auf folgende Punkte: Die Hämmer bestanden aus Eisen. Jeder Hammer wurde etwa 250 ms nach dem Schlag wieder emporgehoben. Es interessiert dabei der Druck-Zeit-Verlauf während eines Hammerschlages; er wurde aufgenommen, indem der Hammer auf ein 2 cm dickes, zylindrisches Eisenstück von 2 cm Durchmesser schlug, welches den Druck auf einen darunter liegenden Piezokristall (X-Schnitt-Quarz mit Eigenfrequenzen über 0,3 MHz) übertrug. Dieser war auf einem im Vergleich zum Hammer recht schweren Eisenklotz befestigt, welcher zur Schwingungsdämpfung in Sand [3] gebettet war. Die durch ein einmaliges Herunterfallen des Hammers erzeugte piezoelektrische Spannung wurde verstärkt (obere Grenzfrequenz 1 MHz) und auf einem Oszillographen in ihrem zeitlichen Verlauf sichtbar gemacht. Abb. 1 zeigt, daß nach jedem Schlag der Hammer wieder abspringt, erneut herunterfällt und so fort. Dasselbe Bild bietet ein auf den Hammer als Beschleunigungsempfänger gesetzter Piezokristall (Biegeschwinger unterhalb seiner Eigenfrequenz) (Abb. 2). Es entsteht eine Schlagfolge, bevor der Hammer von dem Antriebsmechanismus wieder emporgehoben wird. Beim ersten Aufprall hat der Hammer 78,5% seiner

Fallenergie verloren, der erste Nachschlag erfolgt nach 84 ms.

Das in der Unterlage erzeugte Schlagspektrum wurde mit dem oben genannten Druckempfänger aufgenommen, der an einen Hochtonanalysator [4] mit logarithmischem Pegelschreiber angeschlossen war. Die erhaltenen Spektren haben bei

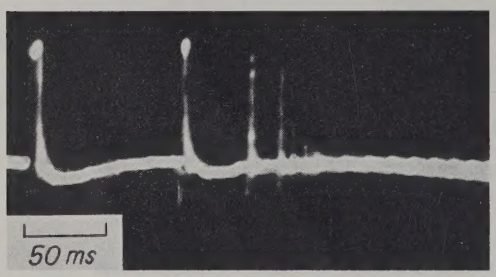

Abb. 1. Der Druck-Zeit-Verlauf beim Schlag auf den Eisenklotz. (Ordinatenmaßstab nicht linear, um die kleinen Nachschläge sichtbar zu machen.)

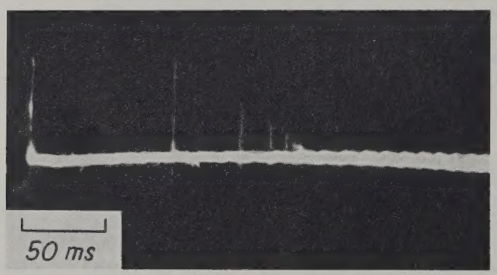

Abb. 2. Der Beschleunigungs-Zeit-Verlauf beim Schlag auf den Eisenklotz. (Ordinatenmaßstab nicht linear, um die kleinen Nachschläge sichtbar zu machen.)

der genormten Schlagfrequenz von 10 s^{-1} eine Liniendichte von 2 Hz. Aus technischen Gründen tritt in dem benutzten Meßverfahren eine geringere Liniendichte auf. Das Spektrum des Schlages auf den Eisenklotz (Abb. 3) ist bis 20 kHz mit einer Abweichung von ± 5 dB konstant.

In dem Spektrum des Schlages auf eine $1 \times 0{,}6$ m^2 große und 28 mm dicke Holzplatte mit 1 mm Linoleumbelag (Abb. 4a) sind die Differenzen zwischen Maxima und Minima größer (15 dB). Außerdem tritt ab 5 kHz ein allgemeiner Abfall nach hohen Frequenzen auf, der etwa 1 dB/kHz beträgt. Er stimmt qualitativ mit der Theorie [5] überein; quantitative Übereinstimmung war nicht zu erwarten, da nicht alle Voraussetzungen der Theorie erfüllt waren. Die experimentelle Relaxationszeit beträgt $2 \cdot 10^{-4}$ s. Nachschläge traten an der Holzplatte nicht auf. Abb. 4b zeigt das Spektrum eines Schlages auf den Eisenklotz, wenn ein 2 mm dickes Stück Schwammgummi zwischen Hammer und Unterlage liegt. Der Abfall beträgt hier 6 dB/kHz, die Relaxationszeit ist größer als 10^{-2} s.

Mit dem Hammerwerk, einem Siemensschen Schallpegelmesser und Oktavsieb wurde der Trittschallpegel einer Decke nach den Vorschriften DIN 52210 gemessen. Man kann während der Messung mit dem Hammerwerk auf dem Fußboden herumfahren, anstatt es an mindestens sechs verschiedenen Stellen auf den Fußboden klopfen zu lassen. Dadurch erreicht man dieselben Ergebnisse, eine schnellere Messung, eine bessere Mittelung sowie einen Überblick über die durch stehende Wellen hervorgerufene Schwankungen. Abb. 5 zeigt einen Ausschnitt aus einem so hergestellten Meßstreifen bei einer festen Oktavsiebeinstellung. Anstelle des Oktavsiebes kann man auch ein schmaleres Filter benutzen.

Abb. 6 zeigt den Trittschallpegel in Abhängigkeit von der Frequenz für eine 32 cm dicke Decke. Diese Decke, eine alte Konstruktion (in dem Hause Bunsenstraße 7 des III. Physikalischen Institutes), ist 507×315 cm^2 groß und besteht

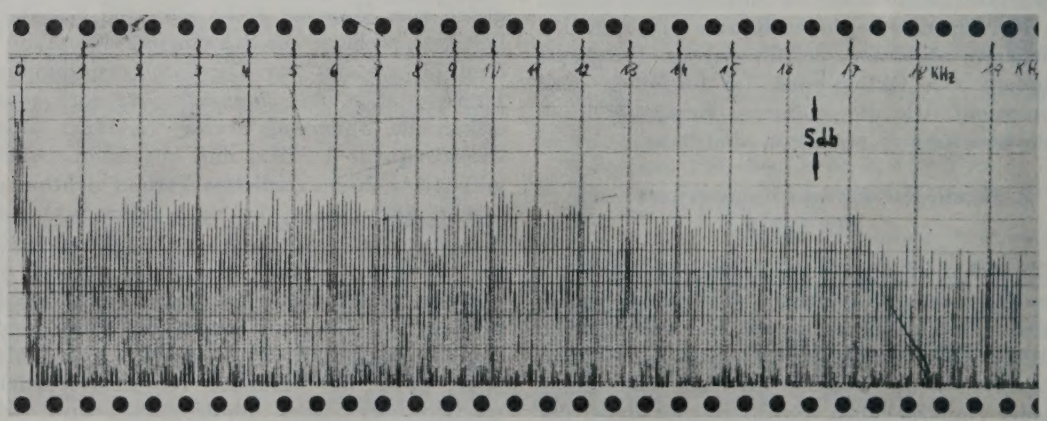

Abb. 3. Das Spektrum des Schlages auf den Eisenklotz.

aus Zementbeton, der zwischen Doppel-T-Träger gestampft ist, aus Zementestrich und aus Linoleum. Der darunter befindliche Raum hat ein Volumen von 40,5 m^3 und die ebenfalls auf Abb. 6 (unten) gezeigte Nachhallzeit. Die Reduktion auf die genormte Absorptionsfläche in diesem Raum betrüge 1,9 dB, ist aber im folgenden nicht berücksichtigt, da es sich nur um Vergleichsmessungen an ein und derselben Decke handelt. Die gestrichelte Kurve auf Abb. 6 zeigt den Trittschallpegel derselben Decke, aber gemessen mit einem Filter von 50 Hz Halbwertsbreite (und 100 Hz Bandbreite bei einem Pegel 40 dB unter dem Maximum) [4]. Hier sind die Meßwerte bereits mit einer Korrektur versehen, welche die konstante Bandbreite umrechnet in eine mit der Frequenz wachsende, wie sie ein Oktavsieb besitzt. Dann stimmen beide Kurven innerhalb der Meßgenauigkeit überein. Soweit die Messungen nach der Hammerwerk-Methode.

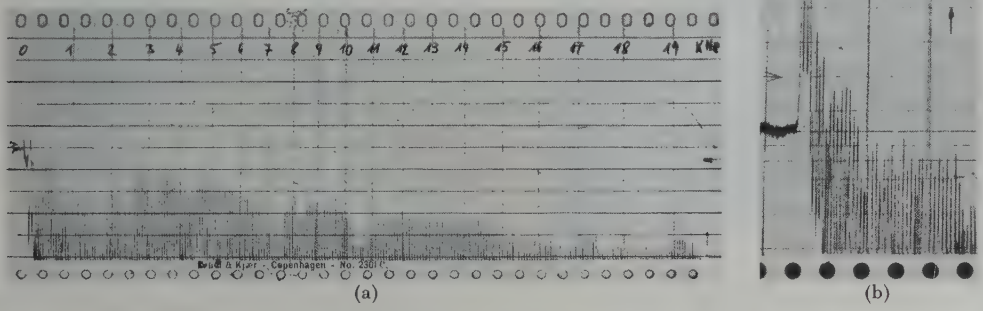

(a) (b)

Abb. 4. Das Spektrum der Schläge auf die Holzplatte (a) und auf den Eisenklotz mit Gummizwischenschicht (b).

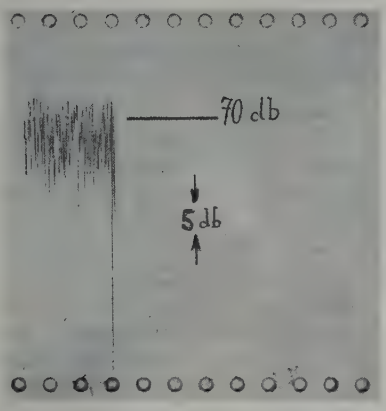

Abb. 5. Schwankungen des Trittschallpegels, wenn man die Aufstellung des Hammerwerkes verschiebt.

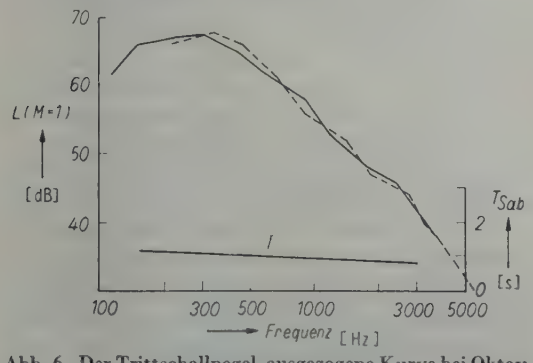

Abb. 6. Der Trittschallpegel, ausgezogene Kurve bei Oktavsieb-Analyse; gestrichelt bei Analyse mit 50-Hz-Filter, umgerechnet auf Oktavbandbreite.

3. Verfahren zur Messung mit sinusförmiger Anregung

Zur sinusförmigen Anregung von Körperschall wurde ein elektromagnetisches System gebaut. Es besteht aus einem 13 kg schweren Permanentmagneten (Type Nr. 20-8617a der Deutschen Edelstahl-Werke, Dortmund), der in einem ringförmigen Spalt von 62 mm Durchmesser, 1,6 mm Breite und 10 mm Tiefe eine Kraftflußdichte von etwa 1,3 $V \cdot s \cdot m^{-2}$ besitzt. In diesem Spalt sitzt eine Spule, die auf einen zylinderförmigen Spulenträger aus Messing gewickelt ist und durch zwei Blattfedern so gehalten wird, daß sie in dem Magnetspalt frei schwingen kann. Abb. 7 zeigt das System, das also einem permanent-dynamischen Lautsprecher ähnlich aufgebaut ist. Nur ist anstelle der Membran ein starrer Fuß angebracht (auswechselbar mit Durchmessern von 30 bis 130 mm), auf den der ganze Magnet gestellt weden kann. Er wird dann von den Blattfedern getragen. Diese wurden so berechnet, daß sie zusammen mit der Masse des Magneten eine Eigenfrequenz von 15,9 Hz ergeben. Die tatsächliche Eigenfrequenz liegt bei 15,6 Hz. Diese Übereinstimmung ist über Erwarten gut.

Abb. 7. Der elektromagnetische Körperschallsender schräg von unten (etwa $^1/_3$ natürlicher Größe).

Wird dieser Körperschallsender auf eine Unterlage, z. B. den Fußboden, gestellt und durch seine Spule ein Wechselstrom I aus einem Verstärker geschickt, so wirkt zwischen Sender und Unterlage eine Kraft K, die dem Strom proportional ist: $K = \alpha I$. Da α hier nicht von der Frequenz abhängt, ist der Effektivwert der Kraft leicht frequenzunabhängig zu machen. (Dies gilt auch bei und unterhalb der Eigenfrequenz. Da in der Eigenfrequenz jedoch besonders große Amplituden auftreten, werden die Verluste größer. Außerdem ist die Justierung der Schwingspule für große Amplituden sehr schwierig. Es empfiehlt sich daher, den Sender nur oberhalb seiner Eigenfrequenz zu benutzen.)

Die Frequenzunabhängigkeit des Effektivwertes der Kraft zwischen Sender und Unterlage wurde gemessen, indem der Sender auf einen piezoelektrischen Druckempfänger gestellt wurde. Das Ergebnis zeigt die Abb. 8. Die untere Grenzfrequenz von 75 Hz ist durch den Kraftverstärker bedingt, die obere bei 1,5 kHz durch die Resonanz des piezoelektrischen Empfängers, der aus Seignettesalz-Kristallen zwischen zwei als Masse wirkenden Messingplatten besteht; durch das Aufsetzen des Körperschallsenders wurde die Masse vergrößert und seine Eigenfrequenz von 3,5 auf 1,8 kHz gesenkt. Ein störender Einfluß von Blattfeder-Resonanzen wurde nicht beobachtet. Durch Verwendung eines Verstärkers mit besserem Ausgangsübertrager konnte die Frequenzkurve noch verbessert werden.

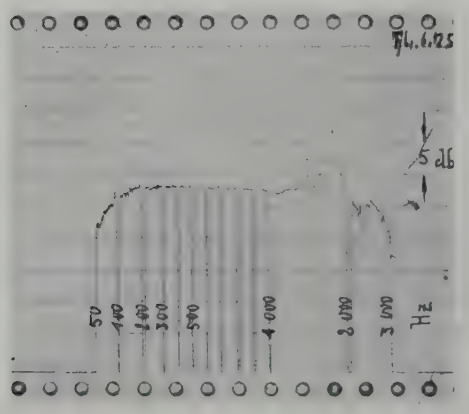

Abb. 8. Die Frequenzkurve des gesamten Systems.

Die Proportionalitätskonstante α zwischen Kraft und Strom des Körperschallsenders wurde wie üblich in einem statischen Versuch bestimmt. Man läßt zwischen Spule und Magnet eine bekannte Gleichkraft wirken, indem man ein Gewicht auf den Magneten setzt. Die hierdurch verursachte Störung der Gleichgewichtslage zwischen Spule und Magnet wird durch einen Gleichstrom kompensiert. Der so erhaltene Wert für α lautet

$$\alpha = 14{,}1 \text{ Newton/A} = 1{,}44 \text{ kp/A} \pm 4\,\%.$$

Ursprünglich war α größer und sank im Laufe der Zeit infolge Alterung des Magneten auf den oben angegebenen Wert.

Oberhalb 1 kHz strahlte der Magnet merklich auch Luftschall ab, den man durch eine über den Magneten gestülpte Dämmhaube genügend vermindern kann. Die Dämmhaube besteht aus einem doppelwandigen Gefäß, das mit Sand in einer 22 mm dicken Schicht gefüllt ist.

Die zur Messung des Trittschallpegels benutzte Apparatur besteht auf der Sendeseite aus einem Schwebungssummer mit Verstärker (90 W) und dem beschriebenen elektromagnetischen Anregesystem. Die Empfangsapparatur setzt sich aus einem DIN-Schallpegelmesser (Siemens & Halske AG) und einem daran angeschlossenen (Neumannschen) Pegelschreiber zusammen. Die Antriebsachse des Pegelschreibers wird mit der Achse des Drehkondensators im Schwebungssummer starr verbunden. Ohne Frequenzmodulation (Wobbelzusatz) des Summers zeichnet der Pegelschreiber die stehenden Wellen des Luftschalles im Empfangsraum über der Frequenz auf, ähnlich wie bei der Messung der Luftschalldämmung. Nun wird der Magnet auf eine andere Stelle auf den Fußboden gesetzt, das Registrierpapier zurückgerollt und eine weitere Kurve über die erste geschrieben. Abb. 9 zeigt, daß sich beide Kurven bis auf die stehenden Wellen decken. Auf diese Weise werden sechs Kurven übereinander

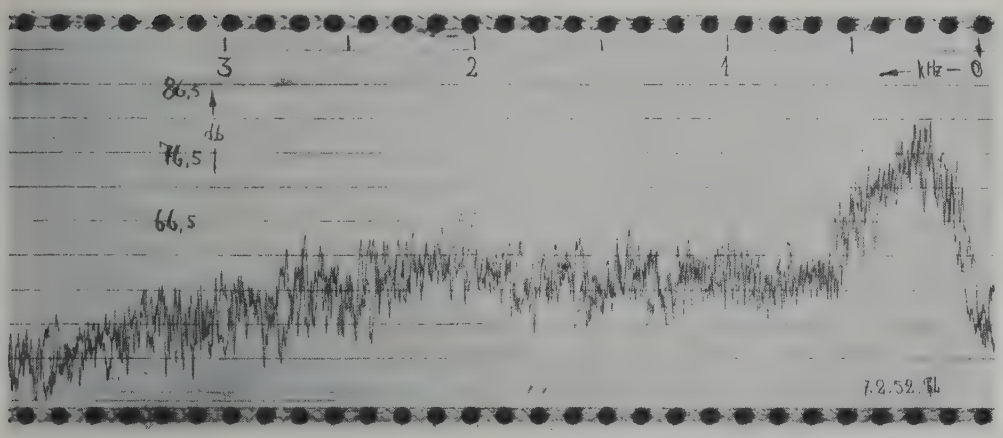

Abb. 9. Ein Registrierstreifen des Trittschallpegels bei sinusförmiger Anregung. Zwei Kurven, gewonnen an verschiedenen Anregungsstellen.

gezeichnet, deren Mittelwert in Abhängigkeit von der Frequenz graphisch ermittelt wird.

An der oben beschriebenen Decke wurde der Trittschallpegel gemessen; die Anregung erfolgte durch das elektromagnetische System mit verschiedenen Fußdurchmessern von 30 bis 130 mm. Die Dicke der als Fuß dienenden Dural-Scheiben betrug 15 mm. Eine Abhängigkeit von der Anregungsfläche ist zu erwarten, sobald deren Durchmesser mit der Biegewellenlänge der Decke vergleichbar wird, sofern der Fuß als starr gegen Biegeschwingungen zu betrachten ist. Dies ist aber nicht erwünscht und eine derartige Starrheit läßt sich wohl gar nicht mit Konstruktionen erreichen, deren Flächengewicht soviel kleiner ist als das der Decke. Die Meßergebnisse (Abb. 10)

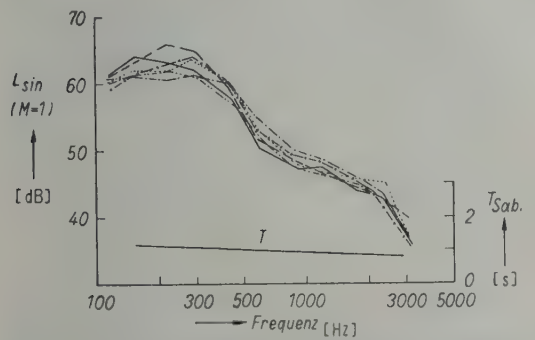

Abb. 10. Der Trittschallpegel bei sinusförmiger Anregung. Sechs verschieden große kreisförmige Anregungsflächen mit Durchmessern von 3 bis 13 cm.

zeigen keine Abhängigkeit des gemessenen Trittschallpegels vom Fußdurchmesser. Vielmehr wird die Streugrenze und damit die Meßgenauigkeit aus dieser Darstellung deutlich. Sie beträgt ± 2 dB.

4. Vergleich der Trittschallmessungen bei schlagartiger und bei sinusförmiger Anregung

Ersetzt man die Anregung einer Decke zu Biegeschwingungen mit dem Hammerwerk durch eine sinusförmige Anregung mit bekannter Kraft K, so ist der Trittschallpegel L auf die Größe dieser Kraft zu beziehen. Man erhält so mit der üblichen Reduktion auf konstante Absorptionsfläche A_0 im Empfangsraum im logarithmischen Maß:

$$L_{sin} = 20 \log p/p_0 - 20 \log K/K_0 + 10 \log A/A_0.$$

Als Bezugswerte wurden die Größen

$$p_0 = 2 \cdot 10^{-5}\,\text{Newton/m}^2 = 2 \cdot 10^{-4}\,\mu\text{bar} = 2 \cdot 10^{-4}\,\text{dyn/cm}^2$$

$$K_0 = 10\,\text{Newton} = 10^6\,\text{dyn} = 1{,}02\,\text{kp}$$

$$A_0 = 10\,\text{m}^2$$

gewählt, weil sie Werte in derselben Größenordnung ergeben wie bei Anregung mit dem genormten Hammerwerk. Man könnte auch andere Bezugswerte festlegen.

Die Definition des Norm-Trittschallpegels, das heißt bei der Messung mit dem Hammerwerk, lautet (in der Schreibweise von KOSTEN u. a. [9]):

$$L_{Norm}\,(M = A_0/A) = 20 \log p/p_0 + 10 \log A/A_0$$

mit $p_0 = 2 \cdot 10^{-5}\,\text{Newton/m}^2 = 2 \cdot 10^{-4}\,\mu\text{bar} = 2 \cdot 10^{-4}\,\text{dyn/cm}^2$,

$A_0 = 10\,\text{m}^2$.

Die Reduktion auf eine bekannte und frequenzkonstante Kraft entfällt hier, da man sich auf die durch das Hammerwerk gegebene Kraft mit seiner durch die örtliche Elastizität bedingten Frequenzabhängigkeit bezieht.

An der oben schon beschriebenen Decke wurde ein Vergleich der Trittschallpegel bei Anregung

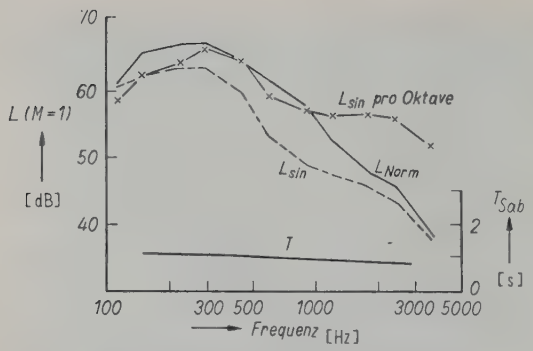

Abb. 11. Der Trittschallpegel; ausgezogene Kurve bei Anregung mit Hammerwerk; gestrichelt bei sinusförmiger Anregung; Kreuze bei sinusförmiger Anregung, aber umgerechnet auf Oktavbandbreite.

mit dem Hammerwerk und mit dem Magnetsystem durchgeführt. Abb. 11 zeigt glatt ausgezogen den Trittschallpegel bei stoßweiser Anregung durch das Hammerwerk und gestrichelt bei sinusförmiger Anregung durch das Magnetsystem. Beide Kurven sind zunächst noch nicht miteinander vergleichbar, da bei der Oktavsiebanalyse die Filterbreite proportional der Frequenz wächst, während sie bei der Sinuserregung konstant bleibt. Die mit dem Magnetsystem gewonnene Kurve wurde daher von konstanter Filterbreite auf Oktavbreite umgerechnet. Das Ergebnis ist ebenfalls in Abb. 11 als ausgezogene Kurve mit Kreuzen eingetragen. Sie stimmt noch nicht mit dem Trittschallpegel bei Anregung mit dem Hammerwerk überein, da die Anregungsspektren beide Male verschieden sind.

Wenn dies so ist, sollte die Differenz der Kurven des Trittschallpegels, einmal gemessen mit dem Hammerwerk, das andere Mal mit sinusförmiger Anregung mit dem Magneten und auf Oktavbandbreite bezogen, das Anregungsspektrum des Hammerwerkes darstellen. Diese Differenz ist als ausgezogene Kurve in Abb. 12 dargestellt und wird zur Bestätigung, daß keine weiteren Einflüsse von wesentlicher Bedeutung da sind, mit dem direkt gemessenen Spektrum verglichen. Letzteres wurde, wie bereits beschrieben, mit einem unter den Hammer auf die Decke gelegten Piezoquarz gemessen. Die Meßwerte sind als Punkte in Abb. 12 eingezeichnet. Man sieht, daß der Frequenzverlauf des Hammerspektrums pro Oktave derselbe ist, wie er aus der Differenz der Trittschallpegel-Kurven gewonnen wurde. Die Streuung der Meßpunkte rührt davon her, daß jeder eingezeichnete Meßpunkt nur einem einzigen Hammerschlag entspricht, während die ausgezogene Kurve aus dem Mittelwert sehr vieler Schläge gewonnen wurde.

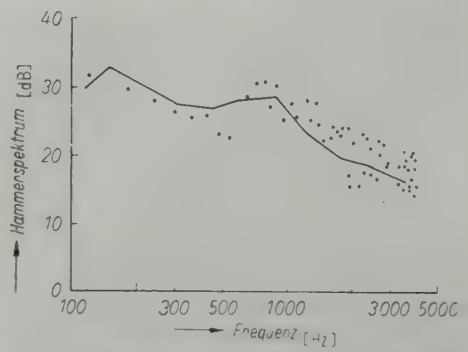

Abb. 12. Das Spektrum des Hammerschlages auf die Decke. Ausgezogene Kurve: Differenz der Trittschallkurven bei Anregung mit Magnetsystem bzw. Hammerwerk; Punkte aus Messung mit untergelegtem Piezoquarz.

5. Messungen auf dem Bau

Die Brauchbarkeit des geschilderten Verfahrens zur Messung des Trittschallpegels bei sinusförmiger Anregung der Decke mit dem Magnetsystem wurde durch Messungen auf dem Bau bestätigt. Zur Verfügung stand eine sogenannte Phönixdeckenkonstruktion, die im wesentlichen aus Stahlbetonrippen besteht, deren Zwischenräume zwischen den Rippen mit Hüttenbims ausgefüllt sind. Das Flächengewicht dieser Konstruktion beträgt 426 kg/m². Es wurden Messungen an zwei gleichen, nur in der Größe verschiedenen Decken ausgeführt: $S_1 = 19{,}6\ m^2$ und $S_2 = 12{,}2\ m^2$. Unter diesen Decken befanden sich Räume von $V_1 = 50{,}7\ m^3$ und $V_2 = 31{,}5\ m^3$ Volumen, deren Nachhallzeiten auf den Abb. 13 und 14 unten eingezeichnet sind. Diese Bilder zeigen außerdem den gemessenen Trittschallpegel (ohne Reduktion auf eine bestimmte Nachhallzeit oder Absorptionsfläche) als ausgezogene Kurven bei Anregung mit dem Hammerwerk und gestrichelt bei Anregung mit dem Magnetsystem, bezogen auf eine anregende Kraft von 10 Newton = 10^6 dyn.

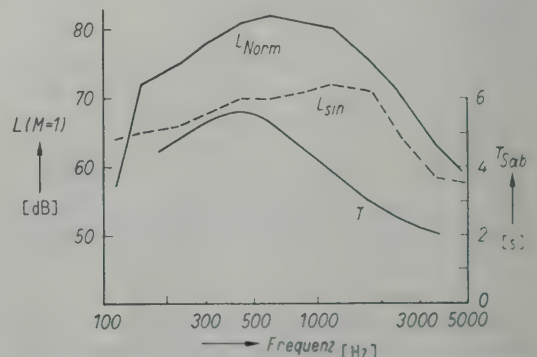

Abb. 13. Messung im Bau: Großes Zimmer. Ausgezogene Kurven: unten Nachhallzeit, oben Trittschallkurve bei Anregung mit Hammerwerk; gestrichelt bei sinusförmiger Anregung.

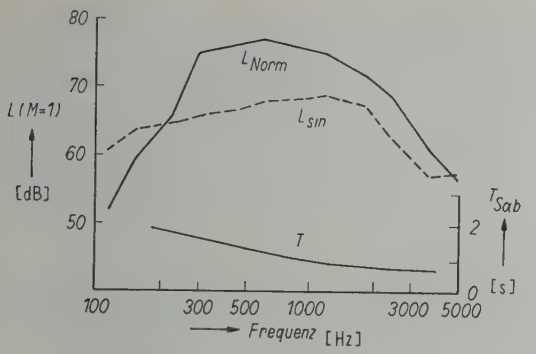

Abb. 14. Messungen im Bau: Kleines Zimmer. Ausgezogene Kurven: unten Nachhallzeit, oben Trittschallkurve bei Anregung mit Hammerwerk; gestrichelt bei sinusförmiger Anregung.

Die Messung erfolgte mit einem Anregungsstrom von 2 A, durch die Schwingspule des Magneten, entsprechend einer Kraft von 24,2 Newton, so daß der empfangene Pegel durchweg über demjenigen lag, der mit dem Hammerwerk gewonnen wurde. Dies ist von Bedeutung für den Störabstand (d.i. die Differenz von Nutz- und Störpegel), der möglichst groß sein soll.

Über die Abhängigkeit der Trittschalldämmung von der Größe der Prüfdecke ist bisher wenig bekannt. In theoretischen Betrachtungen wurden teils [6] der mathematischen Einfachheit halber ebene Wellen, teils [5], [7] Zylinderwellen angenommen. Experimentell wurde die auf einer Decke herrschende Wellenform ermittelt, indem die Decke mit dem Magnetsystem zu Schwingungen von $3 \pm 0{,}15$ kHz angeregt wurde. Die Amplitude wurde in Abhängigkeit von der Entfernung vom Sender mittels eines piezoelektrischen Beschleunigungsmessers [8] abgetastet. Der Sender stand in der Mitte des Zimmers. (Bei Anregung in der Nähe des Randes wird die Streuung der Meßpunkte noch größer.) Um beurteilen zu können, mit welcher Potenz vom Abstand r die Amplitude abnimmt, ist die Amplitudenverteilung in Abb. 15 doppelt logarithmisch dargestellt. Die eingezeichnete Gerade entspricht einer Abnahme mit $r^{-1/2}$, wie sie für Zylinderwellen gilt, und paßt recht gut zu den Meßpunkten. (Es handelt sich um Messungen in einem Neubau auf der oben beschriebenen Phönix-Decke.)

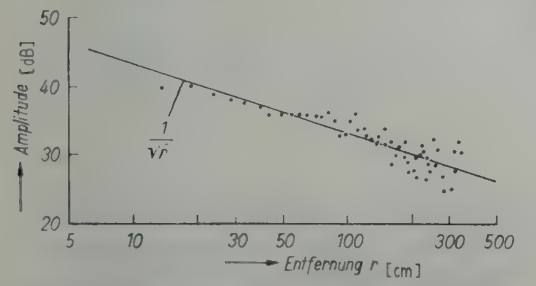

Abb. 15. Die Amplitudenverteilung auf der Deckendiagonalen bei Anregung in der Mitte (0 cm) mit $3 \pm 0{,}15$ kHz.

6. Diskussion

Bei der Messung der Trittschalldämmung mit sinusförmiger Anregung handelt es sich um eine physikalisch durchsichtige Methode zur Prüfung der Eigenschaften von Decken. Sie unterscheidet sich von der üblichen Messung mit einem genormten Hammerwerk wesentlich durch die Benutzung eins konstanten (oder doch wenigstens bekannten) Anregungsspektrums.

Weitere Vorteile der stationären Anregung sind: 1. ein großer Störpegelabstand; 2. die Möglichkeit, die gleichen Apparate benutzen zu können, welche zur Messung der Luftschalldämmung gebraucht werden (nur tritt an die Stelle des Lautsprechers ein Körperschallsender, der übrigens einem Lautsprecher ähnlich konstruiert werden kann); 3. die Möglichkeit der automatischen Registrierung der Meßergebnisse, wie sie bei der Messung der Luftschalldämmung vielfach üblich ist; 4. die Definition einer echten Isolation für den Trittschall. Diese Dämmung müßte die Form besitzen (wieder in der Schreibweise von Kosten u. a. [9]):

$$D\,(M = S/A) = 20 \log \frac{K}{S_0 p} + 10 \log S/A.$$

Hierin bedeuten S die Deckenfläche, K die auf die Decke an einer Stelle ausgeübte Wechselkraft und p den Schalldruck im Empfangsraum mit der gesamten Absorptionsfläche A. Entweder setzt man für S_0 die Fläche S der untersuchten Decke ein. Dann betrachtet man den Mittelwert des anregenden Druckes über die ganze Deckenfläche, während dieser Druck in Wirklichkeit nur auf einer sehr kleinen Anregungsfläche wirksam ist. Oder man setzt für S_0 einen konstanten Bezugswert ein, wie es oben in den Abschnitten 4 und 5 geschehen ist. In beiden Fällen erhält man als Dämmzahl Werte, welche imstande sind, die Trittschalldämmung einer Baukonstruktion zu charakterisieren. Diese Werte sind abhängig von der Frequenz, von den elastischen Eigenschaften der Decke (E-Modul, Biegesteifigkeit, innere Schwingungsdämpfung), ihrer Masse, Dicke, Einspannung am Rande und von ihrer Größe.

Ich danke Herrn Prof. Dr. Erwin Meyer für die Anregung zu dieser Arbeit, sein förderndes Interesse daran und viele wertvolle Ratschläge.

Für die Durchführung der Aufgabe stellte das Bundesministerium für Wohnungsbau die Mittel zur Verfügung.

(Eingegangen am 24. April 1952.)

Schrifttum

[1] DIN 4110, in Zukunft ersetzt durch DIN 52210.

[2] Règles générales applicables, dans des laboratoires et dans la pratique courante, à la mesure de la transmission des sons aériens et des bruits de choc. Edité par le Groupement des Acousticiens de Langue Française, Marseille, April 1951.

[3] Kuhl, W. und Kaiser, H., Geschwindigkeit und Dämpfung von Körperschall in Baumaterialien. Acustica **2** [1952], 179—188.

[4] Tamm, K. und Pritsching, I., Ein Frequenzanalysator mit mechanischem Hochtonfilter. Acustica, Beiheft 1 [1951], AB 43—AB 48.

[5] Cremer, H. und L., Theorie der Entstehung des Klopfschalles. Frequenz **2** [1948], 61.

[6] Brillouin, J., Problèmes de rayonnement en acoustique du bâtiment. Acustica **2** [1952], 65—76.

[7] Cremer, L., Theorie des Klopfschalles bei Decken mit schwimmendem Estrich. Acustica **2** [1952], 167—178.

[8] Meyer, E., Parkin, P. H., Oberst, H. and Purkis, H. J., A tentative method for the measurement of indirect sound transmission in buildings. Acustica **1** [1951], 17—28.

[9] Kosten, C. W., v. d. Eijk, J., Kasteleyn, M. J., van Os, G. J. and de Lange, P. A., Symbols and nomenclature in sound insulation. Acustica **1** [1951], 78—80.

THE ACCEPTABILITY OF SPEECH AND MUSIC WITH A SINGLE ARTIFICIAL ECHO

by R. W. Muncey, A. F. B. Nickson and P. Dubout

Division of Building Research, Commonwealth Scientific and Industrial Research Organization, Australia

Summary

Groups of subjects seated in a room of 0.15 seconds reverberation time assessed whether or not a single artificial echo, added to speech or music previously heard with little or no echo, was disturbing. The artificial echo varied in intensity level from equal to the direct sound to —40 dB and in delay from 30 to 1000 milliseconds. The results obtained for speech differ from those of Haas owing to the different reverberation time. An acceptable-echo-level/delay criterion deduced from the results is shown to be in agreement with pulse work in motion picture theatres.

Sommaire

On a demandé à des groupes de sujets assis dans une salle ayant un temps de réverbération de 0,15 seconde, d'estimer si un écho artificiel simple ajouté à de la parole ou de la musique écoutée auparavant sans écho ou avec un faible écho, gênait ou non l'audition. On a fait varier l'intensité de l'écho artificiel entre l'intensité du son direct et 40 décibels au-dessous de cette intensité, et le retard de l'écho de 30 à 1000 millisecondes. Les résultats obtenus par la parole sont différents des résultats de Haas, car le temps de réverbération n'est pas le même dans les deux cas. On déduit des résultats une valeur acceptable du rapport niveau/retard de l'écho, et on montre qu'elle est en bon accord avec les résultats des essais effectués avec des impulsions dans des cinémas.

Zusammenfassung

Gruppen von Versuchspersonen, die in einem Raum mit einer Nachhallzeit von 0,15 Sekunden saßen, ermittelten, ob ein Einfachecho, das zu Sprache oder Musik hinzugefügt wurde, die vorher mit wenig oder keinem Echo gehört wurde, störend war oder nicht.

Das künstliche Echo wurde in der Schallstärke im Vergleich zum direkten Schall von 0···—40 dB und in der Verzögerungszeit von 30···1000 Millisekunden variiert.

Die Ergebnisse für Sprache unterscheiden sich von denen von Haas wegen der unterschiedlichen Nachhallzeit.

Ein angemessenes Kriterium für das Verhältnis Echointensität zu Verzögerungszeit, das aus den Ergebnissen abgeleitet wurde, ist, wie gezeigt wird, in Übereinstimmung mit Impulsmessungen in Filmtheatern.

1. Introduction

Sounds as heard inside a building consist of an initial direct sound followed by a succession of echoes of varying intensity and delay. Haas [1], [2] measured the intelligibility of speech when the initial sound was followed by one artificial echo and found that for each echo intensity level there occurred a "critical delay difference" at which 50 per cent of his listeners could hear a disturbing echo. The major part of his listening tests were done in a room of 0.8 s reverberation time. An increase in the delay caused an increase in the

number who found the echo disturbing. He found that the critical delay difference was inversely proportional to the number of syllables per second, was increased by decreasing the echo intensity level, was independent of the direction from which the echo came and was increased by an increase in reverberation time.

These results have been used and extrapolated by BOLT and DOAK [3] to provide a tentative criterion for the short-term (0 – 400 ms) transient response of an auditorium for speech. Since there is a good deal of interest also in concert halls it was decided to continue the pioneering work of HAAS into the field of musical sounds and to check how this would affect the BOLT and DOAK criterion.

2. Equipment

The equipment has been designed to enable artificial echoes to be generated by the method used by HAAS, i.e. by recording on a magnetic tape and varying the distance between record and replay heads to obtain the required delays. Since multiple artificial echoes are to be investigated later it was desirable to arrange a succession of replay heads. To obtain small variations in the echo time a tape speed of 1.5 m/s has been adopted and the distance between replay heads is continuously variable to give delays from 22 to 1000 ms. The physical size of the heads is such that delays must be spaced at least 22 ms apart. The erase and the record amplifiers of an E.M.I. type B.T.R.I. tape recorder are used to record the signal on the tape, E.M.I. heads are used for replay and laboratory-made preamplifiers feed the control panel and thence Williamson amplifiers and Australian Rola type 12-OX loudspeakers mounted in vented enclosures. The overall performance of the equipment from 60 to 8000 c/s can be considered adequate. The general layout is shown in Fig. 1.

It was decided early in the work that a definite portion of music or speech should be repeated so that observers became familiar with it and could then make more rapid and consistent judgments. It is possible that by this a systematic error is introduced since a particular phrase may contain a critical combination, but this does not seem likely because the results obtained follow a definite and reasonable pattern. In the tests to be discussed an excerpt of fourteen seconds duration was repeated for each type of sound, of which there were six: slow and fast speech, slow and fast string music and slow and fast organ music.

Each was recorded with a minimum of echoes. Speech was recorded standing close to a directional microphone in the room used for the listening tests, string music was recorded from a quartette ensemble playing out of doors and organ music was obtained with a directional microphone placed close to one speaker of a Compton

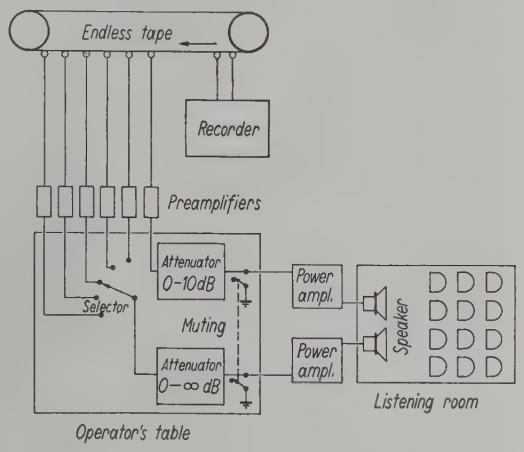

Fig. 1. General layout.

electronic organ. The tempo for the music can best be judged from the melodies given in Fig. 2, each melody taking fourteen seconds. The excerpts of speech were:—slow (about 2½ syllables per second): . . . "two light chairs had been overturned, books and papers from the desk strewed the floor. The grandfather clock which should have stood sentinel on the left as one entered, had fallen" . . . and fast (about 5 syllables per second): . . . "but for Henry Wilson, even though

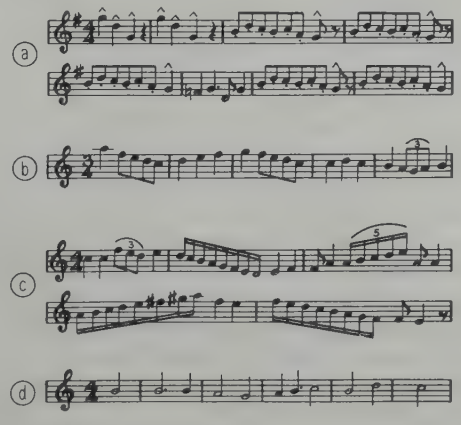

Fig. 2. Melodies of music used:
(a) string music—fast tempo,
(b) string music—slow tempo,
(c) organ music—fast tempo,
(d) organ music—slow tempo.

he had only just brought to the conclusion his most spectacular case, it was hardly likely that a single village eye would be batted for his arrival. Unless indeed a crime were to occur, but Michael had yet to see a place which less suggested crime" . . .

3. Technique

The subjects at each session were seated close together in a room $6 \times 4 \times 3$ m^3 and the sound and the echo were supplied from two loudspeakers placed side by side. It is considered that HAAS has satisfactorily demonstrated that the result with two such sources will be comparable with that for the arrival of the echo from any other direction. (For this test HAAS was working out of doors.) The actual intensity level of the sound and its echo will of course vary slightly from seat to seat but this variation was shown to be less than 2 dB and variability thereby introduced will be far less than the variation of judgment of the observers. The subjects were asked in each test to decide whether they were disturbed by the echo (perceptible non-disturbing echoes were to be rated not-disturbed) and to record their judgment by moving a switch. Electrical means were used to obtain the total number recording 'disturbed' and this was displayed as a meter reading at the operator's bench and recorded by him. Two separate teams were used as observers. The first team comprised the eight persons of the acoustics (and allied) group of the Division. Thirty persons taken from the remainder of the staff of the Division formed the second team from which twenty subjects were selected at random before any session. It was considered that a comparison of the results of the two groups would check that the learning period was about two sessions only and that more experienced subjects would not give a different result in the manner reported by HOPKINSON [4] for glare experiments.

At any one session, about eighteen repetitions of a particular sound type were presented with various combinations of echo delay and level in a randomised order. This was repeated for three other sound types, again in a randomised order. The change of echo was made with the sound muted and the new combination presented by opening the shorting switch. The total sound level was arranged to be of constant intensity, i.e. it was assumed after HAAS that the ear added the sound levels incoherently.

The sounds were presented at a level of 80 dB (peak) above 0.0002 dyne/cm^2 being that desired by the subjects for comfortable listening. Noise level in the room was about 35 dB. The subjects

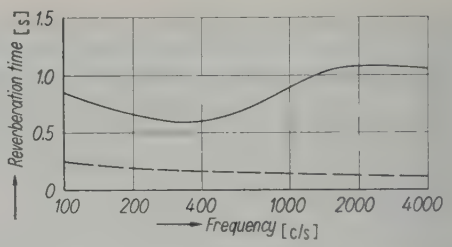

Fig. 3. Reverberation time/frequency characteristics of listening rooms;
——————— reverberant room,
– – – – – – – non-reverberant room.

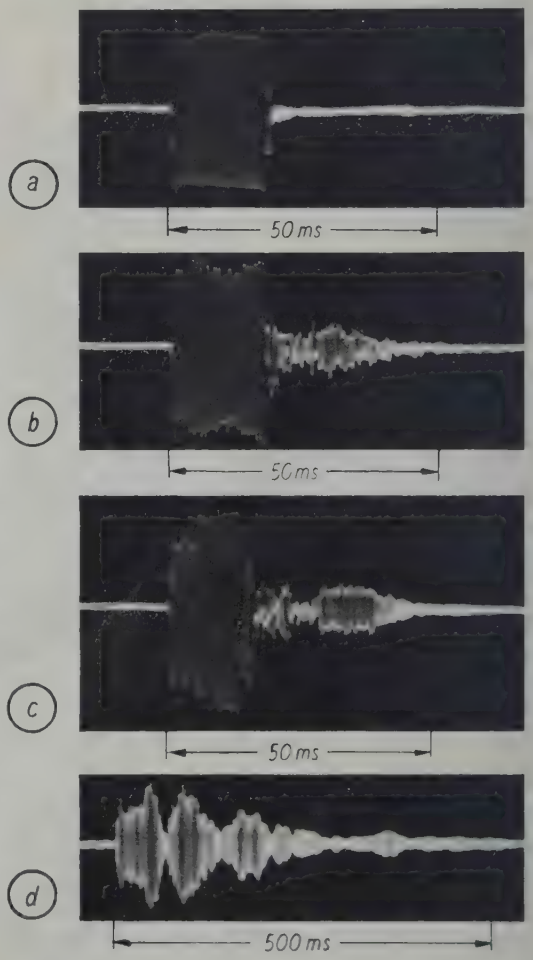

Fig. 4. Response of listening rooms to 20 ms pulses of sound.
(a) Non-reverberant room, microphone near loudspeaker;
(b) non-reverberant room, microphone near centre of room;
(c) non-reverberant room, microphone near rear wall;
(d) reverberant room, microphone near centre of room.

were asked to record their votes during the period of silence between repetitions; voting during presentation of a combination was discouraged. Sessions were limited to 30 min to avoid fatigue effects.

Finally, as a check on the difference between the results of this experiment and those of HAAS, some experiments were made with a similar technique in a room about $7 \times 5 \times 3$ m³ and of about 1.0 s reverberation time.

two groups gave the same answer except that in the group of 20 a percentage of listeners was disturbed by sound with no echoes whereas the group of 8 voted not disturbed. For the fast sound types the same information is plotted in Fig. 7a···c in the form used by BOLT and DOAK giving varying relations between echo intensity level and delays for 20, 50 and 80 per cent of subjects hearing a disturbing echo. It is considered that results for 20 and 80 per cent can be more accurately

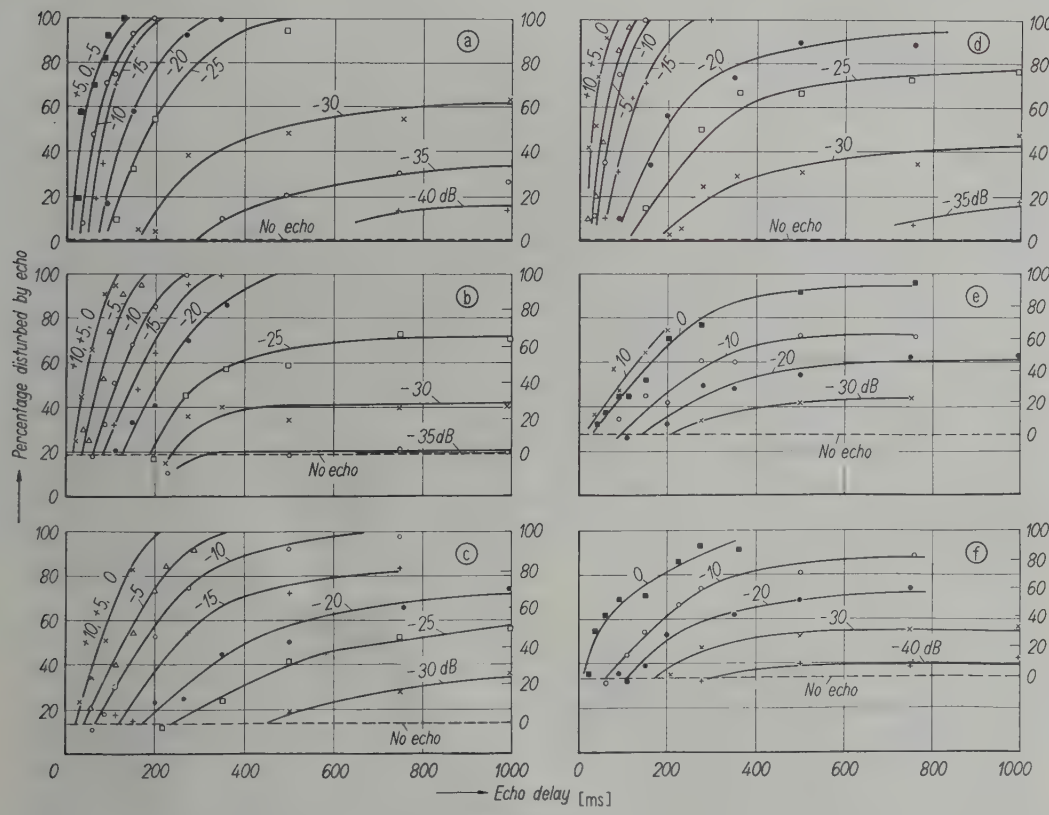

Fig. 5. Percentages of listeners disturbed by single echoes of various sound types (non-reverberant room);
(a) speech—fast tempo,
(b) string music—fast tempo,
(c) organ music—fast tempo,
(d) speech—slow tempo,
(e) string music—slow tempo,
(f) organ music—slow tempo.

4. Results

Reverberation-time/frequency curves for the two rooms used in the experiments are given in Fig. 3; pulse pictures obtained in the two rooms are reproduced in Fig. 4.

The percentage of subjects registering a disturbing echo is plotted as a function of echo delay and echo intensity level for the various types of sound in Fig. 5a···f for the non-reverberant room and in Fig. 6a···c for the reverberant room. The

assessed than those for 10 and 90, as used by BOLT and DOAK.

Each echo combination was presented at least four times except when a reading of all subjects disturbed was obtained at the first two or three presentations (further presentation was then considered unnecessary). There was still a good deal of variation but with four repetitions the 95 per cent fiducial limits were about ± 10 per cent. This is adequate since factors like type of listener and tempo of the sound will undoubtedly intro-

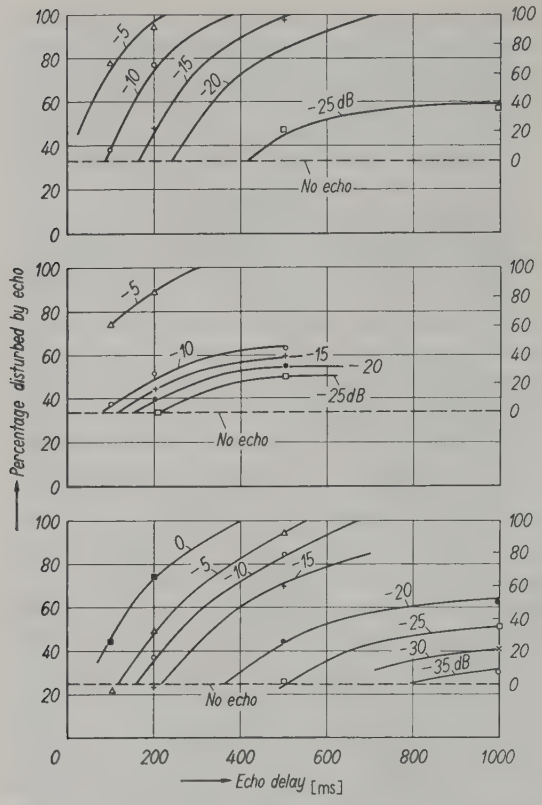

Fig. 6. Percentages of listeners disturbed by single echoes of various sound types (reverberant room);
(a) speech—fast tempo,
(b) string music—fast tempo,
(c) organ music—fast tempo.

the speech or music is slow and, as might be expected from reverberation-time criteria, increasing echoes are tolerated as one moves along the range from speech to string and to organ music. Since obviously one does not design a hall for slow music or speech only, work was concentrated on fast speech and music and most of the discussion is limited to that.

Throughout all tests the sound was occasionally presented without echo. For speech in the non-reverberant room, subjects generally recorded not-disturbed, the average being about two per cent disturbed. For speech in the reverberant room and for music in both rooms a significant number still recorded a disturbing echo. The reverberation undoubtedly contributed but the psychological factor mentioned by HAAS is likely to be a prime factor, particularly for music: "the observer thought that almost always an echo was transmitted and he endeavoured therefore to avoid the blame of being inattentive"—(EHRENBERG's translation). Possibly also for music the ear is used to echoes and therefore prefers them, so that lack of echoes gives an unusual effect rated by some as disturbing. Subjects complained of the difficulty of detecting echoes, particularly with the slow organ music and the percentage disturbed when no echo is added is a rough measure of the difficulty of detecting echoes. It seems reasonable then to treat the percentage disturbed with no echo, obtained from the group of 20, as the line of zero disturbance (since in a hall people

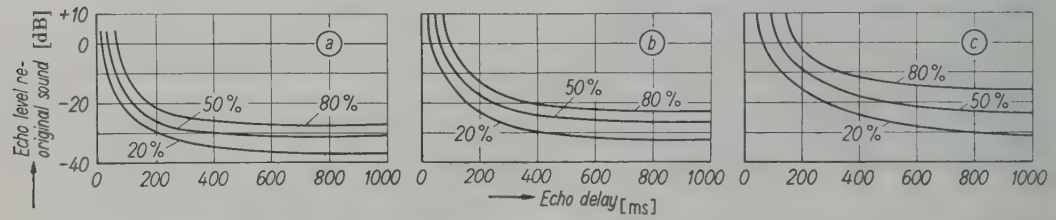

Fig. 7. Acceptable echoes for various percentages of listeners disturbed (non-reverberant room);
(a) speech—fast tempo, (b) string music—fast tempo, (c) organ music—fast tempo.

duce errors equally large. The various average curves as drawn are a reasonable mean and fall inside the fiducial limits.

5. Discussion

The acceptability of an echo added to a sound originally without echo varies with its intensity and delay and with the type of sound and its tempo. An increase in intensity level or delay tends to decrease the acceptability. Louder echoes can be added without listener-disturbance when are less conscious of and are not actually expecting echoes) and to rate percentages on this basis. This has been done on the right-hand scale in Fig. 5 and 6 and these percentages are used in Fig. 7.

The results do not agree exactly with HAAS' claims of the acceptability of short-delay echoes of the order of + 10 dB although + 10 dB echoes are almost as acceptable as those of the + 5, 0 and − 5 dB values. This is probably partly due to the psychological factor mentioned earlier coupled

with subtle changes in the reproduction quality. However from the work of PARKIN and his associates [5], [6] it is quite obvious that sound reinforcement of the order of +10 dB will pass unnoticed when the audience is unconscious of its use. When a speech reinforcement system is in use the optical sense is of importance since this sense will demand that the source is other than the reinforcement speaker and may well explain a 10 dB difference in effect.

HAAS' results concerning the echo disturbance as a function of a given delay and intensity show less disturbance than do those obtained in the non-reverberant room. The lower reverberation is the obvious reason for this fact. HAAS noticed that a decrease in reverberation time decreased his "critical delay time" for echoes of intensity level equal to the original sound. The effect is far more spectacular however for echoes of the order of −10 dB. Check measurements made in a room of reverberation time about one second gave results comparable with those of HAAS. It seems likely that in such a room the echoes from the bounding surfaces are louder than the added echo and being more natural are acceptable.

The new measurements require for speech a more stringent criterion than that previously proposed. P. H. PARKIN of the Building Research Station, Great Britain has informed the authors that the BOLT and DOAK criterion agrees with subjective results at the Shakespeare Memorial Theatre, Stratford-on-Avon. On the other hand there is a striking resemblance between these measurements and the criterion derived from subjective impressions and pulse testing in motion picture theatres and set up recently by MOIR [7] at a meeting of the Society of Motion Picture and Television Engineers. He claims that echoes more than 100 ms after the direct sound should have an intensity level at least 20 dB below the direct sound. This compares extremely well with the derived criterion for speech (Fig. 7a); MOIR would be mainly interested in speech because as A. W. COLLEDGE said at the same meeting "about 80 or 90 per cent of all sound coming out of Hollywood is speech". It appears likely to the present authors that the differing requirements of a motion picture theatre and a live theatre lead to different design criteria. With motion picture theatres where the amplifier gain can be increased to provide an adequate listening level disturbing echoes need not be tolerated. In a live theatre the audience demands an adequate listening level even although this may entail the use of definite echoes.

Finally it should be pointed out that it is fairly certain that a still lower reverberation time in the listening room would not change the acceptability of the echoes since, assuming the sound to decay exponentially, the echoes from the room will be far below the tolerable limit for artificial echoes. Experiments out of doors by the authors gave results similar to those reported here. On the basis of results reported above there is a possibility that echoes of −35 and −40 dB are tolerable at any delay merely because they approach the noise level; however actual listening showed that inputs of −50 dB were not completely masked by noise and hence it must be assumed that the −35 and −40 dB results shown in Fig. 5 can be accepted as substantially correct.

6. Conclusions

Speech with a single artificial echo presented in a non-reverberant room disturbed listeners at intensity levels well below those reported by HAAS. This is due to the lack of room echoes here whereas they were present in earlier experiments. Louder echoes are acceptable with music than with speech. An acceptable-echo-level/delay criterion deduced from the results is in good agreement with a criterion developed from pulse test work in motion picture theatres where numerous echoes to obtain satisfactory listening intensity are not required. Similar criteria derived for string and organ music allow louder and longer delayed echoes and this is in agreement with previous criteria of longer reverberation times for music.

Acknowledgment

The authors desire to acknowledge the assistance of Dr. PERCY JONES of the Conservatorium of Music, University of Melbourne, who made arrangements for the music used in this study.

(Received 18th November, 1952.)

References

[1] HAAS, H., The influence of a single echo on the audibility of speech. (Transl. K. P. R. EHRENBERG). Building Research Station (Great Britain), Library Communication No. 363 (1949).

[2] HAAS, H., Über den Einfluß eines Einfachechos auf die Hörsamkeit von Sprache. Acustica **1** [1951], 49–58.

[3] BOLT, R. H. and DOAK, P. E., Tentative criterion for the short-term transient response of auditoriums. J. acoust. Soc. Amer. **22** [1950], 507–508.

[4] HOPKINSON, R. G., Influence of experience on the sensitivity to discomfort. Nature **169** [1952], 40.

[5] PARKIN, P. H. and SCHOLES, W. E., Recent developments in speech reinforcement systems. Wirel. World **57** [1951], 44–50.

[6] PARKIN, P. H. and TAYLOR, J. H., Speech reinforcement in St. Paul's Cathedral. Wirel. World **58** [1952], 54–57, 109–111.

[7] MOIR, S., Pulse methods in acoustic analysis of rooms. J. Soc. Mot. Pict. Televis. Engrs. **57** [1951], 147–155.

THE EFFECT OF WALL SHAPE ON THE DECAY OF SOUND IN AN ENCLOSURE

by J. W. HEAD

British Broadcasting Corporation, Research Department, London

Summary

A two-dimensional room is considered in which three of the "walls" are straight and the fourth has small, regularly spaced symmetrical projections. The method of FESHBACH [1] is applied to determine the effect of the projections on the natural frequencies and normal modes of the room; explicit formulae are obtained for rectangular, circular and triangular projections.

Recent experimental results obtained by the B.B.C. Research Department [2] suggest that studios or halls with rectangular coffering may have superior subjective properties to those having other types of projection with comparable dimensions. The results here given appear to provide a theoretical reason for this superiority of rectangular coffering.

Résumé

On considère une salle à deux dimensions dont trois des «parois» sont uniformes tandis que la quatrième porte de petites saillies symétriques à espacements réguliers.

On utilise la méthode de FESHBACH [1] pour déterminer l'effet des saillies sur les fréquences propres et les modes normaux de la salle. On donne des formules explicites ayant trait aux saillies en forme de rectangle, de cercle et de triangle.

Des expériences récentes de la B.B.C. Research Department [2] semblent montrer que les salles et studios avec saillies rectangulaires sont meilleures à un point de vue subjectif que celles où les saillies ont d'autres formes, à dimensions comparables.

La présente étude semble donner une raison théorique pour l'avantage des saillies rectangulaires.

Zusammenfassung

Es wird ein zweidimensionaler Raum behandelt, in dem drei der „Wände" glatt sind, während die vierte Wand kleine, regelmäßig angeordnete symmetrische Vorsprünge besitzt. Mit Hilfe der Methode von FESHBACH [1] wird der Einfluß dieser Vorsprünge auf die Eigenfrequenzen und Eigenfunktionen des Raumes bestimmt. Formeln werden für rechteckige, runde und dreieckige Körper abgeleitet.

Die Ergebnisse von Versuchen, die neulich vom B.B.C. Research Department ausgeführt worden sind, weisen darauf hin, daß Aufnahmeräume oder -säle, deren Wände mit rechteckigen Platten ausgekleidet sind, nach subjektiver Wertung den Räumen akustisch überlegen sein dürften, in denen Körper mit vergleichbaren Abmessungen, aber anderer Form, verwendet werden. Die hier angeführten Ergebnisse scheinen die Überlegenheit rechteckiger Platten theoretisch zu begründen.

1. Introduction

The main problem of practical acoustics can be briefly stated—to find a way of designing or adapting studios or concert halls so that they shall be regarded as "good" by speakers, musicians or listeners who have to use them. Although such people may have an immediate subjective appreciation of the qualities of a particular studio or concert hall, it is very difficult satisfactorily to correlate this with any objective quantity under the control of the designer. Recent experimental results obtained by the British Broadcasting Corporation Research Department [2] suggest that rectangular coffering may be more efficient as an agent for improving the subjective quality of studios and halls than other departures from a smooth wall shape having comparable dimensions. As circular cylinders and spheres are widely used in the hope of improving quality, it was considered advisable to investigate whether there was any theoretical reason for this apparent superiority of rectangular coffering.

The mathematical formulation of the problem in the general case in a practically useful way is difficult. We have therefore confined our attention to the case of a nearly-rectangular two-dimensional room in which three of the walls are straight and the fourth has $(n+1)$ small symmetrical projections on base d and having a maximum depth h_1 as in Fig. 1. Each projection is separated from its neighbour by a straight segment of length d, so that the total length a of the wall with projections is $(2n+1)d$; Fig. 1 is drawn with $n=3$, h_1, d are regarded as small

compared with a or b, but may have any relation to the wavelength. FESHBACH [1] derives formulae for the eigenfrequencies and normal modes associated with a boundary having irregularities; we have considered only the case in which the eigenfrequencies are in general distinct. These

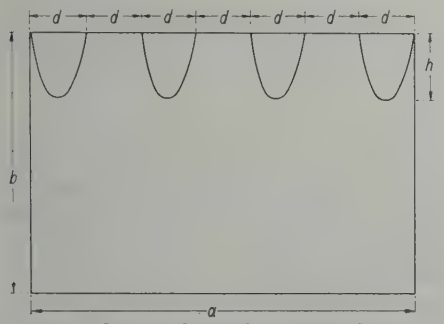

Fig. 1. General shape of room considered.

formulae are briefly explained and applied to our problem in Section 2. The formulae are perfectly general and could theoretically be applied to any shape of projection and to unequal projections unequally spaced. We have considered in detail only three types of projection, namely rectangles, circles and triangles; in each case we have taken the maximum depth h_1 to have the same value $d/2$. Explicit results are obtained in these three cases; they are given in Section 3. Results are discussed in Section 4, their subjective significance in Section 5, and conclusions summarized in Section 6. The Appendix, relevant to Section 5, discusses the general nature of the decay curves associated with one, two, or several significant eigentones.

2. FESHBACH's formulae

The differential equation to be satisfied by the sound potential φ from which pressure and velocity are derived is

$$\nabla^2\varphi = (1/c^2)(\partial^2\varphi/\partial t^2) \qquad (1)$$

with the boundary condition

$$\partial\varphi/\partial n = 0 \qquad (2)$$

at all points of the boundary, n being the outward normal. We thus assume that all boundary surfaces are hard.

When there are no projections, there are a number of eigenfrequencies $\omega/2\pi$ satisfying

$$\omega^2/c^2 = (p^2\pi^2/a^2) + (q^2\pi^2/b^2) \qquad (3)$$

where c is the velocity of sound, and p, q are integers. We regard these eigenfrequencies as in general distinct. With each eigenfrequency is associated a potential

$$\varphi = A\cos(p\pi x/a)\cos(q\pi y/b) \qquad (4)$$

if the axes are taken along two of the straight walls and the origin at their intersection.

We shall denote by $\omega_k/2\pi$ and $\omega_t/2\pi$ two typical eigenfrequencies; the corresponding integers in (3) will be called p_k, q_k and p_t, q_t respectively and the corresponding φ and A in (4) will be called φ_k, A_k and φ_t, A_t respectively. If

$$\begin{aligned} A^2 &= 4/ab \quad (p,\ q \text{ both different from zero}) \\ A^2 &= 2/ab \quad (\text{one of } p,\ q \text{ zero}) \end{aligned} \qquad (5)$$

the potentials φ form an orthonormal set satisfying (1) in the area of the room without projections. This condition of orthonormality is required for the derivation of FESHBACH's formulae (6), (7), (8) and (9) below.

Let R denote the region inside the room with projections, and let S denote the boundary obtained by going round the room anticlockwise and following the curved surface of the projections. Then we define

$$A_{kt} = \int \varphi_k(\partial\varphi_t/\partial n)\,\mathrm{d}S, \quad N_{tt} = \int \varphi_t^2\,\mathrm{d}R. \qquad (6)\ (7)$$

For the room with projections, the eigenfrequency $\Omega_t/2\pi$ corresponding to $\omega_t/2\pi$ is given by FESHBACH [1] as

$$\Omega_t^2 = \omega_t^2 + (c^2 A_{tt}/N_{tt}) + c^4 \sum_k{}' A_{kt}^2/(\omega_t^2 - \omega_k^2) \qquad (8)$$

the symbol Σ' meaning that the term with $k = t$ is omitted. The associated potential function is

$$\Phi_t = \Psi_t + c^2 \sum_k{}' A_{kt}\varphi_k/(\omega_t^2 - \omega_k^2) \qquad (9)$$

where Ψ_t equals φ_t inside S and changes discontinuously to zero on S.

Hence the extent to which Ω_t, Φ_t differ from ω_t, Ψ_t (which are the corresponding quantities when there are no projections) depends upon the coefficients A_{kt}.

We shall see that in the cases for which we obtain A_{kt} explicitly, it is an oscillating function of k for a given t; the highest values of $|A_{kt}|$ obtainable for the various types of projection appear to be of the same order of magnitude, but in determining their effect on (8) and (9) we have to consider not only the magnitude of $|A_{kt}|$ but also of the denominator $(\omega_t^2 - \omega_k^2)$ likely to be associated with it. An individual A_{kt} may acquire unusual importance if associated with an abnormally small value of $(\omega_t^2 - \omega_k^2)$. We shall confine our attention to the broad, general behaviour of three different types of projection for which (6) and (7) can be obtained explicitly, and take little notice of isolated abnormal cases.

3. Explicit results for rectangular, circular and triangular projections

For any type of projection, we obtain A_{kt}, A_{tt} from (6) and N_{tt} from (7). If θ is the angle between the outward normal to the projection and the negative x-axis, we thus obtain

$$A_{kt} = -\sum_{r=0}^{n} A_t A_k \int_{C_r} \cos(p_k \pi x/a) \cos(q_k \pi y/b) \cdot \cdot [(p_t \pi/a) \cos\theta \sin(p_t \pi x/a) \cos(q_t \pi y/b) + (q_t \pi/b) \sin\theta \cos(p_t \pi x/a) \sin(q_t \pi y/b)] \, dS \quad (10)$$

where dS is an element of the circumference C_r of the $(r+1)$th projection, directed so that S increases with x at all points where the tangent to C_r is not parallel to the y-axis. This reduces to

$$A_{kt} = (A_t A_k p_t \pi/4a) \cdot \cdot [\varphi(p_t + p_k;\ q_t + q_k) + \varphi(p_t + p_k; q_t - q_k) + \varphi(p_t - p_k; q_t + q_k) + \varphi(p_t - p_k; q_t - q_k)] + + (A_t A_k q_t \pi/4b) \cdot \cdot [\psi(p_t + p_k; q_t + q_k) + \psi(p_t + p_k; q_t - q_k) + \psi(p_t - p_k; q_t + q_k) + \psi(p_t - p_k; q_t - q_k)] \quad (11)$$

where

$$\varphi(\alpha,\beta) = -\sum_{r=0}^{n} \int_{C_r} \sin(\alpha \pi x/a) \cos(\beta \pi y/b) \cos\theta \, dS, \quad (12)$$

$$\psi(\alpha,\beta) = -\sum_{r=0}^{n} \int_{C_r} \cos(\alpha \pi x/a) \sin(\beta \pi y/b) \sin\theta \, dS;$$

α, β being integers.

The corresponding result for N_{tt} is

$$N_{tt} = A_t^2 \int_0^a \cos^2(p_t \pi x/a)\, dx \int_0^b \cos^2(q_t \pi y/b)\, dy - - A_t^2 \sum_{r=0}^{n} \int_{2rd}^{(2r+1)d} \cos^2(p_t \pi x/a)\, dx \int_g^b \cos^2(q_t \pi y/b)\, dy \quad (13a)$$

where $g = b - f(x - 2rd)$, and $f(x-2rd)$ is the depth of the projection at a distance d along it. The first integral reduces to 1 in all cases. In the $(r+1)$th term of the second we put $x = (2r+\sigma)d$ and obtain

$$N_{tt} = 1 - \frac{1}{4} A_t^2 d \cdot \cdot \int_0^1 \{f(\sigma d) + (b/2q_t\pi) \sin[(2q_t \pi/b) f(\sigma d)]\} \cdot \cdot \{(n+1) + \sum_{r=0}^{n} \cos[(2r+\sigma)(2p_t \pi d/a)]\} d\sigma = 1 - A_t^2 \chi(p_t, q_t), \text{ say,} \quad (13b)$$

$$(14)$$

where $f(x-2rd) = f(\sigma d)$ is the depth of the projection at a distance d along it.

If $f(\sigma d)$ is continuous and differentiable in the whole range $0 \leqq \sigma \leqq 1$, and $f'(\sigma d)$ is always finite, then it follows that

$$a\beta\varphi(\alpha,\beta) = b\alpha\psi(\alpha,\beta). \quad (15)$$

For since θ is the angle between the outward normal to the projection and the negative direction of the axis of x,

$$\cos\theta \, dS = -dy, \quad \sin\theta \, dS = dx.$$

If in the $(r+1)$th terms of $\varphi(\alpha,\beta)$ and $\psi(\alpha,\beta)$ we put $x = (2r+\sigma)d$, the former becomes an integral over the range 0 to 1 with respect to σ which can be integrated by parts. The integrated term vanishes at both limits since $f(0) = f(d) = 0$; the residual integral reduces to the $(r+1)$th term of $\psi(\alpha,\beta)$ multiplied by $(b\alpha/a\beta)$; this proves (15). The proof can be extended to the case in which $f'(\sigma d)$ has a finite number of isolated infinities in the range $0 \leqq \sigma \leqq 1$ provided that $f(\sigma d)$ remains continuous and differentiable. This extension covers the case of circular projections, but not that of rectangular projections, where $f(\sigma d)$ is discontinuous for $\sigma = 0$ or 1.

We now have to apply (12), (13) and (14) to the cases of rectangular, circular and triangular projections respectively, with due consideration for modifications required when (i) p_t, p_k, q_t or q_k is zero, (ii) $p_k = p_t$, and (iii) $q_k = q_t$.

In case (i), (11) will be affected because the product $A_t A_k$ will not have its normal value $4/ab$ (see (5)). (12) will not be directly affected unless case (i) is combined with case (ii) or case (iii), which means that $p_t = p_k = 0$ or $q_t = q_k = 0$. Certain terms in the normal evaluation of (13b) will become indeterminate in case (i) and these should be replaced by their limiting values if p_t or q_t is regarded as tending continuously to zero. Likewise, in cases (ii) and (iii), certain terms in the normal evaluation of (12) become indeterminate. The correct value for $\varphi(\alpha,\beta)$ and $\psi(\alpha,\beta)$ can always be obtained in such cases by taking the limit when α or β is regarded as tending continuously to zero. We therefore do not need to consider these special cases further; they do not change the general nature of the results, and explicit formulae will be given only for p_t, p_k, q_t, q_k, $p_t - p_k$ and $q_t - q_k$ different from zero.

(a) Rectangular projections

In this case, in (12),

$\theta = 0 \quad dS = -dy$ for $b \geqq y \geqq b - \frac{1}{2}d$, $x = 2rd$

$\theta = \pi/2$ $dS = dx$ for $2rd \leqq x \leqq (2r+1)d$, $y = b - \frac{1}{2}d$

$\theta = \pi \quad dS = dy \quad$ for $\quad b - \frac{d}{2} \leqq y \leqq b, x = (2r+1)d$

and in (13b),

$$f(x - 2rd) = \tfrac{1}{2}d.$$

Hence

$$\varphi(\alpha,\beta) = \sum_{r=0}^{2n} \int_{b-\frac{1}{2}d}^{b} \sin(\alpha\pi r d/a)\cos(\beta\pi y/b)\,dy \qquad (16)$$
$$= (-1)^{\beta}(b/\beta\pi)\sin(\beta\pi d/2b)\cdot F(\alpha)$$

where

$$F(\alpha) = \sum_{r=0}^{2n+1} \sin(\alpha\pi r d/a) = \sum_{r=0}^{2n+1} \sin[\alpha\pi r/(2n+1)]$$
$$= \cot[\alpha\pi/2(2n+1)] \quad (\alpha \text{ odd}) \qquad (17)$$
$$\text{or } 0 \qquad (\alpha \text{ even}).$$

Also

$$\psi(\alpha,\beta) = -\sum_{r=0}^{n} \int_{2rd}^{(2r+1)d} \cos(\alpha\pi x/a)\cdot$$
$$\cdot(-1)^{\beta}\sin(\beta\pi d/2b)\cdot dx \qquad (18)$$
$$= (-1)^{\beta+1}(2a/\alpha\pi)\,G(\alpha)\sin(\alpha\pi d/2a)\cdot$$
$$\cdot\sin(\beta\pi d/2b)$$

where

$$G(\alpha) = \sum_{r=0}^{n} \cos[(2r+\tfrac{1}{2})\alpha\pi/(2n+1)]$$
$$= 0 \ (\alpha \text{ odd}) \qquad (19)$$
$$\text{or } \tfrac{1}{2}\sec[\alpha\pi/2(2n+1)]$$
$$(\alpha \text{ even, not a multiple of } (2n+1))$$
$$\text{or } (n+1)\cos[\alpha\pi/2(2n+1)]$$
$$(\alpha \text{ a multiple of } 4n+2).$$

Finally,

$$\chi(p_t,q_t) = (d/4)\int_0^1 [(d/2) + (b/2q_t\pi)\sin(q_t\pi d/b)]\cdot$$
$$\cdot\left\{(n+1) + \sum_{r=0}^{n}\cos[2p_t\pi d(2r+\sigma)/a]\right\} d\sigma$$
$$= (1/8)[d + (b/q_t\pi)\sin(q_t\pi d/b)]\cdot \qquad (20)$$
$$\cdot[(n+1)d + (a/p_t\pi)\sin(p_t\pi d/a)\,G(2p_t)].$$

(b) Circular projections

In this case, in (12) we put

$$x = 2rd + \tfrac{1}{2}d(1-\cos\theta),$$
$$y = b - \tfrac{1}{2}d\sin\theta, \qquad (21)$$
$$dS = \tfrac{1}{2}d\cdot d\theta$$

and the resulting integrals can be evaluated with the help of the identities [3]

$$e^{iz\sin\theta} \equiv J_0(z) + 2\sum_{p=1}^{\infty} J_{2p}(z)\cos 2p\theta +$$
$$+ 2i\sum_{p'=1}^{\infty} J_{2p'-1}(z)\sin(2p'-1)\theta,$$
$$J_{\nu+1}(z) + J_{\nu-1}(z) = 2\nu J_{\nu}(z)/z, \qquad (22)$$
$$J_{\nu+1}(z) - J_{\nu-1}(z) = -2J'_{\nu}(z)$$

where the J's are Bessel functions of the first kind, and ν is arbitrary.

Although $\sin(\alpha\pi x/a)$, $\cos(\alpha\pi x/a)$, $\sin(\beta\pi y/b)$ and $\cos(\beta\pi y/b)$ thus give infinite series in sines and cosines of multiples of θ, only a few terms contribute to the integrals (12) transformed by (21). We find

$$a\beta\varphi(\alpha,\beta) = b\alpha\psi(\alpha,\beta) = ab(-1)^{\beta}H(\alpha,\beta) \qquad (23)$$

$$\text{where } H(\alpha,\beta) = 2G(\alpha)\sum_{p=1}^{\infty}(-1)^{p+1}(2p-1)\cdot$$
$$\cdot J_{2p-1}(\alpha\pi d/2a)\,J_{2p-1}(\beta\pi d/2b). \qquad (24)$$

To evaluate $\chi(p_t,q_t)$ in (14), we put

$$\sigma = \tfrac{1}{2}(1-\cos\theta), \quad f(\sigma d) = \tfrac{1}{2}d\sin\theta$$

and obtain

$$\chi(p_t,q_t) = \frac{d}{16}\int_0^{\pi}[d\sin\theta + (b/q_t\pi)\sin(q_t\pi d\sin\theta/b)]\cdot$$
$$\cdot\left\{(n+1) + \sum_{r=0}^{n}\cos[(4r+1)p_t\pi d/a]\cdot\right.$$
$$\left.\cdot\cos(p_t\pi d\cos\theta/a)\right\}\sin\theta\,d\theta$$
$$= \frac{d}{16}[\tfrac{1}{2}(n+1)\pi d + (n+1)(b/q_t)J_1(q_t\pi d/b) +$$
$$+ (a/p_t)J_1(p_t\pi d/a)\,G(2p_t)] +$$
$$+ (ab/8\pi p_t q_t)H(2p_t,2q_t) \qquad (25)$$

(c) Triangular projections

In this case, in (12), for $2rd \leqq x \leqq (2r+\tfrac{1}{2})d$, we write

$$\theta = \pi/4, \quad x = 2rd + \tfrac{1}{2}\xi d, \quad y = b - \tfrac{1}{2}\xi d,$$
$$dS = d/\sqrt{2}\,d\xi/2,$$

while for $(2r+\tfrac{1}{2})d \leqq x \leqq (2r+1)d$, we write

$$\theta = 3\pi/4, \quad x = (2r+1)d - \tfrac{1}{2}\xi d,$$
$$y = b \quad \tfrac{1}{2}\xi d, \quad dS = d/\sqrt{2}\,d\xi/2.$$

We find

$$\varphi(\alpha,\beta) = (-1)^{\beta}G(\alpha)[2ab^2\alpha/\pi(a^2\beta^2 - b^2\alpha^2)]\cdot \qquad (26)$$
$$\cdot[\cos(\alpha\pi d/2a) - \cos(\beta\pi d/2b)]$$

and (15) applies, so that

$$\psi(\alpha,\beta) = (a\beta/b\alpha)\,\varphi(\alpha,\beta) \qquad (27)$$

while to evaluate $\chi(p_t,q_t)$ we have

$$f(\sigma d) = \sigma d \qquad 0 \leqq \sigma \leqq \tfrac{1}{2}$$

$$f(\sigma d) = (1 \quad \sigma)\, d \qquad \tfrac{1}{2} \leqq \sigma \leqq 1$$

so that

$$\chi(p_t,q_t) = (1/8\pi^2)\left\{\tfrac{1}{2}(n+1)\,d^2\pi^2 + \right. \qquad (28)$$
$$+ (n+1)\,(b^2/q_t^2)[1-\cos(q_t\pi d/b)] +$$
$$+ (a^2/p_t^2)\,G(2p_t)\,[1-\cos(p_t\pi d/a)] +$$
$$+ a^2b^2\,G(2p_t)/(a^2q_t^2 - b^2p_t^2)\cdot$$
$$\left.\cdot\,[\cos(p_t\pi d/a) - \cos(q_t\pi d/b)]\right\}.$$

4. Discussion of results

The outstanding features of these formulae for the various types of projection are:

(i) For circular and triangular projections, but not for rectangular projections

$$a\beta\,\varphi(\alpha,\beta) = b\alpha\,\psi(\alpha,\beta), \qquad (29)$$

$$A_{kt} = 0 \qquad (30)$$

if one of p_t, p_k is odd and the other is even.

(ii) For rectangular projections

$$\varphi(\alpha,\beta) = 0 \qquad (31)$$

if p_t, p_k are both odd or both even,

$$\psi(\alpha,\beta) = 0 \qquad (31)$$

if one of p_t, p_k is odd and the other is even.

(iii) If the wall without projections has any abnormal concentration of eigenfrequencies, the projections will tend to break up this concentration. For if in (8), φ_t and φ_k are different but $\omega_t \approx \omega_k$, the term $c^4A_{kt}^2/(\omega_t^2-\omega_k^2)$ in (8) will be unusually large and Ω_t will therefore differ appreciably from ω_t. Similarly Ω_k will differ from ω_k and therefore from ω_t, and these differences will not in general be equal. From (9) we see that inside the room, Φ_t will be mainly a combination of φ_t and φ_k, while Φ_k will be mainly a different combination. We have here assumed that some of the A_{kt} associated with the abnormal concentration of eigenfrequencies are sufficiently large. A set of projections such that all the A_{kt} associated with a particular concentration of eigenfrequencies were zero or very small would fail to break up that particular concentration.

(iv) The maximum numerical values of $\varphi(\alpha,\beta)$ and $\psi(\alpha,\beta)$ for the various types of projection, and the values of α,β for which they occur, are very approximately calculated and tabulated below:

Table I
Maximum values of $\varphi(\alpha,\beta)$ and $\psi(\alpha,\beta)$

Type of projection	Maximum $\lvert\varphi(\alpha,\beta)\rvert$	Value of $\alpha;\beta$ for maximum	Maximum $\lvert\psi(\alpha,\beta)\rvert$	Value of $\alpha;\beta$ for maximum
Rectangular	a/π	1; $\beta d/b \ll \pi/2$	$2a/\pi^2$	$2n$ or $(2n+2)$; near b/d
Circular	$0.28\,a$	$2n$ or $2n+2$; $\beta d\ b \ll \pi/2$	$0.66\,a/\pi$	$2n$ or $(2n+2)$; near $1.18\,b\ d$
Triangular	$2a/\pi^2$	$2n$ or $2n+2$; $\beta d/b \ll \pi/2$	$\tfrac{1}{2}a$	$2n$ or $2n+2$; near b/d

It is clear from (30) and (31) that if one of p_t, p_k is even and the other odd, only rectangular projections can give a non-zero value for A_{kt}. The essential difference for our present purpose between rectangular projections and other types is that rectangular projections have finite portions which are perpendicular to the wall on which they are based, whereas circular projections have only infinitesimal portions perpendicular to this wall and triangular projections have no such portions.

The maximum values of $\varphi(\alpha,\beta)$ and $\psi(\alpha,\beta)$ are of the same order of magnitude for the three types of projection, but small denominators $(\omega_t^2-\omega_k^2)$ are likely to arise when $p_t \approx p_k$ and $q_t \approx q_k$ so that $\varphi(p_t-p_k;\ q_t-q_k)$ would make a relatively large contribution to A_{kt} for rectangular projections if (p_t-p_k) is odd and small, and (q_t-q_k) is small. Small values of $(\omega_t^2-\omega_k^2)$ can also arise in association with even values of (p_t+p_k) and (q_t+q_k) which would make $\lvert\varphi(\alpha,\beta)\rvert$ or $\lvert\psi(\alpha,\beta)\rvert$ near a maximum in the other cases, but this is much less likely. For non-rectangular projections, small $(\omega_t^2-\omega_k^2)$ will normally be associated with very small A_{kt}.

It thus appears that in the case of rectangular projections the terms $A_{kt}/(\omega_t^2-\omega_k^2)$ will make a more significant contribution to (9) than in either of the other cases.

If the projections were not evenly spaced, or occurred on more than one wall, or the room was three-dimensional, the above procedure could in theory be applied, but would in practice be immensely more complicated. We should not then expect half the A_{kt} to be zero for circular and triangular projections as in the case we have considered, but we can reasonably expect that the contribution of the portions of rectangular projections which are perpendicular to the wall from which they project is to increase sharply many of the A_{kt} which would be small for the other types of projection, and especially to increase certain A_{kt} associated with small $(\omega_t^2-\omega_k^2)$. We are thus led to expect more significant terms in (9) from rect-

angular projections than from other projections similarly distributed and of comparable dimensions.

5. The subjective significance of the results

The B.B.C. Research Department [4], [5], [6] have found that serious faults in studios and halls are often associated with recognisable characteristics of the pulsed-glide decay curves for a limited range of frequencies. In these decay curves, the logarithm of the envelope sound pressure during decay is plotted against time. For a subjectively good studio or hall, the successive pulsed-glide curves obtained as the frequency of the source is slowly increased (but the positions of source and microphone are fixed) should not generally show marked irregularity (departure from linearity) or marked lack of irregularity, and they should not form clearly-defined patterns.

We consider in the Appendix the theoretical decay-curve which would be obtained on the assumption that all but n of the eigentones excited by the source are negligible. We there show that the irregularity of the decay curve is connected with the number and relative importance of the significant eigentones; decay curves of moderate irregularity occur when the two principal eigentones are comparable without being of nearly equal intensity, or when there are several significant eigentones of comparable intensities. Equation (9) shows that the effect of any type of projection is to replace the potential function φ_t (associated with a particular eigentone of the enclosure without projections) by a linear combination of neighbouring eigentone potentials, and therefore in general to reduce the relative importance of eigentones which were outstanding for the enclosure without projections. Projections should therefore improve the subjective quality, and rectangular projections (for which, as we have seen, the difference between Φ_t and Ψ_t in (9) is most marked) should improve the subjective quality more than other types.

6. Conclusions

(a) Rectangular projections alter the natural frequencies and associated normal modes of a smooth-walled rectangular hall or studio more than circular or triangular projections having the same base and maximum depth.

(b) This result is due to the fact that rectangular projections, unlike circular and triangular projections, have finite portions perpendicular to the wall on which they are based.

(c) Rectangular projections are also more effective for breaking up abnormal concentrations of eigenfrequencies than circular or triangular projections.

(d) We have only considered the effect of projections on normal modes in general; for a few isolated particular normal modes the rectangular projections might happen to be relatively ineffective—for example, if q_t and q_k are both multiples of $2b/d$. A slight alteration of d or b would be adequate to correct this ineffectiveness in the rare cases when correction was necessary. Each type of projection will have a different series of modes for which it is thus specially ineffective.

(e) The general effect of projections would appear to be the reduction of the prominence of the leading eigentones at most frequencies. This effect would be most marked where one eigentone is outstanding, or where only two eigentones of nearly equal intensity are significant; no marked effect would be expected from the projections when several eigentones are of comparable importance. Serious faults in actual studios are often correlated with the type of pulsed-glide curve associated with the predominance of one eigentone, or of two eigentones having nearly equal intensity, so that any form of projection would be expected to improve the subjective effect at most frequencies.

(f) The general effect of projections being an overall subjective improvement (conclusion (e)) and the effect of rectangular projections being more marked than that of other types of comparable dimensions (conclusion (a)), we should expect the overall subjective effect of rectangular projections to be superior to that of projections of other types.

(g) Although the case here considered mathematically is necessarily a special one, it should be adequate as a qualitative first approximation for other cases in which we should expect similar results but the mathematical formulation of those results would be very difficult. The theory here set out is to be regarded as a first approximation rather than as a final result, and is put forward tentatively in the hope that it may point the way to a better approximation.

Acknowledgements

The author wishes to acknowledge gratefully the assistance of Mr. P. E. Doak of Manchester University, who by bringing Reference [1] to the author's notice and by constructive criticism enabled the paper to be radically improved. He also wishes to thank the Chief Engineer of the B.B.C. for permission to publish the paper.

(Received 12th November, 1952.)

Appendix

Theoretical pulsed-glide decay curves when n eigentones are significant

We suppose that when the source ceases at $t=0$, n eigentones are significantly excited. Let the initial amplitude, damping rate, frequency and phase of the ith eigentone be respectively C_i, μ_i, $\omega_i/2\pi$ and φ_i. Then the resultant sound pressure P at time t is given by

$$P=\sum_{i=1}^{n} C_i \exp\left[-\mu_i t+\mathrm{i}\left(\omega_i t+\varphi_i\right)\right]. \qquad (1)$$

We assume that the C_i are in descending order of magnitude, and that all differences $\omega_i-\omega_j$ are small compared to the ω_i themselves. The quantity measured by the pulsed-glide technique is proportional to $\log R$, R being the magnitude of the vector P determined by (1), so that

$$R^2=\sum_{i=1}^{n} C_i^2\cdot \mathrm{e}^{-2\mu_i t}+2\sum_{i=1}^{n-1}\sum_{j=i+1}^{n} C_i C_j\cdot \cdot\exp\left[-\left(\mu_i+\mu_j\right)t\right]\cos\left[\left(\omega_i-\omega_j\right)t+\left(\varphi_i-\varphi_j\right)\right]. \qquad (2)$$

If $n=1$, $R=C_1\cdot \mathrm{e}^{-\mu_1 t}$, so that the pulsed glide is a straight line.

If $n=2$, and $\mu_1=\mu_2$, $R\mathrm{e}^{\mu_1 t}$ oscillates with period $2\pi/(\omega_2-\omega_1)$ [s] between C_1-C_2 and C_1+C_2. Hence if $C_1=C_2$, the pulsed-glide will have a dip to $-\infty$ followed by a maximum in each beat cycle interval of $2\pi/(\omega_2-\omega_1)$ [s]. If C_2 is less than, but nearly equal to, C_1, the pulsed-glide will have a maximum and a minimum in each beat cycle, whereas for smaller, but not negligible, values of C_2, the pulsed-glide will merely have an inflexion in each beat cycle. If $\mu_1<\mu_2$, the pulsed-glide will for sufficiently large $C_2<C_1$ have maxima and minima in each beat cycle at first, then mere inflexions, and finally the pulsed-glide will become straight with slope corresponding to the damping rate μ_2. If $\mu_1>\mu_2$, $C_1>C_2$, we can have a pulsed-glide which starts by being straight with slope corresponding to damping rate μ_1, then after a few beat cycles inflexions appear, then maxima and minima, then inflexions, and finally a straight portion of slope corresponding to damping rate μ_2 (the so-called "double-decay" type of pulsed-glide associated with subjectively undesirable effects). If the relative phase of the two eigentones happens to be right, R may pass through a single zero during the time of maxima and minima. Some of the above features may be lost in practical pulsed-glides because R falls below the detectable threshold before they have developed.

We can sum up by saying that if $n=1$, i.e., one eigentone is outstanding, the corresponding pulsed-glide is very straight. If two eigentones predominate above all others and are unequally damped in such a way that they are of equal intensity at a particular instant T during the decay, the corresponding pulsed-glide is very irregular near time T. The extreme case is that of two eigentones of equal intensity and equally damped, for in this case there is in effect a time T once every beat cycle.

If several eigentones are significant, it is still possible, but unlikely, for R to be zero. The conditions for R to be zero are that simultaneously

$$R_x=\sum_{i=1}^{n} C_i\cdot \mathrm{e}^{-\mu_i t}\cos\left[\left(\omega_i-\omega_j\right)t+\left(\varphi_i-\varphi_j\right)\right]=0, \qquad (3)$$

$$R_y=\sum_{i=1}^{n} C_i\cdot \mathrm{e}^{-\mu_i t}\sin\left[\left(\omega_i-\omega_j\right)t+\left(\varphi_i-\varphi_j\right)\right]=0. \qquad (4)$$

There will at most be a finite set S_3 of values of t for which (3) is true before R falls below the threshold. Similarly there will be at most a finite set S_4 of values of t for which (4) is true before R falls below the threshold. In general the sets S_3 and S_4 will have no common member. Either or both may have no members. Thus in general we should not expect R to have a zero when several eigentones are significant though it is possible in particular cases for R to have either a zero or a small value. Extreme values of R require the satisfaction of stringent conditions by the relative phases $(\omega_i-\omega_j)t+(\varphi_i-\varphi_j)$. If we regarded these relative phases in (2) as completely random, we should expect R to be near

$$R_0=\sqrt{\sum_{i=1}^{n} C_i^2\cdot \mathrm{e}^{-2\mu_i t}}. \qquad (5)$$

In general, therefore, when there are several significant eigentones of comparable intensities, we should expect R to oscillate moderately about the value R_0, so that a pulsed-glide of moderate irregularity would be obtained.

References

[1] Feshbach, H., On the perturbation of boundary conditions. Phys. Rev. **65** [1944], 307—318.

[2] Somerville, T. and Ward, F. L., Investigation of sound diffusion in rooms by means of a model. Acustica **1** [1951], 40—48.

[3] Angot, A., Compléments de mathématiques. C. N. E. T., Paris 1949, pp. 361, 368.

[4] Somerville, T., Acoustics in broadcasting. Rep. of Building Research Congress, London 1951, pp. 53—59.

[5] Somerville, T. and Gilford, C. L. S., Composite cathode ray oscillograph displays of acoustic phenomena and their interpretation. B. B. C. Quart. **7** [1952], 1—13. This is substantially the same as:

[6] Somerville, T. and Gilford, C. L. S., B. B. C. Pulsed-glide acoustic displays, parts 1—3. FM-TV Radio Commun. **12** [1952], No. 6, 22, 43; No. 7, 28, 30; No. 8, 22, 38.

REMARKS ON THE CONCEPT OF ACOUSTIC ENERGY

by A. SCHOCH

Institut für theoretische Physik der Universität Heidelberg

Summary

The conventional expressions for acoustic energy—recently found not to be correct in a strict sense—are shown to have characteristic properties by which their use in acoustics can be justified satisfactorily.

Sommaire

On montre que les expressions usuelles pour l'énergie acoustique — récemment prouvées incorrectes d'un point de vue rigoureux — ont des propriétés caractéristiques, qui justifient parfaitement l'usage de ces expressions dans l'acoustique.

Zusammenfassung

Die üblichen Energieausdrücke der Akustik — von denen in letzter Zeit gezeigt worden ist, daß sie nicht streng richtig sind — besitzen charakteristische Eigenschaften, durch die sich ihr Gebrauch in der Akustik befriedigend rechtfertigen läßt.

1. Introduction

The expressions in common use for the energy density E and the energy flux density $\vec{I}$ of a sound wave are

$$E = \frac{1}{2}\left[\varrho\,\vec{u}^2 + \kappa(p-p_0)^2\right] = \\ = \frac{1}{2}\,\varrho\left[\vec{u}^2 + \frac{(p-p_0)^2}{(\varrho c)^2}\right] \tag{1.1}$$

$$\vec{I} = (p-p_0)\,\vec{u}, \tag{1.2}$$

where $\vec{u}$ = particle velocity, p = pressure, ϱ = density, $\kappa = 1/\varrho c^2$ = adiabatic compressibility of the medium, c = velocity of sound; the suffix $_0$ indicates values at equilibrium (medium at rest). The expressions are of second degree in the field variables $\vec{u}$, $p-p_0$, and usually correctness to second order is assumed, if solutions of the first order approximation to the acoustical equations are substituted for $\vec{u}$ and $p-p_0$.

The expressions (1.1), (1.2) have been subjected to criticism by ANDREJEW [1] and recently by J. J. MARKHAM [2], the objections being that

(i) in most of the textbooks it is not specified, whether the expressions refer to Eulerian or Lagrangian representation of the motion, i.e. if E and $\vec{I}$ refer to volumes and areas fixed in space, or to volumes and areas consisting always of the same particles and accordingly changing during the motion;

(ii) second order terms have been omitted in E and $\vec{I}$. Unfortunately, to take account of the missing terms would require solutions of the acoustical equations to the second order of approximation.

The present note is an attempt at a rehabilitation of the expressions (1.1), (1.2) by showing that the continuity equation relating the total energy and the total energy flux can be separated into two independent equations, one of which relates the quantities of (1.1), (1.2)[1]. The latter of these equations is of course well known, though doubts had arisen as to its interpretation [2].

2. Energy equations of hydrodynamics

The following considerations refer to a liquid (or gaseous) medium without any dissipative properties (as for instance viscosity, thermal conductivity, structural relaxation phenomena, etc.). In such a medium the state of stress is given by a scalar pressure p, which is furthermore completely determined by the density ϱ (resp. the volume $1/\varrho$ per unit mass) of the medium:

$$p = p(\varrho). \tag{2.1}$$

The hydrodynamical equations of motion, together with the equation expressing conservation of mass, immediately lead to the following equation:

$$\varrho\left[\frac{\mathrm{D}}{\mathrm{D}t}\left(\frac{\vec{u}^2}{2}\right) - p\,\frac{\mathrm{D}}{\mathrm{D}t}\left(\frac{1}{\varrho}\right)\right] + \nabla(p\vec{u}) = 0. \tag{2.2}$$

[1] This separation has already been used in a paper on the momentum of a sound wave [3].

∇ refers to fixed coordinates and

$$\frac{\mathrm{D}}{\mathrm{D}t} = \frac{\partial}{\partial t} + (\vec{u}\nabla) \tag{2.3}$$

gives, in the usual notation, the rate of change of a quantity attached to a particle, when following that particle in motion.

$p\vec{u} = \vec{I}$, the flow of energy through a material unit surface (i.e. $p(\vec{u}\,\mathrm{d}\vec{\sigma})$, is the work done per unit time on some part of the medium by an adjacent part in contact along the surface element $\mathrm{d}\vec{\sigma}$). $\vec{u}^2/2$ is the kinetic energy per unit mass, and

$$-p\frac{\mathrm{D}}{\mathrm{D}t}\left(\frac{1}{\varrho}\right) = \frac{\mathrm{D}U}{\mathrm{D}t}$$

is to be interpreted as the rate of change of an internal, potential energy U per unit mass of the medium. The existence of a potential energy follows from the assumed relation (2.1) between p and ϱ:

$$U = -\int_{1/\varrho_0}^{1/\varrho} p\,\mathrm{d}\left(\frac{1}{\varrho}\right).$$

U is the work done by compression of the unit mass from volume $1/\varrho$ to $1/\varrho_0$. Apparently the reference value ϱ_0, and with it an additive constant in U, are arbitrary.

By introducing U, (2.2) takes the form

$$\varrho\frac{\mathrm{D}}{\mathrm{D}t}\left(\frac{\vec{u}^2}{2} + U\right) + \nabla\vec{I} = 0. \tag{2.4}$$

Applying (2.3) and using the conservation of mass leads to the equivalent equation [1], [4]

$$\frac{\partial E}{\partial t} + \nabla(\vec{I} + E\vec{u}) = 0, \tag{2.5}$$

with

$$E = \varrho\left(\frac{\vec{u}^2}{2} + U\right) = \text{energy density}. \tag{2.6}$$

The meaning of these equations is conspicuous: The balance of energy is described by (2.5) for an element of volume fixed in space, i.e. in the Eulerian sense (in this case the energy flux is augmented by the convective energy transport $E\vec{u}$), and by (2.4) for a material element of the medium, consisting always of the same particles, i.e. in the Lagrangian sense. (The ∇-operations occurring have to be performed in an Eulerian representation of the field variables in both cases.)

The energy theorem (2.4) can, in its substance, be found in LAMB's Hydrodynamics [5]. A juxtaposition of the alternative forms (2.4), (2.5) of it seems to have been given for the first time by ANDREJEW. The equations have been repeated here for convenient reference.

As was mentioned above, an additive constant is arbitrary in U. In E this corresponds to an arbitrary additive quantity, which is proportional to ϱ. For this reason, it is not possible to fix the scale of energy density by taking the difference of the energy density in the state in question and in some reference state (as ANDREJEW [1] did in his definition of Eulerian energy density). In fact, the conservation law (2.5) would be violated by adding a constant to E. Physically, this means, that potential energy is attached to matter, like internal energy in thermodynamics and like kinetic energy. Things may, however, become more complicated if longe range interaction forces play a part, as e.g. in the presence of electric polarization (piezoelectric media).

3. Decomposition of hydrodynamic energy

The potential energy per unit mass can be written

$$\begin{aligned} U &= -\int_{1/\varrho_0}^{1/\varrho} p\,\mathrm{d}\left(\frac{1}{\varrho}\right) = \\ &= \underbrace{-p_0\left(\frac{1}{\varrho} - \frac{1}{\varrho_0}\right)}_{U_\mathrm{I}} \underbrace{-\int_{1/\varrho_0}^{1/\varrho}(p - p_0)\,\mathrm{d}\left(\frac{1}{\varrho}\right)}_{U_\mathrm{II}} = \\ &= U_\mathrm{I} + U_\mathrm{II}, \end{aligned} \tag{3.1}$$

where p_0 the pressure in the state of rest. Then U_II is, to second order terms, equal to the conventional acoustic energy density (1.1). U_I is in many texts supposed to vanish in the time average. Usually, however, a non-vanishing second order term of U_I is left even in the time average, as has been shown for the case of a plane progressive wave [1], [2]. Therefore the energy of a sound wave in a strict sense comprises both U_I and U_II.

Carrying out the corresponding separation

$$\mathrm{d}U = \mathrm{d}U_\mathrm{I} + \mathrm{d}U_\mathrm{II} = -p_0\,\mathrm{d}\left(\frac{1}{\varrho}\right) - (p - p_0)\,\mathrm{d}\left(\frac{1}{\varrho}\right)$$

in equation (2.2), we derive

$$\varrho\left[\frac{\mathrm{D}}{\mathrm{D}t}\left(\frac{\vec{u}^2}{2}\right) - p_0\frac{\mathrm{D}}{\mathrm{D}t}\left(\frac{1}{\varrho}\right) - (p - p_0)\frac{\mathrm{D}}{\mathrm{D}t}\left(\frac{1}{\varrho}\right)\right] + \nabla(p_0\vec{u}) + \nabla[(p - p_0)\vec{u}] = 0, \tag{3.2}$$

and as

$$\frac{\mathrm{D}}{\mathrm{D}t}\left(\frac{1}{\varrho}\right) = \frac{1}{\varrho^2}\frac{\mathrm{D}\varrho}{\mathrm{D}t} - \frac{1}{\varrho}\nabla\vec{u}$$

on account of the equation of conservation of mass, (3.2) separates into two equations

$$\varrho \frac{\mathrm{D}\, U_{\mathrm{I}}}{\mathrm{D}t} + \nabla \vec{I}_{\mathrm{I}} = 0, \quad \vec{I}_{\mathrm{I}} = p_0 \vec{u}, \tag{3.3}$$

$$\varrho \frac{\mathrm{D}}{\mathrm{D}t}\left(\frac{\vec{u}^2}{2} + U_{\mathrm{II}}\right) + \nabla \vec{I}_{\mathrm{II}} = 0, \quad \vec{I}_{\mathrm{II}} = (p - p_0)\vec{u}, \tag{3.4}$$

which could also be put into the equivalent Eulerian forms corresponding to (2.5).

(3.4) is the conservation theorem usually derived from the first order approximation equations of acoustics and provides the basis for the conventional energy expressions (1.1) and (1.2). With the definition (3.1) of U_{II} it holds rigorously, and not only within the framework of the linearized acoustical equations.

4. Discussion of U_{I} and I_{I}

As U_{I}, $\vec{I}_{\mathrm{I}}$ contain the field variables linearly, solutions to the second order of approximation are required to give values of the energy quantities correct to second order. In principle, first order solutions would therefore be insufficient for the computation of acoustic energy.

It seems, however, that the contributions U_{I}, $\vec{I}_{\mathrm{I}}$ are far less important in acoustics than U_{II}, $\vec{I}_{\mathrm{II}}$. To understand the physical meaning of the I-terms, let us compute the total I-energy contained in a fixed quantity of matter ($\mathrm{d}\tau$ = element of volume):

$$\int \varrho\, U_{\mathrm{I}}\, \mathrm{d}\tau = -p_0 \int \varrho \left(\frac{1}{\varrho} - \frac{1}{\varrho_0}\right) \mathrm{d}\tau = -p_0 (V - V_0).$$

Here V and V_0 are respectively the instantaneous and the equilibrium volumes of the quantity in question. Apparently the total I-energy equals the work done by the equilibrium pressure p_0 during the change of the volume. Therefore, the total I-energy is zero, if there is no change of the total volume. This condition would be fulfilled for a medium contained in a rigid vessel, a case which may, however, not be regarded as strictly realizable.

But the following is a case of practical interest: Suppose a source of sound waves (e.g. a vibrating piezoelectric disc) positioned in an extended medium and put into action for a limited time. After some time, the sound waves cover a region as sketched in Fig. 1. Then the I-energy in a part of the medium entirely containing the wave packet (i.e. in a part bounded by the surface of the source and any material surface S as indicated in Fig. 1) will be zero, if the source assumes its initial volume after having been switched off. That is, U_{I} does not contribute to the total energy of the sound waves.

In a steady-state sound field, maintained by periodic vibrations of the surface of the source, we similarly find that the energy flux $\vec{I}_{\mathrm{I}}$ does not contribute to the energy radiation from the source. The I-energy traversing a material surface S enclosing the source is per unit of time

$$\oint_S p_0 (\vec{u}\, \mathrm{d}\vec{\sigma}) = p_0 \frac{\mathrm{D}V}{\mathrm{D}t}$$

if V, for the time being, denotes the instantaneous volume enclosed by S. The time average of this (in the Lagrangian sense) becomes zero because of the assumed periodic motion. The absence of radiation due to I-energy might have been inferred from the case of a finite wave train considered in the preceding paragraph: There is no net transport of I-energy because the total amount of it contained in the wave train is zero.

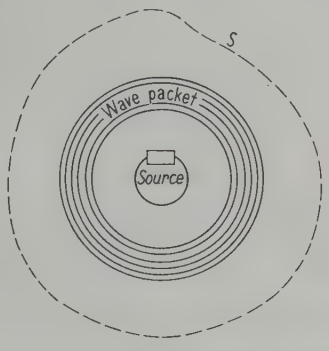

Fig. 1. A wave packet enclosed within a surface S on which the medium is at rest.

The statements may be illustrated by the case of a plane progressive wave, where an exact solution is available. If the motion is taking place in x-direction and is excited by a piston at $x = 0$, the displacement ξ of which is varying according to $\xi = f(t)$, the solution is most conveniently written in Lagrangian representation (i.e. x denoting the coordinates of the undisplaced particles). Approximated to second order it reads [6], [1], [7], [3]:

$$\xi(x,t) = f\left(t - \frac{x}{c_0}\right) + \frac{\alpha x}{2c_0^2}\left[f'\left(t - \frac{x}{c_0}\right)\right]^2, \tag{4.1}$$

if the initial conditions are imposed:

$$f(t) = 0, \quad f'(t) = 0 \qquad \text{for } t = 0$$

$$\xi(x,0) = 0, \quad \frac{\partial \xi}{\partial t} = u(x,0) = 0 \qquad \text{for } x > 0.$$

Herein is $c = \sqrt{\mathrm{d}p/\mathrm{d}\varrho}$ the instantaneous velocity of sound, $\alpha = 1 + \frac{\varrho_0}{c_0}\left(\frac{\mathrm{d}c}{\mathrm{d}\varrho}\right)_0$, and the suffix $_0$ indicates values in the equilibrium state.

With the piston returning to its initial position after having excited a sound wave, (4.1) shows that also every particle returns to its initial position after the passage of the wave train[2]. The volume of that part of the medium which is covered by the wave train is therefore equal to the equilibrium volume. Thus the total I-energy is zero, as stated above, and as had been shown earlier [3].

From (4.1) one easily deduces that

$$U_{\mathrm{I}} = -p_0\left(\frac{1}{\varrho} - \frac{1}{\varrho_0}\right) = -\frac{p_0}{\varrho_0}\frac{\partial \xi}{\partial x} =$$

$$= \frac{p_0}{\varrho_0}\left(\frac{u}{c_0} - \frac{\alpha}{2}\frac{u^2}{c_0^2}\right).$$

The expression in terms of the particle velocity u shows that the (Lagrangian) time average of U_{I} does not usually vanish, in spite of zero values of the time average of u and of the total I-energy.

That there is—in the time average—no I-energy flow in the case of periodic motion is immediately evident from the vanishing time average of $p_0 u$.

5. Conclusion

On account of the properties of U_{I} and $\vec{I}_{\mathrm{I}}$ and under the conditions prevailing in acoustics, it would therefore seem a reasonable convention to consider the contributions $\varrho\left(\frac{\vec{u}^2}{2} + U_{\mathrm{II}}\right) = E_{\mathrm{II}}$ and $\vec{I}_{\mathrm{II}}$ as the acoustic energy density and energy flux density proper. E_{II} has the property of never being negative, whereas ϱU_{I} has not. (That $U_{\mathrm{II}} \geqq 0$ follows from the hydrodynamic stability of the medium, which requires $\mathrm{d}p/\mathrm{d}\left(\frac{1}{\varrho}\right) < 0$.)

In a dissipative medium, a potential energy no longer exists. Equation (2.4) has then to be generalized by adding the heat flow to $\vec{I}$ and interpreting U as the internal energy in the sense of thermodynamics. But the separation of this generalized equation into two equations corresponding to (3.3) and (3.4) is still possible, with the same expressions for U_{I}, $\vec{I}_{\mathrm{I}}$ as above, satisfying the same conservation equation (3.3). It is the generalization of (3.4) which contains the thermodynamics. This means that dissipation (sound absorption) feeds from E_{II}, whereas (3.3) describes only some reversible shifting about of mechanical energy. This consideration may serve as further argument for the distinction of part II as acoustic energy.

The present note was stimulated by a discussion with Dr. P. J. Westervelt, who directed the author's attention to the papers by J. J. Markham. The author would like to thank Dr. Westervelt and Dr. Markham for discussion and correspondence.

(Received 10th November, 1952.)

[2] This would not be true if $f(t), f'(t)$ were not simultaneously zero for $t = 0$. A start of the piston with a finite velocity —which would produce a shock wave —shall, however, be excluded here. It could not, moreover, be realized with a finite mass of the piston.

References

[1] Andrejew, N., J. Phys. USSR **2** [1940], 305.
[2] Markham, J. J., Phys. Rev. **86** [1952], 712.
[3] Schoch, A., Z. Naturforsch. **7a** [1952], 273.
[4] Richter, G., Z. Phys. **125** [1947], 98.
[5] Lamb, H., Hydrodynamics, 6. ed. Chapt. I, Cambridge University Press 1932.
[6] Fubini-Ghiron, E., Alta Frequenza **4** [1935], 530.
[7] Westervelt, P. J., J. acoust. Soc. Amer. **22** [1950], 319.

Berliner Studiengesellschaft für Ultraschall

Unter dem Vorsitz von Privatdozent Dr.-Ing. J. J. Gruetzmacher ist kürzlich die „Berliner Studiengesellschaft für Ultraschall" mit dem vorläufigen Sitz im Institut für Schwingungsforschung an der Technischen Universität Berlin, Berlin-Charlottenburg 2, Jebensstr. 1, gegründet worden. Sie hat sich die Durchführung von Forschungs- und Entwicklungsarbeiten auf dem Gebiet des Ultraschalls zur Aufgabe gemacht. Eine Reihe namhafter Fachleute aus Wissenschaft und Industrie steht der Gesellschaft als korrespondierende Mitglieder mit Rat und Tat zur Seite. Neben Problemen der Grundlagenforschung sollen zunächst insbesondere solche der Verfahrens-, Verkehrs- und Fertigungstechnik behandelt werden; mit biologischen und medizinischen Forschungsstellen besteht gleichfalls eine enge Zusammenarbeit. W. Weber

27. April 1953

ZUR AKUSTISCHEN ZÄHIGKEITSGRENZSCHICHT

Von E. MEYER und W. GÜTH

III. Physikalisches Institut der Universität Göttingen

Zusammenfassung

Es wird die akustische Zähigkeitsgrenzschicht untersucht, indem in fortschreitenden Schallwellen die Luftbewegung in der Nähe einer starren Grenzfläche durch beleuchtete Schwebeteilchen mikroskopisch sichtbar gemacht wird.

Summary

The acoustic viscous boundary layer is investigated for sound waves in air in the neighbourhood of a rigid wall using illuminated floating particles seen under a microscope.

Sommaire

On a étudié la couche limite visqueuse acoustique en rendant visible au microscope, par l'éclairage de particules en suspension, le mouvement de l'air, dans une onde sonore progressive, au voisinage d'une surface rigide.

1. Einleitung

Die Luftteilchen in einer fortschreitenden Schallwelle führen lineare Schwingungen in der Schallausbreitungsrichtung aus. Bringt man eine ebene starre Fläche parallel der Ausbreitungsrichtung in das Schallfeld, so wird in größerem Abstand von dieser die Bewegung der Luftteilchen unbeeinflußt bleiben. Ihre Schwingungsamplitude ist unabhängig vom Abstand konstant. An der Grenzfläche selbst haftet die Luft, und infolge ihrer Zähigkeit wird ihre Bewegung in der Nähe der Grenzfläche gehemmt. Man wird also eine der Abb. 1 entsprechende Geschwindigkeitsverteilung erwarten, wobei die Länge der Pfeile die jeweilige Geschwindigkeitsamplitude andeutet. Sie ist in großem Abstand konstant und verringert sich zur Grenzfläche hin.

Die mathematische Beschreibung des Vorganges findet sich bei KIRCHHOFF, RAYLEIGH, CRANDALL und CREMER [1]···[4].

Die aus der Herleitung der Schallwellengleichung geläufige Newtonsche Kraftgleichung

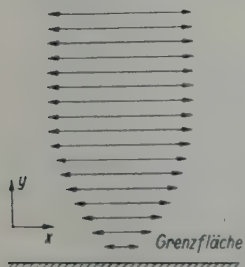

Abb. 1. Vermutete Schnelleverteilung über der Grenzfläche.

$$\varrho_0 \frac{\partial v}{\partial t} = -\frac{\partial p}{\partial x}$$

wird durch einen Summanden erweitert, der der Zähigkeit Rechnung trägt

$$-\eta \frac{\partial^2 v}{\partial y^2} + \varrho_0 \frac{\partial v}{\partial t} = -\frac{\partial p}{\partial x}. \quad (1)$$

Darin sind v die Schnelle in der x-Richtung (Abb. 1), p der Druck, ϱ_0 die Dichte, η die Zähigkeit der Luft.

Die Vereinfachung in der Behandlung der Gl. (1) besteht in der Annahme, daß der Druck p unabhängig von der Höhe y über der Grenzfläche ist. $\partial/\partial t$ wird durch $i\omega$ ersetzt. Aus Gl. (1) wird dann:

$$\eta \frac{\partial^2 v}{\partial y^2} - i\omega \varrho_0 v = \frac{\partial p}{\partial x}. \quad (2)$$

Ihre Lösung lautet:

$$v(y) = -\frac{1}{i\omega \varrho_0} \cdot \frac{\partial p}{\partial x}\left(1 - e^{-\sqrt{\frac{i\omega\varrho}{\eta}}\, y}\right) = \\ = v_0\left(1 - e^{-\sqrt{\frac{i\omega\varrho}{\eta}}\, y}\right); \quad (3)$$

v_0 ist der Betrag der Schnelle im freien Schallfeld.

Die Schnelle im Abstand y von der Grenzfläche ist nach Gl. (3)

$$|v(y)| = v_0 \sqrt{1 - 2e^{-\sqrt{\frac{\omega\varrho}{2\eta}}\, y} \cos \sqrt{\frac{\omega\varrho}{2\eta}}\, y + e^{-2\sqrt{\frac{\omega\varrho}{2\eta}}\, y}}. \quad (4)$$

Die zur Gl. (4) gehörige Kurve ist in Abb. 2 skizziert. Sie oszilliert mit einer exponentiell abklingenden Amplitude um die Gerade $|v| = v_0$. Den in Abb. 2 mit $\lambda = 2\pi(\omega\varrho/2\eta)^{-1/2}$ bezeichneten Abstand nennt CREMER die „Zähigkeitswellenlänge" oder die „akustische Grenzschichtdicke". Ersteres, da ja die Gl. (3) formal eine Welle, die Zähigkeitswelle, beschreibt, die von der Grenzfläche her in der y-Richtung fortschreitet.[1] Die Zähigkeitswellenlänge wächst also, wie man aus Gl. (3) und im folgenden aus Abb. 6 sieht, um-

[1] Die Analogie zum elektrischen Skineffekt ist offensichtlich, der ja auch auf einer in das Metall eindringenden Welle beruht.

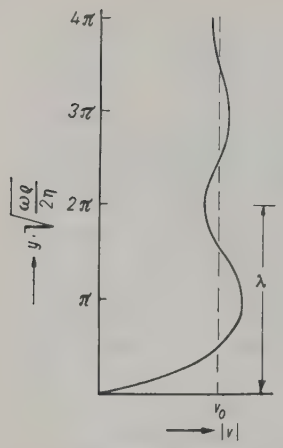

Abb. 2. Skizze des Kurvenverlaufs zu Gl. (4).

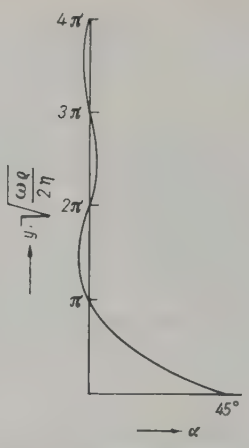

Abb. 3. Skizze des Kurvenverlaufs zu Gl. (5).

gekehrt proportional der Wurzel aus der Frequenz.

Die Phasendifferenz, mit der ein Luftteilchen in der Höhe y gegen ein senkrecht darüber im freien Schallfeld befindliches Luftteilchen schwingt, ist nach Gl. (4) gegeben durch

$$\operatorname{tg}\chi = \frac{e^{-\sqrt{\frac{\omega\varrho}{2\eta}}y}\sin\sqrt{\frac{\omega\varrho}{2\eta}}y}{1 - e^{-\sqrt{\frac{\omega\varrho}{2\eta}}y}\cos\sqrt{\frac{\omega\varrho}{2\eta}}y}. \qquad (5)$$

Die zu Gl. (5) gehörige Kurve ist in Abb. 3 skizziert.

2. Aufbau der Apparatur und Messung

In einem langen Rohr mit rechteckigem Querschnitt wird vom linken Ende her die im Rohr enthaltene Luft durch einen Lautsprecher zu Längsschwingungen angeregt (vgl. Abb. 4). Die vom Lautsprecher abgestrahlte Schallenergie wird am rechten Ende des Rohres durch einen 2 m langen Schluckkeil aus Schlackenwolle absorbiert, so daß sich zwischen Lautsprecher und Keil eine fortschreitende Schallwelle ausbildet. Der Rohrquerschnitt (5×7 cm^2) ist so klein, daß keine Querwellen entstehen können. Zwischen Lautsprecher und Keil sind in den beiden Seitenwänden Fenster angebracht, zwischen denen ein Glasröhrchen[2] von 2 cm Durchmesser liegt. Seine äußere Oberfläche dient als Grenzfläche, über der die Luftbewegung beobachtet wird.

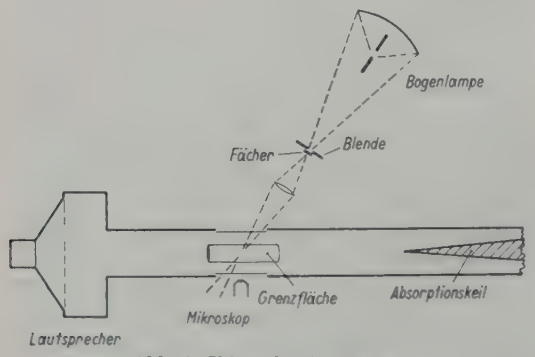

Abb. 4. Skizze der Apparatur.

Die Schwebeteilchen sind winzige mittels eines Zerstäubers in die Luft geblasene Öltröpfchen. Sie werden durch eine Dunkelfeldbeleuchtung im Mikroskop sichtbar gemacht. Als Lichtquelle dient eine Beck-Bogenlampe, die im Augenblick des Photographierens stark überlastet wird. Der Spiegel der Bogenlampe bildet die Lichtquelle auf eine Blende ab, vor der zur Phasenmessung ein durch einen Synchronmotor betriebener Fächer den Lichtstrahl periodisch kurz unterbricht. Ein Beleuchtungsobjektiv bildet den Fächer in die Objektebene über der Grenzfläche ab. Das von der Lichtquelle ausgeleuchtete Gebiet über der Grenzfläche wird durch ein Mikroskop beobachtet.

Abb. 5. Aufnahme einer Tröpfchenbahn.

Die Öltröpfchen (etwa 10^{-5} cm Durchmesser) schwingen unter dem Einfluß des Schallfeldes hin und her und machen die Schallelongation der Luftteilchen völlig mit. Ihre Bahnen sind im Mikroskop als horizontale Striche sichtbar. Mit Hilfe eines elektrischen Feldes (etwa 8000 V/cm) können die Tröpfchen in vertikaler Richtung auf die Grenzfläche zubewegt werden, da sie durch den Zerstäubungsprozeß fast immer elektrisch geladen sind. Man sieht dann im Mikroskop die Striche sich auf die Grenzfläche zubewegen und dabei kürzer werden, bis sie als Punkt auf ihr enden. Macht man von dem ganzen Vorgang eine Zeitaufnahme, so kommt die Aufnahme Abb. 5 zustande. Man sieht darauf deutlich das erste

[2] Es wurde eine gewölbte Grenzfläche gewählt, weil bei einer ebenen die Flächenteile, die vor und hinter der Objektebene liegen, bei dem intensiven Gegenlicht das Bild teilweise überstrahlen würden.

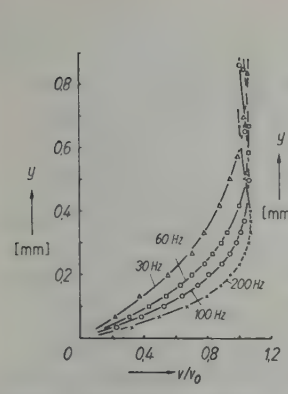

Abb. 6. Berechnete Schnelleprofile (Kurven) und eingetragene Meßwerte für verschiedene Frequenzen.

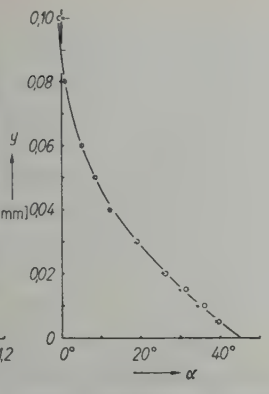

Abb. 7. Berechnetes Phasenprofil (Kurve) und eingetragene Meßwerte für die Frequenz 60 Hz;
○ linke Schattengrenze,
× rechte Schattengrenze.

Maximum der Geschwindigkeitsamplitude, wie es nach Abb. 2 zu erwarten ist.

Solche Bilder wurden für die Frequenzen 30, 60, 100 und 200 Hz aufgenommen und ausgemessen. Abb. 6 zeigt die Ergebnisse.

In Abb. 5 ist innerhalb der Tröpfchenbahn ein dunkler Streifen zu sehen. Er dient der Bestätigung der Gl. (5). Der oben erwähnte Synchronmotor wird aus demselben elektrischen Generator wie der Lautsprecher betrieben; die Frequenz, mit der der Lichtstrahl unterbrochen wird, stimmt daher mit der Schallfrequenz überein. Da der Fächer in die Objektebene abgebildet wird, ist die Tröpfchenbahn an einer Stelle scharf unterbrochen. Weil die der Grenzfläche nahen Luftschichten gegen die entfernteren phasenverschoben schwingen (vgl. Gl. (5)), verschiebt sich der dunkle Streifen in der Nähe der Grenzfläche etwas zur Seite. Die Auswertung einer Phasenmessung zeigt Abb. 7.

Die beschriebene Methode der Sichtbarmachung und Ausmessung der Schallausschläge (bzw. Schallschnellen) eignet sich auch gut dazu, in engen Kapillaren, deren lichte Weite mit der Zähigkeitswellenlänge vergleichbar ist, die Schalldämpfung zu untersuchen. Über diese Versuche wird in einer späteren Arbeit berichtet werden.

(Eingegangen am 27. August 1952.)

Schrifttum

[1] Kirchhoff, G., Poggendorfs Ann. Phys. **134** [1868], 177.
[2] Lord Rayleigh, Theory of sound, Vol. II, XIX. D. van Nostrand Co., New York 1926.
[3] Crandall, I. B., Theory of vibrating systems and sound. Macmillan & Co., London 1929.
[4] Cremer, L., Über die akustische Grenzschicht vor starren Wänden. Arch. elekt. Übertragung **2** [1948], 136.

ON A VARIATIONAL PRINCIPLE IN ACOUSTICS*

by Osman K. Mawardi

Acoustics Laboratory, Massachusetts Institute of Technology, Cambridge 39, Massachusetts, U.S.A.

Summary

The present paper describes an investigation of the propagation of sound inside an acoustic labyrinth. The latter consists of a tube of rectangular cross-section interrupted at periodic intervals by thin partitions with staggered openings. By virtue of the expected periodicity of the wave function in the labyrinth, Floquet's theorem can be employed to determine the velocity potential anywhere in the structure as a function of the potential in the space between any two consecutive partitions. This property is used in developing a variational principle which yields the propagation constant of acoustic waves travelling down the labyrinth. The phase velocity and attenuation for the simpler type of waves propagated have been evaluated by the previous principle. The accuracy of the method is believed to be quite satisfactory.

Sommaire

On donne dans le présent article les résultats d'une étude sur la propagation du son dans un labyrinthe. Celui-ci est un tube de section rectangulaire partagé à intervalles constants par des cloisons minces ayant des ouvertures en chicane. Comme la fonction d'onde doit être périodique dans le labyrinthe, on peut utiliser un théorème de Floquet pour déterminer le potentiel des vitesses en tout point de la structure en fonction du potentiel dans l'espace compris entre deux cloisons successives quelconques. On utilise cette propriété pour établir un principe de variation qui fournit la constante de propagation d'une onde acoustique parcourant le labyrinthe. On a également évalué, par application de ce principe, la vitesse de phase et l'affaiblissement dans le cas d'un type simple d'onde se propageant dans le système. On estime que la précision de cette méthode est tout à fait satisfaisante.

* This work has been supported in part by the Office of Naval Research, U.S.A.—Presented at the Eighth International Congress on Theoretical and Applied Mechanics, Istanbul, Turkey, 1952.

Zusammenfassung

Die vorliegende Arbeit beschreibt eine Untersuchung über die Schallausbreitung in einem akustischen Labyrinth. Dieses besteht aus einem Rohr von rechteckigem Querschnitt, das in periodischen Abständen von dünnen Zwischenwänden mit gegeneinander versetzten Öffnungen unterteilt wird. Mit Hilfe der erwarteten Periodizität der Wellenfunktion im Labyrinth kann das Theorem von FLOQUET benutzt werden, um das Geschwindigkeitspotential an einer beliebigen Stelle des Rohres aus dem Potential im Raum zwichen zwei aufeinander folgenden Trennwänden zu bestimmen. Diese Eigenschaft wird benutzt, um ein Variationsprinzip zu entwickeln, mit dem die Fortpflanzungskonstante der akustischen Wellen, die durch das Labyrinth wandern, sich bestimmen läßt. Die Phasengeschwindigkeit und die Dämpfung für die einfacheren Wellentypen wurden nach diesem Prinzip berechnet. Die Genauigkeit der Methode scheint befriedigend zu sein.

1. Introduction

In several acoustic installations, constrictions are introduced inside ducts in order to increase the attenuation of sound waves travelling down the duct. A survey [1] of the technical literature reveals that the effect of discontinuous constrictions on the propagation of sound waves has been extensively investigated. The mathematical methods used in these studies have borrowed heavily from analogous problems in electromagnetic waveguides [2]. An exact solution for the propagation through discontinuous constrictions, however, is difficult and often intractable. As a result, one has to resort to approximate methods. Of these, the variational techniques appear to be the most fruitful, judging from the wide variety of cases which have been investigated by their means.

The presence of periodic discontinuities in the duct adds appreciably to the complexity of the situation. Information on this class of problem is scanty and only a few isolated instances have been treated [3]. A renewed interest in the understanding of the propagation down structures with periodic discontinuities was aroused, following the encouraging preliminary results of the use of an acoustic labyrinth [4] (Fig. 1) as an acoustic termination.

The purpose of the present paper is to work out a generalized theory for the propagation of waves down the labyrinthlike structure of Fig. 1. The results are presented in the form of a propagation constant derived from a variational principle developed herein.

2. Formulation of the problem

A well known proposition in acoustics states that the velocity potential inside a region can be determined as a function of the value of the potential or its gradient at the boundary. This functional relation follows from a direct application of Green's second identity which leads to:

$$\Phi(\mathbf{r}) = \int_S [G(\mathbf{r},\mathbf{r}')\,\partial_n \Phi(\mathbf{r}') - \Phi(\mathbf{r}')\,\partial_n G(\mathbf{r},\mathbf{r}')]\,\mathrm{d}S \qquad (1)$$

where $G(\mathbf{r},\mathbf{r}')$ is the Green's function for the domain under consideration, $\Phi(\mathbf{r})$ is the velocity potential and $\mathbf{r}$, $\mathbf{r}'$ are position vectors referred to some origin O. Choosing a Green's function which has a vanishing gradient at the boundary, the above expression becomes:

$$\Phi(\mathbf{r}) = \int_S [G(\mathbf{r},\mathbf{r}')\,\partial_n \Phi(\mathbf{r}')]\,\mathrm{d}S. \qquad (2)$$

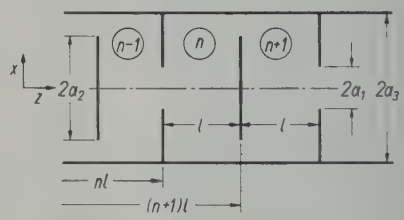

Fig. 1. Schematic diagram for labyrinth structure.

Let a coordinate system x, y, z be defined (Fig. 1) such that the z-axis coincides with the "axis" of the labyrinth. Let it be assumed that the prevailing symmetry of the system will make the motion independent of the y-coordinate. For any cell n, enclosed between the two parallel planes $z = nl$ and $z = (n+1)l$, it is found by means of eq. 2:

$$\Phi^{(n)}(x,z) = \int_S [G^n(x,z;x',z')\,\partial_n \Phi^{(n)}(x',z')]_{z'=nl}\,\mathrm{d}S + \int_S [G^{(n)}(x,z;x',z')\,\partial_{n'} \Phi^{(n)}(x',z')]_{z'=(n+1)l}\,\mathrm{d}S. \qquad (3)$$

The superscript n refers to quantities related to the domain $nl \leqq z,\ z' \leqq (n+1)l;\ 0 \leqq x,\ x' \leqq a_3$. Only one half of the labyrinth need be considered, by virtue of its axial symmetry. A similar relation derived for the cell $(n+1)$ is,

$$\Phi^{(n+1)}(x,z) = \qquad (4)$$
$$= \int_S [G^{(n+1)}(x,z;x',z')\,\partial_n \Phi^{(n+1)}(x',z')]_{z'=(n+1)l}\,\mathrm{d}S + \int_S [G^{(n+1)}(x,z;x',z')\,\partial_n \Phi^{(n+1)}(x',z')]_{z'=(n+2)l}\,\mathrm{d}S.$$

The domain of the cell $(n+1)$ extends over

$$(n+1)l \leqq z,\ z' \leqq (n+2)l;\ 0 \leqq x,\ x' \leqq a_1.$$

The labyrinth walls being rigid, the normal velocity will vanish at the boundaries. By virtue of its symmetry, the x-component of the velocity will

vanish on the axis. The boundary conditions will further require the velocity to be continuous across the openings, i.e., for any n,

$$\partial_z \Phi^{(n)}[x,(n+1)l] = \partial_z \Phi^{(n+1)}[x,(n+1)l] \quad a_2 \leqq x \leqq a_3$$
$$\text{or} \quad \partial_z \Phi^{(n)}(x,nl) = \partial_z \Phi^{(n-1)}(x,nl) \quad 0 \leqq x \leqq a_1 \tag{5}$$

according to the case on hand.

The propagation problem will be formally solved, once the potential function is determined from the set of eqs. 3 and 4 in a manner compatible with eq. 5.

3. Construction of Green's function

The Green's function for the cell n satisfies the differential equation

$$\left(\frac{\partial^2}{\partial x^2}+\frac{\partial^2}{\partial z^2}+k^2\right) G^{(n)}(x,z;x',z') = -\delta(x-x')\,\delta(z-z') \tag{6}$$

subject to the conditions,

$\partial_n G = 0$ at $x=0$, a_3 and at $z=nl$, $z=(n+1)l$.

Let $G^{(n)} =$ (7)

$$= \sum_m \frac{2-\delta_{om}}{a_3} \cos\left(\frac{m\pi x}{a_3}\right) \cos\left(\frac{m\pi x'}{a_3}\right) G_m^{(n)}(z,z'),$$

where $\delta_{om} = 1$, $o = m$; $\delta_{om} = 0$, $o \neq m$.

A substitution of eq. 7 in eq. 6 shows that

$$\left[\frac{\partial^2}{\partial z^2} + k^2 - \left(\frac{m\pi}{a_3}\right)^2\right] G_m^{(n)}(z,z') = -\delta(z-z'). \tag{8}$$

The general solution of the above equation is (9)

$$G_m^{(n)} = \begin{cases} (A\sin K_m z' + B\cos K_m z')\cos K_m[(n+1)l-z] & z' < z \\ \cos K_m[(n+1)l-z'](A\sin K_m z + B\cos K_m z) & z < z' \end{cases}$$

where $K_m^2 = k^2 - \left(\frac{m\pi}{a_3}\right)^2$ and $nl \leqq z, z' \leqq (n+1)l$.

Using the boundary conditions, the ratio of the arbitrary constants can be determined and it is found

$$\frac{A}{B} = \frac{\sin K_m nl}{\cos K_m nl}. \tag{10}$$

From an integration of both sides of eq. 8, it follows that

$$\partial_z G_m^{(n)}(z,z')\Big|_{z=z'+0}^{z=z'-0} = -1 \tag{11}$$

whence

$$B = \frac{\cos(K_m nl)}{K_m \sin K_m l}. \tag{12}$$

The general expression for the Green's function is finally found to be

$$G^{(n)} = \sum_m \frac{(2-\delta_{om})}{a_3 K_m \sin K_m l} \cos\left(\frac{m\pi x}{a_3}\right) \cos\left(\frac{m\pi x'}{a_3}\right) \begin{cases} \cos\{K_m[(n+1)l-z]\}\cos[K_m(nl-z')] & z' < z \\ \cos\{K_m[(n+1)l-z']\}\cos[K_m(nl-z)] & z < z', \end{cases} \tag{13}$$

$$nl \leqq z,\ z' \leqq (n+1)l.$$

4. Derivation of variational principle

The mathematical procedure in solving the problem on hand is considerably simplified by introducing the concept of the propagation constant. Since the higher modes are expected to be rapidly attenuated it will be assumed that,

$$\Phi(x,nl) = \Phi[x,(n+2)l]\,e^{2\alpha ml}, \quad \pm m, \pm n = 0,1,2\ldots \tag{14}$$

The previous expression (eq. 14) can be considered as following from a direct application of FLOQUET's theorem applied to the periodic structure studied. The constant α is in general a complex quantity, the real part of which vanishes when no attenuation is present. The real part cannot be negative when no sources are included in the labyrinth.

The two eqs. 3 and 4 can be rewritten as,

$$\Phi^{(n)}(x,z) = -\int_0^{a_1} G^{(n)}(x,z;x',nl)\,\partial_{z'}\Phi^{(n)}(x',z')\Big|_{z'=nl} dx' + \int_{a_2}^{a_2} G^{(n)}[x,z;x',(n+1)l]\,\partial_{z'}\Phi^{(n)}(x',z')\Big|_{z'=(n+1)l} dx', \tag{15}$$

$$\Phi^{(n+1)}(x,z) = -\int_{a_2}^{a_3} G^{(n+1)}[x,z;x',(n+1)l]\cdot \cdot \partial_{z'}\Phi^{(n+1)}(x',z')\Big|_{z'=(n+1)l} dx' + \int_0^{a_1} G^{(n)}[x,z;x',(n+2)l]\cdot \cdot \partial_{z'}\Phi^{(n+1)}(x',z')\Big|_{z'=(n+2)l} dx'.$$

The negative sign appearing in front of some of the integrals follows from the accepted convention of letting the positive direction of the gradient be along the outwards normal. Since the velocity is continuous across the opening, then matching the velocity deduced from the two expressions (eq. 15) yields,

$$2\,\partial_z \Phi^{(n)}(x,z)_{z=(n+1)l} = \tag{16}$$
$$= (1-e^{-2\alpha l}) \int_0^{a_1} \partial_z G^{(n)}(x,z;x',z')\,\partial_{z'}\Phi^{(n)}(x',z')\Big|_{\substack{z'=nl \\ z=(n-1)l}} dx',$$
$$a_2 \leqq x \leqq a_3.$$

The last expression made use of the properties:

$$\partial_z [G^{(n)}(x,z;x',z')]_{\substack{z=(n+1)l \\ z'=nl}} = -\partial_z [G^{(n+1)}(x,z;x',z')]_{\substack{z=(n+1)l \\ z'=(n+1)l}},$$
$$\partial_z [G^{(n)}(x,z;x',z')]_{z=(n+1)l=z'} = -\partial_z [G^{(n+1)}(x,z;x',z')]_{z=(n-1)l=z'}. \tag{17}$$

By a similar line of argument a similar relation for the velocity distribution across the opening at $z=nl$, yields

$$2\partial_z \Phi^{(n)}(x,z)_{z=nl} = (1-e^{2\alpha l}) \int_{a_2}^{a_3} \partial_z G^{(n)}(x,z;x',z')\, \partial_{z'} \Phi^{(n)}(x',z') \Big|_{\substack{z'=(n+1)l \\ z=nl}} dx', \quad 0 \leqq x \leqq a_1. \tag{18}$$

For simplicity, let the following notation be introduced

$$\partial_z \Phi^{(n)}(x,z)_{z=nl} = f_1^{(n)}(x), \qquad \partial_z \Phi^{(n)}(x,z)_{z=(n+1)l} = f_2^{(n)}(x), \tag{19}$$

then the question to be considered deals with the solution of the simultaneous integral equations,

$$2f_2^{(n)}(x) = (1-e^{-2\alpha l}) \int_0^{a_1} \partial_z [G^{(n)}(x,z;x',z')]_{\substack{z'=nl \\ z=(n+1)l}} f_1^{(n)}(x')\, dx'$$

$$2f_1^{(n)}(x) = (-1+e^{2\alpha l}) \int_{a_2}^{a_3} \partial_z [G^{(n)}(x,z;x',z')]_{\substack{z'=(n+1)l \\ z=nl}} f_2^{(n)}(x')\, dx'. \tag{20}$$

Elimination of $f_1^{(n)}(x)$ from these two relations yields,

$$f_2^{(n)}(x) = -\frac{1}{4}(1-e^{2\alpha l}) \cdot \int_0^{a_1} \int_{a_2}^{a_3} \partial_z [G^{(n)}(x,z;x',z')]_{\substack{z'=nl \\ z=(n+1)l}} \times \partial_z [G^{(n)}(x',z';x^*,z^*)]_{\substack{z^*=(n+1)l \\ z'=nl}} \cdot f_2^{(n)}(x^*)\, dx'\, dx^* (1-e^{2\alpha l}). \tag{21}$$

Denoting

$$\int_0^{a_1} \partial_z [G^{(n)}(x,z;x',z')]_{\substack{z'=nl \\ z=(n+1)l}} \cdot \partial_z [G^{(n)}(x',z';x^*,z^*)]_{\substack{z^*=(n+1)l \\ z'=nl}} dx'$$

by $K^n(x,x^*)$ which by virtue of its construction is a positive definite function [5], then the above expression (eq. 21) can be rewritten,

$$f_2^{(n)}(x) - = -\frac{1}{2}(\cosh 2\alpha l - 1) \int_{a_2}^{a_3} K^n(x,x^*) f_2^{(n)}(x^*)\, dx^*. \tag{22}$$

Inspection of the above relation (eq. 22) reveals that the propagation constant can be estimated by a variational formula. The eq. 22 is a canonical FREDHOLM integral equation of the second kind, and the unknown constant plays the part of the proper value of the equation. Thus multiplying both sides of eq. 22 by $f_2^{(n)}(x)$ and integrating between the limits $a_2 - a_3$, we find

$$\frac{1}{\frac{1}{2}(\cosh 2\alpha l - 1)} = \frac{\int_{a_2}^{a_3} \int_{a_2}^{a_3} f_2^{(n)}(x)\, K^n(x,x^*)\, f_2^{(n)}(x^*)\, dx\, dx^*}{\int_{a_2}^{a_3} f_2^{(n)2}(x)\, dx}. \tag{23}$$

The above expression is identified with the ratio of two definite positive quantities and as a result $(\cosh 2\alpha l - 1)$ is stationary [6] for first order variation of the function $f_2^{(n)}(x)$.

5. Evaluation of stationary quantity

In order to determine the quantities to the left hand side of eq. 23, suitable trial functions $f_2^{(n)}(x)$ have to be evaluated. The static solution is a reasonable guess. The latter is analogous to the determination of the lines of current in a conducting plate ABCD (Fig. 2), the electrodes of which are at PB and DQ. This problem has been solved exactly by MOULTON [7], who gave the distribution in terms of elliptic functions. A close approximation found by assuming the constrictions far apart (i.e., AD $\gg$ DC) yields results more amenable to easy computations. This problem also had been previously worked [8]. The complex potential in the vicinity of the aperture say at $z=(n+1)l$ $(a_2 \leqq x \leqq a_3)$ is given by the results of ref. [8] as

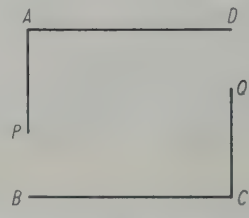

Fig. 2. Idealized conducting strip used to calculate the distribution of velocity in the aperture.

$$w = \frac{2A}{\pi} \arcsin \left[\frac{\sin \frac{(a_3 - Z)\,\pi}{2a_3}}{\sin \frac{(a_3 - a_2)\,\pi}{2a_3}} \right] \qquad (24)$$

where Z is the complex number $(x + jy)$. When the arbitrary constant A is made equal to a_3, then the flux of fluid through the aperture is given by

$$\int_{a_2}^{a_3} f_2^{(n)}(x)\,dx = a_3. \qquad (25)$$

The kernel is found to be:

$$K^n(x, x^*) = \frac{4}{a_3^2}\, a_1 \cos^2 k l + \qquad (26)$$

$$+ \frac{a_3}{\pi} \cos K_1 l \sin \frac{\pi a_1}{a_3} \left(\cos \frac{\pi x}{a_3} + \cos \frac{\pi x^*}{a_3} \right) \cos k l +$$

$$+ \frac{1}{2} \cos^2 K_1 l \left(a_1 + \frac{a_3}{2\pi} \sin \frac{2\pi a_1}{a_3} \right) \left(\cos \frac{\pi x}{a_3} \cos \frac{\pi x^*}{a_3} \right) + \ldots$$

Substitution of eq. 24 and eq. 25 into eq. 23 yields for the propagation constant

$$\cosh 2\alpha l =$$

$$1 - \frac{3/2 \left(1 - \frac{a_2}{a_3}\right) + 3/2\pi \sin \frac{\pi a_2}{a_3}}{2 \left[\frac{a_1}{a_3} \cos k l - \sin^2 \frac{\pi a_2/a_3}{\pi} \sin \frac{\pi a_1}{a_3} \cos K_1 l \cos k l + \frac{1}{2} \left(\frac{a_1}{a_3} + \frac{1}{2\pi} \sin \frac{2\pi a_1}{a_3} \right) \sin^4 \frac{\pi a_2}{2a_3} \cos^2 K_1 l + \ldots \right]} \qquad (27)$$

which can be written formally,

$$\cosh 2\alpha l = 1 - C/2D.$$

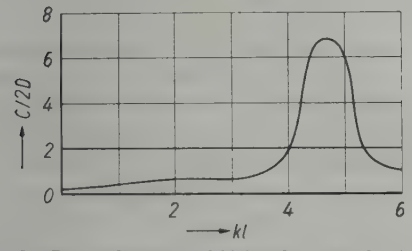

Fig. 3. $C/2D$ as a function of kl for the case of $a_1/a_3 = 0.8$, $a_2/a_3 = 0.5$ and $l/a_3 = 3/\pi$. Attenuation occurs whenever $0 > C/2D > 2$.

The propagation constant α then becomes a pure imaginary whenever $|1 - C/2D| \leqq 1$; it, however, will have a real positive part indicating attenuation in the propagated wave, whenever $|1 - C/2D| > +1$. Since the series of D converges quite rapidly, only the first few terms have been retained.

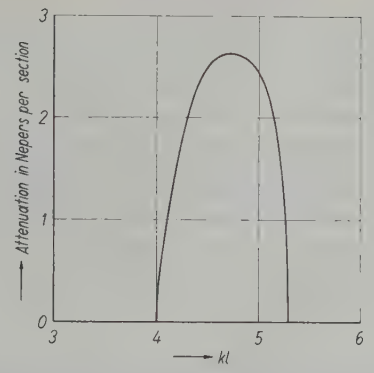

Fig. 4. Real part of propagation constant corresponding to Fig. 3. Only one attenuating band has been computed.

In order to investigate the attenuation bands for the labyrinth $C/2D$, a typical case has been drawn in Fig. 3. Attenuation is present whenever $0 > C/2D > 2$. The corresponding propagation constant has been computed and is shown in Fig. 4.

(Received 6th November, 1952.)

References

[1] Miles, J.W., Quart. appl. Math. **7** [1949], 45.

[2] Watson, W. H., Physical principles of waveguide transmission. Clarendon Press, Oxford 1947.
Marcuvitz, N., Waveguide Handbook; Radiation Laboratory Series. McGraw-Hill Book Co., New York 1951, p. 143 ff.

[3] Ingård, U. and Pridmore-Brown, D., J. acoust. Soc. Amer. **23** [1951], 689.

[4] Mawardi, O. K., J. acoust. Soc. Amer. **23** [1951], 146.

[5] Bateman, H., Messenger of Math. **37** [1908], 91.

[6] Equation (23) is a variational equation of a type first studied by Schwinger. The results of some of his investigations can be found in the Massachusetts Institute of Technology, Radiation Laboratory reports (1941—1945). See also Marcuwitz's Handbook, ref. [2].

[7] Moulton, F., Proc. Lond. math. Soc. **3** [1905], 104.

[8] Lees, C. H., Proc. phys. Soc. **23** [1911], 1361.
Shoefield, F. H., Phil. Mag. **(7) 6** [1928], 567.

ACOUSTIC IMPEDANCE MEASUREMENT BY THE TRANSMISSION-CHARACTERISTIC METHOD

by A. F. B. NICKSON and R. W. MUNCEY

Division of Building Research, Commonwealth Scientific and Industrial Research Organization, Australia

Summary

The transmission-characteristic method for measuring acoustic impedances has been developed to the stage where it is an accurate, simple and versatile method. The most suitable chamber dimensions are derived, construction of chambers is described and the impedance of a selected material at various angles of incidence is given for a wide range of frequencies.

Sommaire

On a perfectionné la méthode de mesure de l'impédance acoustique, dite méthode de la caractéristique de transmission, de façon à la rendre précise, simple et universelle.

On a calculé les dimensions les plus convenables à donner à la chambre, on décrit le mode de réalisation de cette chambre et on donne, pour une gamme étendue de fréquences, l'impédance d'un matériau choisi, mesurée sous des angles d'incidence différents.

Zusammenfassung

Die Methode der „Übertragungs-Charakteristik" zur Messung von akustischen Impedanzen ist zu einer genauen, einfachen und vielseitigen Methode entwickelt worden. Die günstigsten Kammerabmessungen werden abgeleitet, der Bau der Kammern wird beschrieben und die Impedanz eines ausgewählten Materials wird für verschiedene Einfallswinkel und für einen weiten Frequenzbereich mitgeteilt.

1. Introduction

The classical methods for measuring the acoustic properties of bounding surfaces employ the reverberation chamber which yields the absorption coefficient and the impedance tube which measures the specific normal acoustic impedance. Both methods have serious shortcomings. In a reverberation chamber it is difficult to achieve satisfactory diffusion for frequencies below 500 to 1000 c/s, the absorption coefficient is somewhat dependent on the size and shape of the chamber in which the test is made and in actual use the coefficients seem to be too high. The shortcomings of the impedance tube are that it operates at normal incidence only and has artificial mounting conditions.

Consequently it is strange that the transmission-characteristic (t.c.) method first proposed by WENTE [1] and used by HARRIS [2] and others has not been widely adopted; with it measurements can be made at definite angles of incidence, mounting conditions can be close to standard and the use of low frequencies is comparatively simple. High accuracy is required only in measuring audio frequencies. As this can be done by comparison methods, it is not difficult. The Division of Building Research has been investigating the t.c. method and is finding it most useful.

HARRIS has shown that the impedance of a material can be calculated from the change of bandwidth and resonant frequency of the normal modes of vibration of a rectangular chamber when the material is substituted for one wall of the chamber. His equations are given below. His analysis is not rigorous in that he does not actually consider the case of forced vibrations; nevertheless the equations he derives are the same as those obtained by a more rigorous treatment.

Consider a (bare) rectangular chamber whose dimensions are l_{xb}, l_{yb} and l_{zb} and suppose that material is introduced to cover the y-z wall so that the new x-dimension is l_x. Then, use the following symbols:

ν_b = the frequency of the mode of vibration with no material in the chamber,

ν_c = the frequency of the mode of vibration with the material in the chamber,

k_b = the bandwidth with no material in the chamber (taken as half the frequency difference between frequencies at which the response has dropped 3 dB from maximum),

k_c = the bandwidth with the material in the chamber,

ϱ = the density of the air,

c = the velocity of sound in air at the particular conditions,

n_x, n_y, n_z = the number of nodal planes in the x, y and z directions,

σ_x, σ_y, σ_z = coefficients of value ½ or unity depending on whether the corresponding n_x, n_y, n_z are zero or non-zero,

λ = the wave length of the sound,

$\eta_x = 2 l_x \nu / c$, $\eta_y = \ldots$ etc.,

$\zeta \varrho c$ = the impedance of the material,

$Z = \varrho c \gamma \exp \mathrm{j} \Phi$ = the impedance of the chamber wall.

HARRIS shows that the impedance of the material measured is given by

$$\zeta = \frac{2 l_x}{\lambda} \cdot \frac{\coth(-\mathrm{j}\pi\chi)}{\chi}$$

where the real and imaginary parts of χ^2 are

$$\mathrm{Re}(\chi^2) = n_x^2 \left(\frac{l_x}{l_{xb}}\right)^2 - \frac{4 l_x^2 (\nu_b^2 - \nu_c^2)}{c^2} + \frac{2\sigma_x \eta_x}{\pi} \cdot \frac{\sin \Phi}{\gamma},$$

$$\mathrm{Im}(\chi^2) = \frac{4 \nu l_x^2}{\pi c^2} \cdot \left(k_c - k_b + \frac{\sigma_x l_{yb} l_{zb} k_b}{2(\sigma_x l_{yb} l_{zb} + \sigma_y l_{zb} l_{xb} + \sigma_z l_{xb} l_{yb})}\right).$$

2. The chambers

The transmission-characteristic method uses normal modes of vibration of the chamber which are separated in frequency (or which can be separated by microphone placement). It is desirable therefore to proportion the room so that the separation in frequency of the lower modes is as uniform as possible.

The frequencies of the normal modes of vibration are given by

$$2 \frac{l_{xb} \nu}{c} = \sqrt{n_x^2 + \left(\frac{l_{xb}}{l_{yb}}\right)^2 n_y^2 + \left(\frac{l_{xb}}{l_{zb}}\right)^2 n_z^2}.$$

By writing $(l_{xb}/l_{yb})^2 = D$ and $(l_{xb}/l_{zb})^2 = E$ it can readily be seen that the two modes of vibration, (P_1, Q_1, R_1) and (P_2, Q_2, R_2), will have the same frequency if and only if

$$P_1^2 + DQ_1^2 + ER_1^2 = P_2^2 + DQ_2^2 + ER_2^2.$$

The locus of points satisfying this condition is a straight line on the D, E plane. Fig. 1 shows all such loci for which the values of P_1, Q_1, etc. are less than three. Now it is desirable that the dimensional ratio chosen for the chambers should be such that the corresponding (D, E) points do not fall upon the loci and, in fact, the distance away from a line is some measure of the separation of the two modes in question. Hence it is necessary to fix the dimensions so that the corresponding point falls in one of the spaces of the diagram.

The examination can be made as follows. The ratio $1 : D : E$ is chosen to fall in an open space of the diagram (e.g. H, J, K) and the modal frequencies calculated based upon the lowest modal frequency equal to unity. The frequency ratios corresponding to three areas H, J and K are given in Table I. These and other series were examined for uniformity of spacing and separation and the ratio 1 : 0.785 : 0.5 chosen as the most satisfactory.

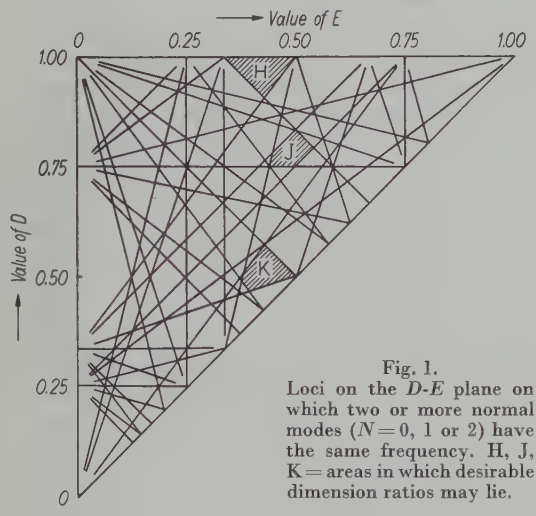

Fig. 1.
Loci on the D-E plane on which two or more normal modes ($N = 0$, 1 or 2) have the same frequency. H, J, K = areas in which desirable dimension ratios may lie.

Table I

Frequencies of normal modes for various chamber dimensional ratios

Area		H	J	K
Dimension ratio	$1 : D : E$	1 : 0.96 : 0.43	1 : 0.785 : 0.5	1 : 0.52 : 0.43
Modal frequencies	1.0.0	1.00	1.00	1.00
	0.1.0	1.44	1.25	1.10
	0.0.1	1.47	1.41	1.52
	1.1.0	1.76	1.60	1.49
	1.0.1	1.78	1.73	1.82
	0.1.1	2.06	1.89	1.88
	2.0.0	2.00	2.00	2.00
	1.1.1		2.13	2.13
	2.1.0		2.36	2.28
	2.0.1		2.45	2.51
	0.2.0		2.50	2.20
	1.2.0		2.69	2.42
	2.1.1		2.74	
	0.0.2		2.82	
	0.2.1		2.87	

Having fixed the dimension ratio it is necessary to decide the largest dimension of each chamber. An overlap of frequency range is desirable and a ratio of about two to one appears reasonable. The useful frequency range can be covered by six sizes as follows:

Lowest mode frequency	100	200	400	800	1600	3200	c/s
Greatest chamber dimension	1.73	0.864	0.432	0.216	0.108	0.054	m

Chambers have been constructed so that at least two are of the same material and have the same wall thickness making them thermally similar. When such a pair is placed in the same thermal environment the internal temperature (and consequently the wave velocity) of the two will drift equally. This drift is reduced in the laboratory as the space in which the chambers are placed is insulated to lessen the rate of temperature change.

The two largest chambers have been constructed in 10.2 cm concrete blocks hard-plaster-rendered inside, those with greatest dimensions 0.864 m, 0.432 m and 0.216 m have been made from 2.54 cm (nominal) wood lined with 0.16 cm aluminium sheet, and the three smallest are constructed in 1.48 cm brass. The masonry chambers have concrete doors with refrigerator type seals and locks and the samples are placed inside; the remainder have one open side which can be covered by the lid or by the sample and in this way measurements can be made on *in situ* materials.

In the masonry and wooden boxes, sound is produced by a small loudspeaker mounted in one corner, and in the diagonally opposite corner a small microphone connected to a vacuum tube voltmeter measures the amplitude of the sound. In the brass boxes sound is introduced from outside by a tube stuffed with wires and is detected by a microphone also outside and connected to the box with a similar tube. As indicative of the wall hardness it is sufficient to say that in the box $1.73 \times 1.37 \times 1.22$ m^3 (volume of 2.89 m^3) the R.T. is 13.5 s at 100 c/s and in the brass box $10.8 \times 8.58 \times 7.63$ cm^3 (volume of 706 cm^3) the R.T. is 0.5 s at 1600 c/s. These decays correspond to Sabine absorption coefficients of 0.004 and 0.007 respectively. Consequently in the present measurements the walls have been taken as being infinitely hard and no correction is applied in the second equation. For experimental purposes the expressions for $\mathrm{Re}(\chi^2)$ and $\mathrm{Im}(\chi^2)$ of Section 1 may be approximated to

$$\mathrm{Re}(\chi^2) = n_x^2 \left(\frac{l_x}{l_{xb}}\right)^2 - \frac{2\eta_x^2 \Delta\nu}{\nu} \qquad (1)$$

and $$\mathrm{Im}(\chi^2) = \frac{2\eta_x^2}{\nu}(k_c - mk_b) \qquad (2)$$

where $$\Delta\nu = \nu_b - \nu_c$$

and $$m = 1 - \frac{\sigma_x l_{yb} l_{zb}}{2(\sigma_x l_{yb} l_{zb} + \sigma_y l_{xb} l_{zb} + \sigma_z l_{xb} l_{yb})}.$$

3. Experimental procedure

The equations (1) and (2) involve accurate determination of small frequency increments. The required accuracy is obtained by measuring each frequency in terms of a standard frequency of good stability. A stable oscillator, the frequency of which can be varied, is used to locate the particular frequency to be measured. A second oscillator is adjusted to a frequency close to that of the first oscillator (the second frequency being known exactly in terms of the standard crystal frequency) and the frequency difference between the two oscillators measured by means of the Lissajous figure formed on the screen of a cathode ray tube when the two frequencies are applied to the deflecting plates. In this manner the frequency of the variable oscillator is determined to a high degree of accuracy, the estimated error being less than one part in 10 000. The equipment is described in detail elsewhere [3].

4. Calculations

The calculations required can be shortened by using conformal transformations in the manner shown by Morse and Bolt [4] who give several maps covering a range of impedances for the transformation of χ^2 to $\ln(\zeta/\eta)$. For many experimental measurements the maps are not sufficiently contoured or extensive and failing considerable calculation and re-drawing the following procedure was adopted:

$$\zeta = \eta_x \frac{\coth(-\mathrm{j}\pi\chi)}{\chi} = -\mathrm{j}\pi\eta_x \frac{\coth W}{W}$$

where $$W = \mathrm{j}\pi\chi.$$

$\coth W/W$ can be expanded as terms of a series containing one set of real terms and one set of imaginary terms. When this is done it is found that the first two terms in each set are sufficient to cover most of the acoustic impedances in which interest is shown. Equating the real and imaginary parts of ζ with the real and imaginary parts of the expansion multiplied by the quantity η_x gives two equations for the two parts of ζ in terms of the real and imaginary parts of χ^2. (These latter are determined from experiment.) The results obtained in this manner can be expressed as follows:

(I) $n_x = 0$:

$$\frac{R}{\varrho c} = \frac{c}{4\pi l_x} \cdot \frac{(k_c - mk_b)}{(k_c - mk_b)^2 + (\nu_b - \nu_c)^2},$$

$$\frac{X}{\varrho c} + \frac{\pi\eta}{3} = \frac{c}{4\pi l_x} \cdot \frac{-(\nu_b - \nu_c)}{(k_c - mk_b)^2 + (\nu_b - \nu_c)^2};$$

(II) $n_x = 1, 2 \ldots l_x = l_{xb}$ (box with removable side):

$$\frac{R}{\varrho c} = \frac{c}{2\pi l_x} \cdot \frac{(k_c - m k_b)}{(k_c - m k_b)^2 + (\nu_b - \nu_c)^2},$$

$$\frac{X}{\varrho c} = \frac{c}{2\pi l_x} \cdot \frac{-(\nu_b - \nu_c)}{(k_c - m k_b)^2 + (\nu_b - \nu_c)^2};$$

(III) $n_x = 1, 2 \ldots \; l_x \neq l_{xb}$ (box without removable side):

$$\frac{R}{\varrho c} = \frac{c}{2\pi l_x} \cdot \frac{(k_c - m k_b)}{(k_c - m k_b)^2 + [(\nu_b - \nu_c + \alpha)(l_x/l_{xb})^2]^2},$$

$$\frac{X}{\varrho c} = \frac{c}{2\pi l_x} \cdot \frac{-(\nu_b - \nu_c + \alpha)(l_x/l_{xb})^2}{(k_c - m k_b)^2 + [(\nu_b - \nu_c + \alpha)(l_x/l_{xb})^2]^2},$$

where $$\alpha = \frac{n_x^2 \nu}{\eta_x^2}(1 - l_x/l_{xb}).$$

The accuracy of these relations is such that the maximum errors are less than 5 per cent for values of $\frac{\nu_b - \nu_c}{\nu} < \pm \frac{0.02}{\eta_x^2}$ and $\frac{k_c - m k_b}{\nu} < \frac{0.04}{\eta_x^2}$ with $l_x/l_{xb} = 0.95$.

Note in (I) and (II) that a material of half the R and X impedance is necessary to give the same bandwidth and frequency shift for a grazing wave as for a normal or oblique wave, which agrees with the values used for σ ($\sigma = \frac{1}{2}$ for $n = 0$, $\sigma = 1$ for $n = 1$) since usually $\pi\eta/3 \ll X/\varrho c$.

5. Bare wall impedances

The value of the impedance of the test specimen has been expressed in terms of the frequencies of the normal modes of vibration and the resonance bandwidths associated with those modes by equations (1) and (2). Each equation contains a correction term for the impedance of the wall opposite the sample, the effect of the other bare walls being eliminated by the analysis. In the first of these equations the correction term can easily be computed but in the second a knowledge of the bare wall impedance is necessary.

Harris [2] points out that the impedance could be calculated from a knowledge of the sound velocity and the room dimensions, but rejects this method because of the large error likely to be introduced in the impedance by small errors in the sound velocity. He then proposes that the pressure distribution in the chamber be explored and, assuming equal wall impedances for the case when $n_x > 1$, shows how the impedance may be evaluated. This technique cannot however be applied to the case where $n_x = 1$ because the minimum pressure is theoretically zero and consequently the impedance of any wall of a chamber cannot be determined below twice the lowest modal frequency. Further, the wall impedances have been found to be so high that it is doubtful if measured minima would give as good an accuracy as the calculations using the velocity of sound.

It was decided therefore to adopt the method using the velocity of sound and to assume its value to be 340.5 m/s at 15 °C with a temperature coefficient of 0.602 m/s per degree centigrade. These figures were based on evidence from various sources, notably Abbey and Barlow [5] and Hardy, Telfair and Pielemeier [6]. This value may be expected to be within ± 0.2 m/s and such an error has no significant effect upon the order of the calculated impedance.

Morse and Bolt [4] have shown that the frequency factor for a standing wave when all the walls are fairly hard has the form $\exp(-j\omega_n t - k_n t)$ where ω_n and k_n can be written

$$\omega_n = \pi c \sqrt{\frac{\mu_x^2 - \kappa_x^2}{l_x^2} + \frac{\mu_y^2 - \kappa_y^2}{l_y^2} + \frac{\mu_z^2 - \kappa_z^2}{l_z^2}}$$

$$k_n = \frac{c}{4} \sqrt{\frac{4\pi\,\mu_x \kappa_x}{\eta_x l_x} + \frac{4\pi\,\mu_y \kappa_y}{\eta_y l_y} + \frac{4\pi\,\mu_z \kappa_z}{\eta_z l_z}}$$

and the various μ's and κ's are the respective wave number and attenuation parameters.

A series expansion for ω_n and k_n gives the value

$$\mu_x^2 - \kappa_x^2 = n^2 - \frac{2\sigma\eta}{\pi}(s_1 + s_2)$$

and $$\frac{4\pi\,\mu_x \kappa_x}{\eta} = 4\sigma(g_1 + g_2)$$

where $$s = \frac{\varrho c}{Z}\sin\Phi, \quad g = \frac{\varrho c}{Z}\cos\Phi.$$

The approximate value of k_n for the damping constant when all walls are fairly hard is therefore

$$k_n = \frac{c}{4}\left[\frac{4\sigma_x(g_{x1} + g_{x2})}{l_x} + \frac{4\sigma_y(g_{y1} + g_{y2})}{l_y} + \frac{4\sigma_z(g_{z1} + g_{z2})}{l_z}\right]$$

or if values of g are the same for each surface of the box, k_n is found to be equal to

$$2c\,K \cdot \frac{\cos\Phi}{Z/\varrho c} \quad \text{where} \quad K = \frac{\sigma_x}{l_x} + \frac{\sigma_y}{l_y} + \frac{\sigma_z}{l_z}.$$

In a similar manner a value may be obtained for ω_n,

$$\omega_n^2 = \pi^2 c^2 \left[\frac{n_x^2 - \frac{2\sigma_x \eta_x}{\pi}(s_{x1} + s_{x2})}{l_x^2} + \right.$$
$$\left. + \ldots(y)\ldots + \ldots(z)\ldots\right].$$

Remembering that $$\left(\frac{2\nu}{c}\right)^2 = \frac{n_x^2}{l_x^2} + \frac{n_y^2}{l_y^2} + \frac{n_z^2}{l_z^2}$$

and calling this frequency ν_{b1} as being the value if the walls are infinitely hard, the value for ω is found to be

$$\omega_c^2 = \pi^2 c^2 \left[\left(\frac{2\nu_{b1}}{c}\right)^2 - \frac{8 s \nu_{b1}}{\pi c} \cdot K\right]$$

and ω_c is the value of frequency measured with fairly hard walls. This equation may be put into the form

$$\frac{\nu_c^2 - \nu_{b1}^2}{\nu_{b1}} = \frac{2c K}{\pi}\left(\frac{\sin \Phi}{Z/\varrho c}\right).$$

From equations (1) and (2), the value of $Z = \varrho c \gamma \cdot \exp j \Phi$ can be obtained from the solutions

$$\gamma = \frac{2c K}{k_n}\left[1 + \pi^2\left(\frac{\nu_c^2 - \nu_{b1}^2}{\nu_{b1} k_n}\right)^2\right]^{-\frac{1}{2}},$$

$$\Phi = \text{arc tan}\,\frac{\pi\left(\nu_c^2 - \nu_{b1}^2\right)}{\nu_{b1} k_n}.$$

Measurements made on the softest of the three wall types used (the wooden surface lined with sheet metal) resulted in a specific impedance $120 \angle -60$ at 400 c/s. This gives a value of $\sin \Phi/\gamma$ as 0.0065 that is small compared with the value of $2\eta_x^2 \frac{\Delta\nu}{\nu}$ and may therefore be neglected.

6. Results of experiment

To illustrate the use of the t.c. method for measuring the acoustic impedance of a material, it was decided to measure one material over a large frequency range, and for as many angles of incidence as could be conveniently measured in any one box. As the normal modes in any box come closer together and the bandwidths become wider as the frequency increases, there is a limit to the range of frequencies that can be measured in any box. For the material measured this ratio was about 3:1 in the larger boxes and 2:1 in the second smallest box. In the smallest box only a small range was covered because of inefficiency of the loudspeaker and microphone units when used with tubes filled with fine wires. The material for which the measurements were made was a soft fibreboard, 1.27 cm thick, weighing 0.38 g/cm². Samples of this material from a standard batch were cut and glued into position in the boxes with a cold water glue. The samples were allowed to remain for five days before measurements were made. The experimental procedure was to measure the frequencies and bandwidths of modes in one box before the sample was glued in, referring at intervals to any one selected mode in a thermally similar chamber. In this way all the modal frequencies of the chamber could be obtained as a ratio using the arbitrary selected mode which was kept under observation. Five days later when the glued sample was ready to be measured, the modal frequencies in the chamber were again measured and the new bandwidths determined, referring occasionally to the initially selected mode in the other thermally similar chamber. As this would have changed from the previous occasion when measured, this value in conjunction with the ratios determined at the start will give the values of the bare box modes as they would be if there was no sample present. The new modal frequencies being then measured enable the frequency shifts to be calculated. The bandwidths of these peaks are also measured.

In some cases the peaks interfere with one another, and this difficulty can be overcome occasionally by using the decay of sound at the particular frequency being considered. The simple relation $k_n = 6.91/T$ relates bandwidth to time of decay, and thus the bandwidth can be measured when it is not possible to reduce the peak intensity sufficiently on either side to enable k_n to be measured in the normal way. A Brüel and Kjær level recorder (type 2301) was found useful for this purpose although its resolving time was rather too long for some cases. Varying the position of the microphone also helps to operate modes when close together.

Table II gives the values of $R/\varrho c$ and $X/\varrho c$ measured for the sample at various frequencies and angles of incidence for a number of different boxes. The greatest practical difficulty was that although the samples were cut from two sheets of a known batch, each sample had necessarily a different glued joint. All that could be done here was to mix and apply the glue in the same way each time, place weights on the surface and then measure the samples after five days when the joints could be considered reasonably similar.

Table III gives the mean values of $R/\varrho c$ and $X/\varrho c$ when divided first into frequency groups 100—200, 200—400 c/s, etc., and angular groups 0—30, 30—60, 60—90°. This enables an overall picture of the behaviour of the fibreboard for three different angles of incidence and a large range of frequencies to be obtained. These values are plotted in Fig. 2.

7. Discussion of results

To discuss the results profitably it is necessary to refer to the average results of the measurements shown in Table III and Fig. 2 rather than to the individual measurements in Table II. The important feature is that the acoustic impedance of the material depends on the angle of incidence of the sound wave. This is clearly shown in the figure, where it can be seen that the impedance for incident angles 0—30° is greater than for angles 30—60°, and the latter group has a greater

Table II

Mode	Frequency	$R/\varrho c$	$X/\varrho c$	θ
Box 1				
001	98.6	100	−50.2	88
100	124.4	80.8	−57.5	0
010	138.7	62.7	−60.2	87
101	158.4	34.6	−49.6	37
011	170.4	49.6	−59.7	87
110	186.3	19.8	−38.8	47
002	197.0	34.5	−48.4	87
111	210.8	41.2	−43.6	53
102	232.6	23.0	−36.9	57
012	241.1	16.6	−32.1	86
200	248.7	26.6	−40.2	0
201	267.5	67.2	−35.1	16
112	276.0	10.9	−26.9	62
020	277.2	33.3	−39.3	87
210	284.8	51.5	−35.4	26
021	293.8	6.78	−20.3	85
003	295.4	6.15	−23.6	86
211	301.4	51.9	−36.3	32
Box 2				
001	197.4	29.4	−40.3	85
100	251.1	31.8	−41.6	0
010	276.3	20.2	−35.3	85
101	319.1	22.4	−34.4	38
011	341.4	25.8	−34.7	86
110	372.7	18.9	−30.7	48
002	394.0	13.2	−26.8	85
111	423.1	15.2	−28.3	54
102	466.5	15.0	−26.7	58
012	483.6	9.04	−23.4	85
200	502.2	17.7	−27.6	0
112	544.6	8.82	−18.6	63
020	547.8	9.75	−17.5	85
210	573.1	14.7	−24.3	27
003 / 021 ?	593.6	8.38	−20.6	85
211	602.2	2.35	−11.4	33
Box 3				
001	385.2	18.9	−26.5	84
100	499.8	22.7	−29.9	0
010	546.4	6.65	−17.6	83
101	627.0	15.0	−19.7	35
011	675.7	18.0	−26.3	85
110	740.8	20.8	−17.5	46
002	778.8	17.1	−14.4	86
111	835.0	15.8	−16.3	52
102	924.2	19.9	− 7.9	56
012	951.8	12.9	−12.3	85
200	999.1	14.4	−12.3	0
201	1066	4.85	−10.0	16
020	1098	10.4	−14.1	85
210	1140	16.3	−10.3	24
003 / 021 ?	1166	13.7	−11.7	86
Box 4				
001	744.1	2.00	− 7.15	76
100	1043	40.1	− 0.64	0
010	1098	13.4	− 8.05	85
101	1287	8.75	− 1.77	32
011	1331	10.1	−11.6	84
110	1501	9.65	−20.0	45
002	1523	3.58	− 3.12	83
111	1656	4.95	− 5.53	52
102	1848	10.1	+ 0.22	54
200	2082	31.9	+ 9.49	0
Box 5				
001	1551	10.2	−11.5	81
010	1951	11.2	− 8.59	83
100	2210	6.71	− 8.42	0
011	2498	8.18	− 4.66	84
101	2709	9.50	− 1.08	42
110	2941	10.3	− 3.54	47
002	3130	8.11	− 2.08	87
111	3313	8.49	− 5.02	54
012	3681	7.93	− 6.65	84
102	3803	6.31	− 2.53	59
020	3879	3.14	− 4.95	80
021	4059	0.90	− 3.42	73
112	4231	2.76	− 7.46	64
Box 6—sample A				
001	3165	15.3	− 2.65	87
010	3920	17.5	− 1.91	88
100	4382	6.92	− 8.04	0
011	4847	1.80	− 2.50	74
Box 6—sample B				
001	3155	10.4	− 4.82	84
010	3904	13.6	− 6.72	84
100	4700	8.19	− 5.73	0
011	4838	0.95	− 4.37	74

Table III

Frequency range [c/s]	N	Mean $R/\varrho c$	Mean $X/\varrho c$	Range of angle θ
100—200	5	55.2	−51.9	60°—90°
200—400	8	17.6	−29.8	
400—800	6	11.5	−20.0	
800—1600	6	11.8	−11.6	
1600—3200	5	10.6	− 4.56	
3200—6400	7	6.55	− 4.36	
100—200	2	27.2	−44.2	30°—60°
200—400	6	28.1	−34.8	
400—800	6	12.9	−20.4	
800—1600	4	13.5	−11.5	
1600—3200	4	8.71	− 3.38	
3200—6400	3	5.83	− 5.00	
100—200	1	80.8	−57.5	0°—30°
200—400	4	44.3	−38.1	
400—800	3	18.4	−27.2	
800—1600	3	11.8	−10.9	
1600—3200	1	6.71	− 8.42	
3200—6400	2	7.56	− 6.89	

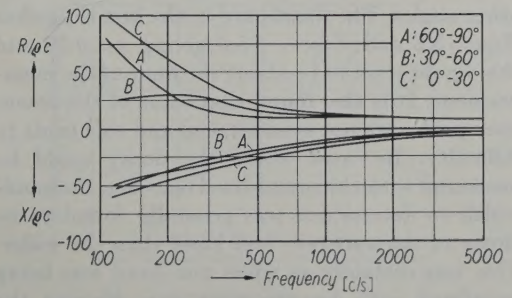

Fig. 2. Frequency characteristic of 1.25 cm fibreboard at different angles of incidence.

impedance than for angles 60—90° over most of the frequency range from 100—5000 c/s. This means that for this sample the absorption coefficient calculated from $\alpha = \frac{8R\varrho c}{R^2 + X^2}$ will increase as the angle of incidence departs from the normal. This is to a certain extent a confirmation of the suggestion that the absorption coefficient would alter with angle of incidence of a material of normal impedance $Z/\varrho c$ in the manner of $1 - \left|\frac{Z\cos\theta - \varrho c}{Z\cos\theta + \varrho c}\right|^2$. This expression has a maximum at $\theta = \arccos \varrho c/Z$ and is zero when $\theta = \pi/2$. Although there are several modes in the boxes for which geometrically the angle of incidence is $\pi/2$, it is found in practice that the presence of the material modifies the wave behaviour in such a manner that the angle of incidence is not greater (in the present cases) than 88°, and would be less than this for a material of a smaller normal impedance. The manner in which the curves cross around 200 c/s when the impedance of the sample for angles 30—60° becomes smaller than for angles 60—90° cannot be explained in this way but the effect is quite real for the material used. In the case of the lower frequencies, the above formula would not be satisfactory as a representation of the variation of α with θ. This method however gives the value of $R/\varrho c$ and $X/\varrho c$ for an actual angle of incidence $\theta = \arccos \sqrt{\mathrm{Re}\,(\chi^2)/\eta_x^2}$, and α can then be calculated as $\frac{8R\varrho c}{R^2 + X^2}$.

There are several difficulties in using the t.c. method for measurement of acoustic impedance and some attention has to be paid to them. The obvious one is that only materials of medium impedance can be measured satisfactorily, because after the first two or three modes the bandwidths become so wide as to mask each other and make it difficult to determine the presence of peak frequencies. If this small number of modes is satisfactory, the range of incident angles is limited to 0° or 90° and it is difficult to measure any other angles. The fibreboard in the last range has $R/\varrho c = 5.8$ and $X/\varrho c = -5.0$ giving $\alpha = 0.79$ and this would seem to be about the limit of the measurement. It is also found that some of the resonance peaks are not symmetrical and this leads to difficulty. In cases where the decay could be measured with the sound-level recorder, the bandwidth so determined was generally found to be closer to the narrower half band than the wider. This was certainly so when one band was being interfered with by the next one. Moving the microphone position was sometimes found to be helpful as this is equivalent in effect to suppressing the interfering mode.

The third difficulty is due to the change in the velocity of sound with temperature. This is important as small frequency shifts are often to be measured, and it has been overcome by using two thermally similar chambers in each measurement. It is important to watch that the frequency shifts measured are due solely to the sample and not partly to a change of temperature while the measurements are being made.

8. Conclusions

This investigation has shown that the transmission-characteristic method is a powerful tool for measuring the acoustic impedance of materials at various frequencies and various angles of incidence. Certain limitations are to be expected when measuring the softer materials and the method then requires modification. The obvious difficulty is due to increasing bandwidths while the modal frequencies are coming closer together, but this may be partly overcome by varying the position of the microphone in the box. The boxes may be portable and can be easily placed against materials already erected for which measurements are required. The method provides an excellent means of comparing the impedance of various materials at different frequencies as required by the experimental work on acoustic models. The fact that allowance can be made for the bare wall impedance means that for most measurements boxes made of wood lined with metal sheet will be satisfactory provided proper attention is given to the sealing of the box.

Acknowledgments

The method used for examining chamber dimension ratio developed from discussions of one of the authors with J. W. Head of the B.B.C. Research Laboratories of Balham, England. His assistance is gratefully acknowledged.

(Received 4th November, 1952.)

References

[1] Wente, E. C., Characteristics of sound transmission in rooms. J. acoust. Soc. Amer. **7** [1935], 123—126.

[2] Harris, C. M., Application of the wave theory of room acoustics to the measurement of acoustic impedance. J. acoust. Soc. Amer. **17** [1945], 35—45.

[3] Nickson, A. F. B., An accurate method of measuring frequency in the audio range. J. sci. Instrum. **29** [1952], 391—393.

[4] Morse, P. M. and Bolt, R. H., Sound waves in rooms. Rev. mod. Phys. **16** [1944], 69—150.

[5] Abbey, R. L. and Barlow, G. E., Velocity of sound in gases. Austral. J. sci. Res. A **1** [1948], 175—189.

[6] Hardy, H. C., Telfair, D. and Pielemeier, W. H., Velocity of sound in air. J. acoust. Soc. Amer. **13** [1942], 226—233.

The mercury thermometer

An instrument for the measurement of high-intensity ultrasonic waves

by O. LINDSTRÖM

Division of Physical Chemistry,
The Royal Institute of Technology, Stockholm, Sweden

Zusammenfassung

Ein gewöhnliches Quecksilber-Thermometer wird als Leistungsmesser für Ultraschall angewandt. Diese einfache Methode ist überraschend genau, der mittlere Fehler beträgt etwa ein Prozent.

In the quantitative study of the chemical and biological effects of ultrasonic waves the determination and control of the sound intensity is a question of fundamental importance.

The instrument readings on the power control panel of the high frequency generator, e.g. of plate voltage and plate current of the rectifier, yield accurate expressions for the electric power input. Under constant conditions there is in general a linear relationship between the electric power input and the acoustic output of the transducer. The quotient between the acoustic output and the electric input may be called the power conversion ratio, p.c.r. for brevity. Unfortunately the p.c.r. is not a stable apparatus constant which may be evaluated once for all but a rather changeable magnitude influenced by many factors difficult to control. Because of this variancy it is necessary in accurate work to make frequent determinations of the p.c.r. in order to secure a defined acoustic output.

It should here be pointed out that the p.c.r. and the underlying linear relation refer to the primary acoustic output from the transducer. In general the sound intensity is evaluated by means of any instrument placed at some distance from the transducer. When the liquid in the interspace between the transducer and the instrument is cavitating the p.c.r. as determined in this way will decrease because of the reflexion of sound at the gas bubbles formed in the cavities. Cavitation has therefore to be avoided, e.g. by working at low acoustic intensities, using degassed liquids or increasing the hydrostatic pressure in the liquid. A convenient method is to arrange a fast circulation of the liquid so that the gas bubbles are swept out of the sound field before they have attained a disturbing magnitude. This was done in the experiments reported here. (At high rates of liquid circulation the transmitted power will be reduced due to an effect of the streaming liquid, therefore it is necessary to maintain constant conditions even with regard to the liquid circulation [1].)

A great many methods have been designed for the determination of the intensity of powerful ultrasonic waves in liquids. Most of them are based either on the sound pressure or on the heating action of the acoustic waves [2]. The former methods, in which the sound pressure is measured by means of a suspended reflector, yield absolute intensity values. However, these methods are complicated because of the tendency of the reflector to remain fixed in certain preferred positions, a phenomenon which is observable even in the case of a (slightly) conical reflector. The thermal methods do not easily give absolute values but are potentially more simple and rapid. An accurate thermal method, calibrated with the aid of an absolute sound pressure method, therefore seems to be most suited for the continuous control of the p.c.r. during a series of experiments. It was then realized that an ordinary mercury thermometer might offer some advantages, the mercury bulb being sufficiently large and the instrument itself a most reliable temperature indicator. The degree of reproducibility of such a thermometer method was evaluated in the following experiments.

The most suitable position for the thermometer was found to be the one demonstrated in Fig. 1. It is easy to arrange the thermometer in this symmetrical position with the aid only of an ordinary laboratory stand, and the error in the position thus achieved is of the order of 1 mm. The important reason, however, for arranging the thermometer bulb in the acoustic fountain and not in the liquid bulk is that the surface of the fountain acts as a kind of curved reflector, which focusses the acoustic waves on the thermometer bulb so that a much larger temperature difference is obtained.

In these experiments the liquid medium consisted of transformer oil, which was circulated and thermostated to $24.22 \pm 0.10\,^{\circ}C$. The constant oil temperature is a prerequisite in order to secure a fairly constant p.c.r. value, because of the temperature variation of the transducer's resonance frequency. (Of course this does not imply that it is necessary to work with a thermostated liquid when applying this thermometer method.) The statistical variations in the acoustic energy (equal to ± 5 % and due to fluctuations in the power supply) and the variation in the oil temperature made it necessary to evaluate the appropriate temperature difference as a mean value over a short period of time. Simultaneously the variations in the electric input were recorded by means of a printing potentiometer so that an accurate mean value for the electric input could be computed. The small differences in the power input between the separate experiments were corrected for with the aid of the approximate linear relationship between the temperature difference and the power input. It has to be pointed out that the separate runs are independent of each other since the thermometer was taken away and the laboratory stand removed between each experiment.

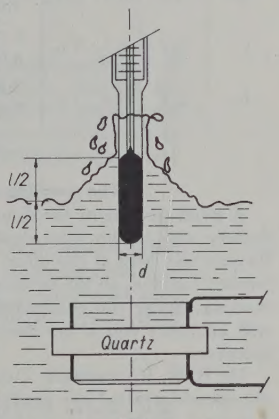

Fig. 1.
Position of the thermometer in the ultrasonic field.

The results of some runs with four different thermometers are given in the Table. It is recognized that in spite of the rather simple procedure the standard deviation is sufficiently small, of the order of one per cent for the two more accurate thermometers A and D. This error could probably, if necessary, be reduced by means of some mechanical ar-

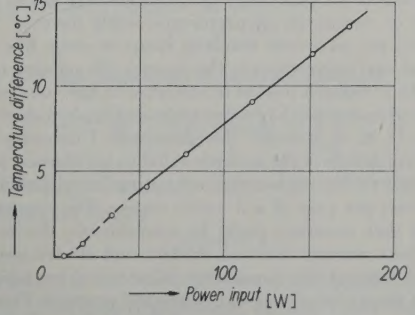

Fig. 2. Temperature difference versus electric power input.

rangement permitting a more exact and defined thermometer setting.

In Fig. 2 a typical curve for the temperature difference versus power input is reproduced. As the thermometer bulb at low intensities is partly situated in the air there is some uncertainty at the smallest values. This error vanishes when the acoustic fountain is high enough to cover the whole bulb.

Longer continuous exposures of the order of thirty minutes or more must be avoided since the thermometer may then be damaged due to cavitation which may be set up in the mercury bulb.

The writer wishes to thank Professor O. LAMM for his kind interest and encouragement. Thanks are also due to the Swedish State Council of Technical Research.

Stockholm, 7th September, 1952.

Thermometer	Scale div. [°C/cm]	Hg bulb d [cm]	Hg bulb l [cm]	Temperature diff. [°C]	Mean value [°C]	Max. error [%]	Stand. dev. [%]
A	2.3	0.8	2.6	9.35 9.25 9.12 9.25 9.09 9.31	9.23	1.5	1.1
B	3.1	0.7	2.3	7.94 7.83 7.97 7.96 8.00 8.15	7.98	2.1	1.3
C	5.2	0.7	1.6	8.75 8.52 8.80 8.66 8.57 8.43	8.62	2.2	1.6
D	2.1	0.6	1.8	7.93 7.99 8.01 8.20 8.02 8.06	8.04	2.0	1.0

References

[1] LINDSTRÖM, O., Acta Chem. Scand. **6** [1952], 1313.

[2] BERGMANN, L., Der Ultraschall. S. Hirzel Verlag, Zürich 1949.

The teaching of acoustics

A joint meeting of the Acoustics Group of the Physical Society and of the Education Group of the Institute of Physics was held at the office of the Institute in Belgrave Square, London, on the evening of the 19th November. The meeting, under the chairmanship of Mr. WEST, was very well attended and a live discussion followed the opening speeches.

Dr. R. W. B. STEPHENS (Imperial College) in the opening speech stressed the study of vibrations as being fundamental to physics as a whole and pointed out the close association of modern acoustical theory with that of other branches of physics, e.g. the similarity of DEBYE's theory of specific heats with the theory of room acoustics. He suggested that the treatment of acoustics as a Cinderella subject in schools and colleges arose from the crowded nature of the present syllabuses and the very small proportion of acoustic questions set in physics examination papers. The speaker then pointed out how acoustics permeated into the fields of aeronautics, light electrical engineering, rheology, medicine, etc., and examples quoted from this wide sphere of application could do much to make the teaching of the subject more alive and attractive.

Mr. E. NIGHTINGALE, an experienced teacher and writer of school text-books, dealt with the teaching of acoustics in schools. He indicated, by means of demonstrations, how much of the earlier teaching can be illustrated experimentally with simple apparatus by the energetic and enthusiastic schoolmaster. A suggested list of topics for lecture demonstrations was presented by the speaker.

Dr. E. G. RICHARDSON (Durham University) dealt with the University aspect of acoustics instruction and research and pointed out that while in England there are no institutions or university departments solely devoted to the subject, yet advanced teaching exists in some five or six colleges and universities in the country. He pointed out the need for a research worker in acoustics to have undergone a balanced training in hydrodynamics and applied electronics.

Mr. D. M. A. MERCER (Southampton University) gave tentative details of the acoustic syllabus for honours physics students at his University consisting of approximately 7 lectures per year of a 3 year's course. The speaker suggested that acoustics could be conveniently divided into 3 sections, namely classical, modern and electro-acoustics, and he stressed the importance of electrical analogies and circuit theory in present-day acoustical practice. This point was also emphasised by other speakers, and also the need for an adequate mathematical background for the advanced worker in acoustics.

Dr. H. LOWERY, author of "The background of music", spoke of the difficulty of teaching music students who had only a negligible knowledge of science or mathematics, and said that he started with orchestration as the basis of his instruction. Lieutenant ROBERTS, who had been concerned with the teaching of young boys training to be army musicians, also found the purely musical approach the most successful method. Dr. W. H. GEORGE (Chelsea Polytechnic) pointed out that musical acoustics was a very specialised subject; he thought that the theory of vibrations should be presented as a basic part of all physical theory and thereby do much to overcome the prejudice that a knowledge of music is essential to a study of acoustics.

Professor FLOYD spoke of the necessity of giving pre-medical students a good understanding of the mechanism of the human ear, Dr. E. J. IRONS urged the use of graphs to illustrate wave-motion and Mr. S. H. HUMBY cited examples of how the ordinary architect was often years behind in his knowledge of the acoustic design of rooms. Other points emerging from later speakers were the correlation of acoustic with electromagnetic theory, and the possibility of making more space for acoustics in the school syllabus by incorporating the theory of harmonic motion and wave-motion in the applied mathematics course.

A brief summary of the acoustics questionnaire sent to teaching institutions and industrial organisations by the Acoustics Group of the Physical Society was also presented by Dr. STEPHENS. On the educational side it revealed that instruction in acoustics was a normal part of the B. Sc. honours degree course in physics, but a few courses were also associated with equivalent degree examinations in music, architecture and engineering. Nearly 50 firms replied to the industrial questionnaire but only one or two salient features will be quoted here. It was surprising for instance to find only one out of seven firms in the acoustics material industry recruiting staff who have already received education in acoustics of a university degree standard. The electrical engineering and radio and telecommunication industries appear to be the chief industrial users of acoustic specialists, but it must not be overlooked that many find employment in the Post Office research section, the B.B.C. and Government research establishments. In the case of those industries who have research associations, it is the general practice for the various firms to pass over their acoustical problems to these associations. R.W.B.S.